EFFECT OF ALTERNATIVE GLYCOSYLATION ON INSULIN RECEPTOR PROCESSING IN 3T3-L1 ADIPOCYTES

By

JOSEPH BUMSUH HWANG

A DISSERTATION PRESENTED TO THE GRADUATE SCHOOL
OF THE UNIVERSITY OF FLORIDA IN PARTIAL FULFILLMENT
OF THE REQUIREMENTS FOR THE DEGREE OF
DOCTOR OF PHILOSOPHY

UNIVERSITY OF FLORIDA

1999

This work is dedicated to my wife, Hyunok, and my parents.

ACKNOWLEDGMENTS

It is my honor to acknowledge the individuals to whom I am indebted for their support in the completion of my doctoral degree. First, I would like to give my utmost appraisal to my mentor, Dr. Susan Frost. Her energy and enthusiasm for science were inspiring and greatly appreciated. Her patience and encouragement in times of frustration exemplify her as a mentor. I was also fortunate to have received guidance from my committee members, Dr. Nancy Denslow, Dr. Ben Dunn, Dr. William Dunn, and Dr. Peter McGuire. I am grateful for their interest and devotion in shaping me into a successful scientist. It has been my pleasure to have worked with former and present members of Dr. Frost's lab. I have enjoyed listening and arguing with Dr. Maxine Fisher on her view points of life and I have enjoyed the healthy competition between Dr. Mike Thomson and myself. I also thank Melissa McInerney and Greg Marshall for being so entertaining. I would also like to give my sincere thanks to all the graduate students who have given me their support, encouragement, and friendship. I also thank my friends from the Gainesville Korean Baptist

Church for their eternal love and friendship. I will always be grateful to my parents for their prayers and for the joys of being a family. Finally, I would like to express my greatest joy and thanks to my wife and companion, Hyunok. Without her dedication and sacrifice I would not have achieved nor realized my full potential.

TABLE OF CONTENTS

ACKNOWLEDGMENTS. iii

LIST OF FIGURES. viii

LIST OF TABLES xi

ABBREVIATIONS. xii

ABSTRACT xvii

CHAPTERS

1. OVERVIEW. 1

    Introduction. 1
        3T3-L1 Adipocytes. 1
        Insulin Receptor 6
        N-linked Oligosaccharide Processing. 11
        GRP78 and "Quality Control". 21

2. MATERIALS AND METHODS 35

    Materials 35
    Methods 36
        Cell Culture 36
        Antibody Production. 37
        Peptide Purification of Anti-IRβ Antibody. 41
        Total Membrane Isolation 46
        Subcellular Fractionation. 49
        Markwell Assay for Protein Concentration Determination 51
        Metabolic Labeling 53
            [35S]methionine/cysteine. 53
            [3H]mannose 54
        Immunoprecipitation. 56
        SDS-Polyacrylamide Gel Electrophoresis 58
            One-dimensional gel electrophoresis 58
            Two-dimensional gel electrophoresis 58
        Electrotransfer and Immunoblot Analysis. 61

Glycosidase Digestions 63
Furin Digestion. 65
Glycogen Assay 67
Glucose Transport. 69
Autophosphorylation Assay. 71

3. GENERAL CELLULAR CHANGES IN RESPONSE TO GLUCOSE DEPRIVATION 73

Introduction. 73
Results 78
Glucose Transport. 78
Glycogen Content 81
Glycosylation of GLUT1 and GLUT4 81
Subcellular Distribution of GLUT1 and GLUT4. . . 86
Induction of Molecular Chaperones. 86
Conclusions 88

4. IDENTIFICATION AND CHARACTERIZATION OF INSULIN RECEPTOR PROCESSING INTERMEDIATES. 93

Introduction. 93
Results 96
Subcellular Localization of the Insulin Receptor in 3T3-L1 Adipocytes. 96
Time-dependent Accumulation of the Alternative Proreceptor 99
Synthesis of the Insulin Receptor. 99
Characterization of the Oligosaccharide Structure on the Insulin Receptor 101
Functional Activity of the Alternative Proreceptor 109
Conclusions .111

5. ROLE OF GRP78 AND PROTEOSOMES IN ALTERNATIVE PRORECEPTOR DEGRADATION .114

Introduction. 114
Results 115
Insulin Receptor Processing and Turnover 115
Interaction of GRP78 with the Alternative Proreceptor 119
Proteasome-mediated Degradation of the Alternative Proreceptor 124
Conclusions .129

6. REPROCESSING OF THE ALTERNATIVE PRORECEPTOR WITH GLUCOSE REFEEDING 132

Introduction 132
Results. 135
Restoration of Processing of the Alternative Proreceptor 135
Proteasome-mediated Degradation of the Intermediate Proreceptor. 142
Model of Reprocessing Mechanism. 146
Conclusions 148

7. CONCLUSIONS AND FUTURE DIRECTIONS 152

Conclusions 152
Future Directions 156

LIST OF REFERENCES 161

BIOGRAPHICAL SKETCH. .172

LIST OF FIGURES

Figure page

1-1 - Insulin Receptor Plays a Key Role in Mediating Insulin Action 5

1-2 - A Model of Insulin Receptor Processing. 7

1-3 - A Model of GRP78 Interacting with Newly Synthesized Proteins 33

2-1 - Dot Blot Analysis of IRβ Prebleed and Test Bleed. .42

2-2 - Immunoprecipitation of IR Using Affinity Purified IRβ Antibody 47

2-3 - Subcellular Fractionation of 3T3-L1 Adipocytes. . .50

2-4 - *N*-glycosidase F and Endoglycosidase H Digestions. .64

3-1 - Sugars Used for Dolichol-linked Core Oligosaccharide. 76

3-2 - Effect of Glucose or Fructose on Insulin-stimulated Glucose Uptake. 79

3-3 - Effect of Glucose or Fructose on Glycogen Content .83

3-4 - Effect of Glucose Deprivation on Glycosylation of GLUT1 and Expresion of GRP78 84

3-5 - Effect of Tunicamycin Treatment on the Migration of GLUT1 85

3-6 - Subcellular Localization of GLUT1, GLUT4, and GRP78. 87

3-7 - Effect of Glucose Deprivation on the Expression of ER Molecular Chaperones 89

3-8 - Two-dimensional Analysis of ER Molecular Chaperones .90

4-1 - Subcellular Distribution of IR in 3T3-L1 Adipocytes .97

4-2 - Time-dependent Accumulation of Alternative Proreceptor. 100

4-3 - Synthesis of IR 102

4-4 - Effect of Glycosylation on IR Migration 103

4-5 - Digestion of the Alternative Proreceptor with Furin 105

4-6 - A Model of Insulin Receptor Species Resulting from Two Furin Cleavage Sites. 106

4-7 - Insulin-stimulated Autophosphorylation of IR. . . 110

5-1 - IR Processing and Turnover. 116

5-2 - Co-precipitation of GRP78 with IR 120

5-3 - ATP-dependent Interaction of IR with GRP78. . . . 121

5-4 - Two-dimensional Analysis of IR and GRP78. 123

5-5 - Effect of Lactacystin on Degradation of the Alternative Proreceptor. 125

5-6 - Effect of MG132 on Degradation of the Alternative Proreceptor. 128

5-7 - Effect of Lysosomal Inhibitors on Degradation of the Alternative Proreceptor 130

6-1 - Processing of the Alternative Proreceptor in the Presence of Glucose. 136

6-2 - Effect of Endo H Treatment during Glucose Refeeding 138

6-3 - Effect of Tunicamycin Treatment during Glucose Refeeding 139

6-4 - Labeling the Alternative Proreceptor with [3H]mannose. 141

6-5 - Processing of [3H]mannose-labeled Alternative Proreceptor in the Presence of Glucose 143

6-6 - Effect of MG132 on Degradation of the Intermediate Proreceptor. 145

6-7 - Model of Reprocessing Mechanism 147

LIST OF TABLES

Table page

1-1 - *N*-linkede Glycosylation Sites on the IR 9

4-1 - Subcellular Distribution of IR. 96

ABBREVIATIONS

μCi	microCurie
μg	microgram
μL	microLiter
μM	microMolar
βME	β-mercaptoethanol
Asn-X-Ser/Thr	*N*-linked glycosylation site
ATPase	adenosine triphophatase
BFA	brefeldin A
BiP	immunoglobulin heavy chain-binding protein
BSA	bovine serum albumin
CFTR	cystic fibrosis transmembrane conductance regulator
DMEM	Dulbecco's modified Eagle's medium
DTT	dithiothreitol
ECL	enhanced chemiluminescence
EDTA	ethylenediamine tetraacetic acid
Endo H	endoglycosidase H

ER	endoplasmic reticulum
FBS	fetal bovine serum
GFAT	glucosamine:fructose 6-P aminotransferase
Glc	glucose
GlcNac	N-acetylglucosamine
GLUT	glucose transporter
GLUT1	glucose transporter 1
GLUT4	glucose transporter 4
GRP	glucose-regulated protein
GRP78	glucose-regulated protein of 78kDa
GRP94	glucose-regulated protein of 94kDa
H	cell homogenate
Hac1p	homologous to ATF and CREB
HDM	high density membrane
Hsc70	heat-shock cognate of 70kDa
Hsp70	heat-shock protein of 70kDa
IEF	isoelectric focusing
IgG	immunoglobulin G
IR	insulin receptor
IRα	insulin receptor α-subunit
IRβ	insulin receptor β-subunit
IRE1p	an integral membrane endonuclease

KDa	kiloDalton
KLH	Keyhole limpet hemocyanin
KRP	Krebs-Ringer phosphate buffer
LDM	low density membrane
Man	mannose
MAPK	mitogen-activated protein kinase
MG132	N-carbobenzyloxy-leucinyl-leucinyl-leucinal
NgF	*N*-glycosidase F
p36	aglycoform of GLUT1
p37	aberrantly glycosylated glycoform of GLUT1
p46	constitutive form of GLUT1
PAS	protein A-Sepharose
PBS	phosphate buffered saline
PDI	protein disulfide isomerase
PGI	phosphoglucose isomerase
PGM	phosphoglucose mutase
PI	isoelectric point
PI3	phosphatidylinositol 3
PI3K	PI3 kinase
PM	plasma membrane
PMI	phosphomannose isomerase

PMM	phosphomannose mutase
PMSF	phenylmethylsulfonyl-fluoride
PP1C	type 1 serine/threonine phosphatase
PPIase	peptidyl-prolyl isomerase
PTG	protein targeting to glycogen
RIPA	radioimmune precipitation buffer
SDB	sample dilution buffer
SDS	sodium-dodecyl-sulfate
SDS-PAGE	SDS-polyacramide gel electrophoresis
SNARE	soluble N-ethylmaleimide-sensitive fusion protein attachment protein receptor
Sulfo-MBS	sulfo-m-maleimidobenzoyl-N-hydroxysuccinimide ester
TAP	transporter activating protein
TBS-T	Tris-buffered saline containing Tween
TCA	trichloroacetic acid
TEMED	N,N,N',N'-tetramethylethylenediamine
TES	Tris/EDTA/Sucrose buffer
TES-P	TES containing phenylmethylsulfonyl-fluoride
TGN	trans Golgi network

Tris	tris(hydroxymethyl)aminomethane
t-SNARE	target-SNARE
UPR	unfolded protein response
UPRE	UPR element
VAMP	vesicle-associated membrane protein
v-SNARE	vesicle-SNARE

Abstract of Dissertation Presented to the Graduate School
of the University of Florida in Partial Fulfillment of the
Requirements for the Degree of Doctor of Philosophy

EFFECT OF ALTERNATIVE GLYCOSYLATION ON INSULIN RECEPTOR PROCESSING IN 3T3-L1 ADIPOCYTES

By

Joseph Bumsuh Hwang

December, 1999

Chairperson: Susan C. Frost
Major Department: Biochemistry and Molecular Biology

The mature insulin receptor (IR) is a cell surface heterotetrameric glycoprotein composed of two α- and two β-subunits. In 3T3-L1 adipocytes as in other cell types, the receptor is synthesized as a single polypeptide consisting of uncleaved α- and β-subunits, migrating as a 190kDa glycoprotein. To examine the importance of *N*-linked glycosylation on IR processing, we have used glucose deprivation as a tool to alter protein glycosylation. Western blot analysis shows that glucose deprivation led to a time-dependent accumulation of an alternative proreceptor of 170kDa in a subcellular fraction consistent with ER localization. Co-precipitation assays provided evidence that the alternative proreceptor bound GRP78, an ER molecular chaperone. *N*-glycosidase F treatment showed that the alternative proreceptor contained *N*-linked oligosaccharides. Yet, endoglycosidase H insensitivity indicates an aberrant oligosaccharide structure. Using pulse-chase methodology, we show that the synthetic rate was similar between the normal and alternative proreceptor. However, the normal proreceptor was processed into α- and β-subunits ($t_{1/2}$ = 1.3h ± 0.6h) while the alternative proreceptor was degraded ($t_{1/2}$ = 5.1h ± 0.6h). Inhibition of the lysosome or cytoplasmic proteasome, with lactacystin or MG132, did not prevent loss of the alternative proreceptor. However, both lactacystin and MG132 resulted in an increase in "processing" of the alternative proreceptor into the β-subunit. Upon refeeding cells that were initially deprived of glucose, the alternative proreceptor was processed to a higher molecular weight form and gained sensitivity to endoglycosidase H. This "intermediate" form of the proreceptor was also degraded although a small fraction escaped degradation resulting in cleavage to the α- and β-subunits. The addition of MG132 in the chase medium with 25mM glucose prevented degradation of the intermediate proreceptor and caused an increase in processing into the β-subunits. These data provide evidence for the first time

that glucose deprivation leads to the accumulation of an alternative proreceptor which can be post-translationally glycosylated with the readdition of glucose inducing both accelerated degradation and maturation.

CHAPTER 1
OVERVIEW

3T3-L1 Adipocytes

Based on their ability to store and subsequently release lipid, adipocytes play a central role in metabolic homeostasis. The hormonal regulation of proteins involved in this process has been under intense scrutiny for many years. More recently, adipocytes have been shown to have endocrine function. For example, adipocytes alone secrete leptin, the *ob* gene product, which is hypothesized to regulate body weight by interacting with a hypothalamic receptor to control satiety (Golden et al., 1997). Overexpression of leptin in humans signals the development of insulin resistance and obesity. Little attention has been placed on the protein processing path in adipocytes which is ultimately responsible for the correct synthesis, folding, and targeting of membrane and secretory proteins intimately involved in homeostasis.

The 3T3-L1 adipocytes are insulin-responsive cells that have been extensively used as a model system to examine insulin action. Isolated adipocytes are only viable for a few hours and thus, not feasible for use in studying long term effects of insulin. Thus, a 3T3-L1 preadipocyte cell line was established from fibroblasts of a mouse embryo (Green and Meuth, 1974; Green and Kehinde, 1976). 3T3-L1 adipocytes, differentiated from 3T3-L1 preadipocytes, offer a model system to study responses to insulin. Since the development of 3T3-L1 adipocytes, many insulin-dependent mechanisms have been examined.

The insulin-responsive glucose transporter, GLUT4, has been shown to translocate from an intracellular compartment to the cell surface upon insulin stimulation (Calderhead et al., 1990; Piper et al., 1991; Blok et al., 1988). Recent studies have shown that GLUT4 containing vesicles are biochemically distinct from other vesicular compartments in that they are enriched in VAMP2 (vesicle-associated membrane protein), a v-SNARE protein, but not VAMP3, which is localized to the constitutively recycling endosomes (Martin et al., 1998; Sevilla et al., 1997). Complementary receptors called SNAREs (soluble N-ethylmaleimide-senitive fusion protein attachment protein receptors), v-SNARE (vesicle-SNARE) and t-SNARE (target-membrane SNARE), are involved in vesicle membrane to target membrane recognition and fusion of membranes. VAMP2, which is enriched in vesicles containing GLUT4, has been shown to interact with syntaxin 4, the major plasma membrane t-SNARE in adipocytes (Volchuk et al., 1996). It was not until mid 1999, that Min et al. (1999) showed that insulin stimulates the dissociation of a novel syntaxin 4-binding protein, isolated from a 3T3-L1 adipocyte library. This led to the increase in interaction between syntaxin 4 (t-SNARE) and its partner VAMP2 (v-SNARE). This docking event initiates membrane fusion, which occurs by yet an unknown mechanism.

Insulin also affects glycogen metabolism. It is known that insulin stimulation leads to the dephosphorylation of glycogen synthase, glycogen phosphorylase, and phosphorylase kinase, which results in activation of glycogen synthase and inactivation of phosphorylase and phosphorylase kinase. This leads to a net increase in the rate of glycogen synthesis. Insulin leads to these changes by activating type I serine/threonine phosphatase, PP1C, which leads to the dephosphorylation of these rate-limiting enzymes. Recently, Brady et al. (1997) have isolated a novel protein called PTG, an abbreviation for Protein Targeting to Glycogen, from the 3T3-L1 adipocyte library. PTG, which binds to glycogen, recruits PP1C to glycogen. Thus, it has been proposed that PTG acts as a scaffolding protein which recruits PP1C and its substrates (glycogen synthase, phosphorylase, and phosphorylase kinase) to the glycogen molecule.

Although much effort has been placed on understanding the signaling events responsible for the changes in cellular metabolism in response to insulin, the intracellular proteins responsible for the activation of insulin-induced metabolic changes remain controversial. As shown in Figure 1-1, insulin has been shown to activate both PI3 (phosphatidylinositol 3) kinase and MAPK (mitogen-activated protein kinase) [White and Kahn, 1994]. However, Wiese et al. (1995) have shown that the activation of MAPK or PI3 kinase by insulin is not sufficient for the insulin-stimulated uptake of glucose, lipogenesis, and glycogen synthesis in 3T3-L1 adipocytes. Whichever pathway is responsible for the insulin-induced metabolic changes, it is certain that insulin must bind to its receptor (IR) to initiate the signaling cascades that lead to the metabolic changes. Thus, IR plays a key role in mediating the effects of insulin.

In order for the cells to mediate the pleiotrophic effects of insulin, circulating insulin must first bind to its receptor on the surface of cells. It is the processing (i.e., protein glycosylation, protein folding, and targeting) of IR in 3T3-L1 adipocytes that will be the

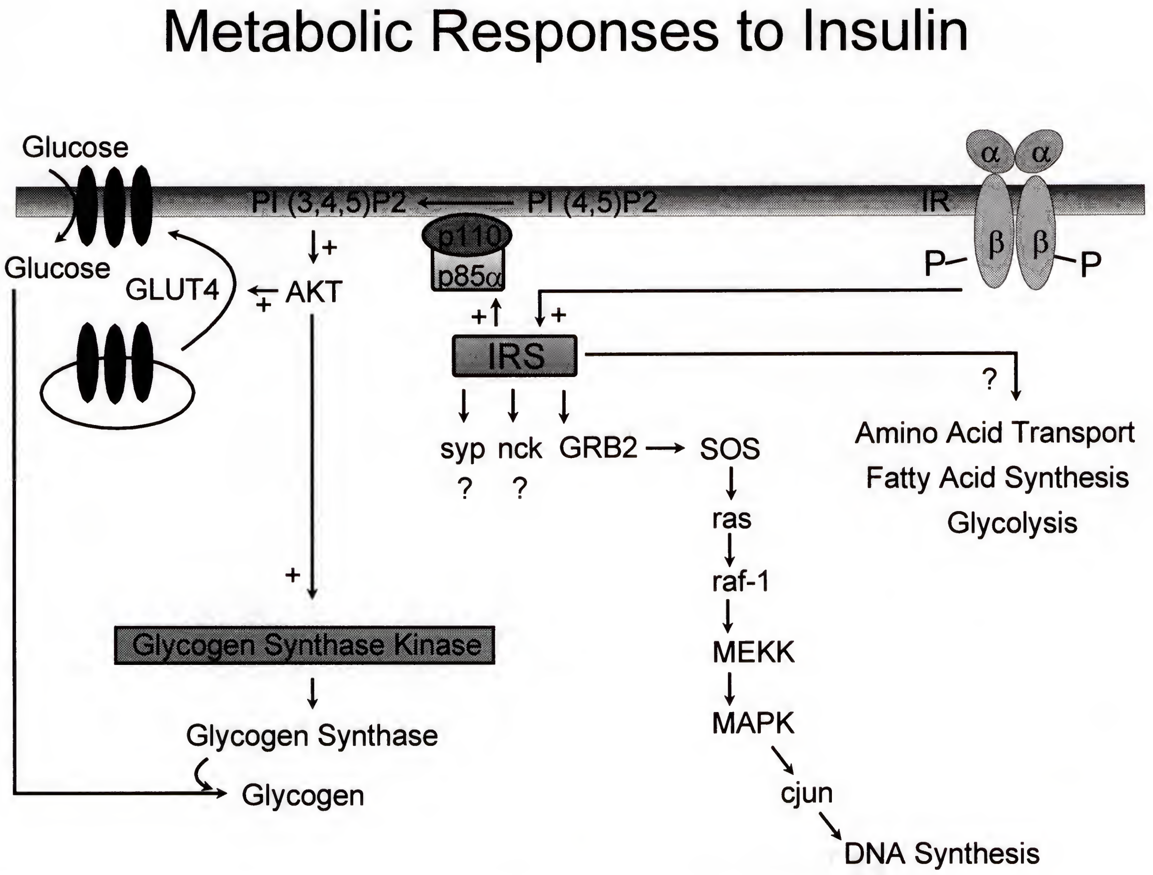

Figure 1-1 - Insulin Receptor Plays a Key Role in Mediating Insulin Action This model was modified from White and Kahn, 1994. See text for explanation.

focus of this research. Since 3T3-L1 adipocytes express large amounts of the insulin receptor, approximately 200,000 receptors per cell (Reed et al., 1981; White and Kahn, 1994), 3T3-L1 adipocytes provide a good model system to examine insulin receptor processing.

Insulin Receptor

The insulin receptor (IR) has been extensively used as a model to examine the effect of glycosylation on processing and function. The IR is a membrane-bound glycoprotein belonging to the tyrosine kinase receptor family. Cell surface receptors bind extracellular insulin which leads to autophosphorylation and activation of its tyrosine kinase, resulting in downstream activation of glucose uptake as well as glycogen, fatty acid, and DNA synthesis (White and Kahn, 1994).

The mature receptor is a heterotetramer composed of two α-subunits (135kDa) and two β-subunits (95kDa). However, as shown in Figure 1-2, the receptor is initially synthesized as a single polypeptide (1,372 amino acids for mouse) containing the domains for both the α-subunit (721 amino acids) and β-subunit (619 amino acids) [Knutson, 1991]. In the lumen of the endoplasmic reticulum (ER), the

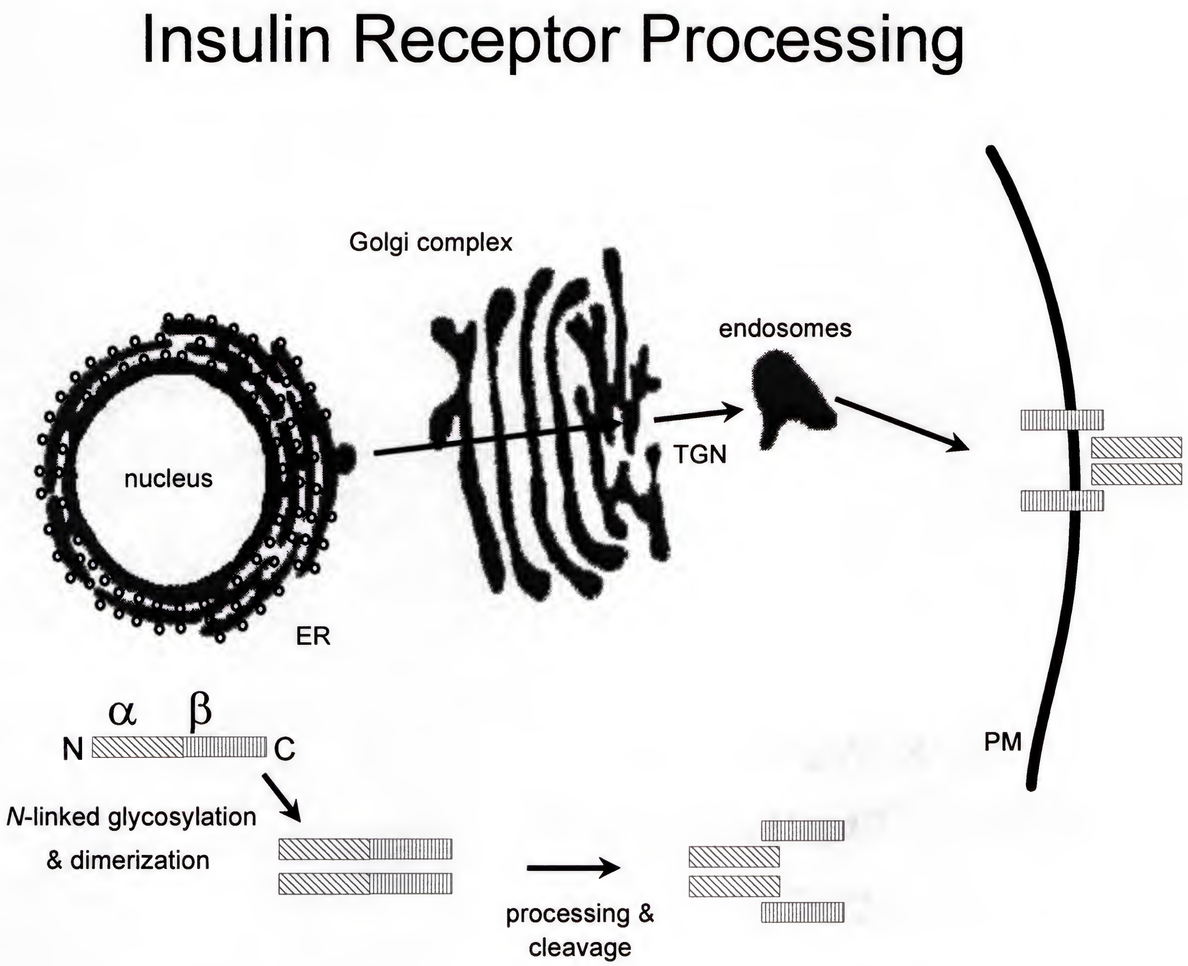

Figure 1-2 - A Model of Insulin Receptor Processing See text for explanation. Insulin receptor is represented as α and β. N and C represent amino-terminus and carboxy-terminus, respectively.

ER signal peptide (first 27 amino acids) at the amino-terminus of the proreceptor is cleaved off. Then, the proreceptor is co-translationally *N*-glycosylated on both the α- and β-subunits as shown by the incorporation of metabolically labeled monosaccharides, sensitivity to glycosidase digestions, and binding to specific lectins (Herzberg et al., 1985; Hedo et al., 1983). Oligosaccharide processing begins in the ER and continues through the Golgi.

In addition to the oligosaccharide processing, the proreceptor undergoes dimerization and acquisition of function with respect to ability to bind insulin (Ronnett et al., 1984). During processing in the ER, the proreceptor undergoes dimerization and acquisition of function within 1.5h. In the trans Golgi network (TGN), the proreceptor is proteolytically cleaved by furin at a consensus sequence of basic amino acid residues (RKRR), yielding a heterotetramer composed of two α- and two β-subunits (Zhou et al., 1999). Furin, a serine endoprotease belonging to the family of subtilisin-like proprotein convertases, is reponsible for this cleavage *in vivo* (Robertson et al., 1993) and *in vitro* (Bravo et al., 1994). An additional 1.5h is required for the insertion of the active receptor into the plasma membrane. Ultimately, the

N-linked oligosaccharide structures are composed of both high mannose and complex carbohydrates, the latter of which contains galactose, fucose, *N*-acetylglucosamine, and sialic acid. Elucidation of the primary sequence of the IR has identified 14 potential *N*-linked glycosylation sites on the α-subunit and 4 potential *N*-linked glycosylation sites on the β-subunit (Ebina et al., 1985; Ullrich et al., 1985)

Table 1-1 - *N*-linked Glycosylation Sites on the IR

IR subunit	Position (Asn-X-Thr/Ser)	*N*-linked glycosylation	Reference
α^1	Asn^{43}	yes	Caro et al.,1994
α^2	Asn^{52}	yes	Caro et al.,1994
α^3	Asn^{105}	yes	Caro et al.,1994
α^4	Asn^{138}	yes	Caro et al.,1994
α^5	Asn^{242}	potential	
α^6	Asn^{282}	potential	
α^7	Asn^{322}	potential	
α^8	Asn^{364}	potential	
α^9	Asn^{424}	yes	Bastian et al.,1993
α^{10}	Asn^{445}	yes	Bastian et al.,1993
α^{11}	Asn^{541}	potential	
α^{12}	Asn^{633} (Asn^{635})	potential	
α^{13}	Asn^{651} (Asn^{653})	potential	
α^{14}	Asn^{698} (Asn^{700})	potential	
β^1	Asn^{769} (Asn^{759})	yes	Leconte et al.,1994
β^2	Asn^{782} (Asn^{772})	yes	Leconte et al.,1994
β^3	Asn^{920} (Asn^{910})	yes	Leconte et al.,1994
β^4	Asn^{933} (Asn^{923})	yes	Leconte et al.,1994

There are 14 *N*-linked glycosylation sites (represented as Asn-X-Thr/Ser, where X is any amino acid except proline) on the α-subunit and 4 sites on the β-subunit. The position of the asparagine residue reflects the insulin receptor (IR) amino acid sequence from both human and mouse (in parenthesis).

[Table 1-1]. In addition, the β-subunit has also been shown to contain an *O*-linked carbohydrate (Herzberg et al., 1985; Collier and Gorden, 1991; Leconte et al., 1994). Once mature, the IR is targeted to the plasma membrane, where it can bind to circulating insulin.

Initial studies examining the effect of glycosylation on IR processing were performed using tunicamycin treatment which inhibits *N*-linked glycosylation and leads to the accumulation of an aglyco-proreceptor in an intracellular compartment (Ronnett et al., 1981; Reed et al., 1981; Ronnett et al., 1984; Goldstein et al., 1988). The use of castanospermine and 1-deoxynojirimycin (glucosidase inhibitors) also leads to accumulation rather than processing (Arakaki et al., 1987). A direct correlation between aberrant glycosylation and processing/function has recently been addressed using site-directed mutagenesis of individual *N*-linked glycosylation sites. Mutation of the asparagines within the four *N*-linked consensus sequences of the β-subunit has no effect on processing, but inhibits signaling because of defective autophosphorylation and tyrosine kinase activity (Leconte et al., 1992; Weng and Spiro, 1997). Interestingly, only the third and fourth α-linked sites regulate the functional status of the receptor. In the α-subunit, mutation of the first four *N*-linked glycosylation sites (Collier et al., 1993) or mutation of the first or second pair of sites (Caro et al., 1994) leads to accumulation of the proreceptor in the ER. Individual mutations have no effect on processing or function (Caro et al., 1994; Bastian et al., 1993). Thus, it has been proposed that specific *N*-linked oligosaccharide sites (both location and number) in the IR differentially affect processing and gain of function.

Studies conducted using glycosylation inhibitors or site-directed mutagenesis to examine the effect of glycosylation on IR processing reveal the importance of proper glycosylation on IR processing and function (see below). However, none has investigated the reversibility of the altered glycosylation, due to the irreversibility of glycosylation inhibitors and site-directed mutagenesis.

Thus the goal of this research was to use glucose deprivation as a reversible tool to influence insulin receptor processing in a physiological setting.

N-linked Oligosaccharide Processing

Post-translational processing of membrane-bound glycoproteins occurs in the processing compartments of ER and Golgi. During the journey of a protein from the ER to the trans Golgi network (TGN), the newly translated polypeptide must be glycosylated, folded into its native structure, acquire function, and be targeted to its functional compartment. These monumental steps are assisted by various enzymes, such as oligosaccharide transferases and IR molecular chaperones that are localized to specific membrane compartments.

N-linked glycosylation occurs co-translationally inside the ER lumen. Co-translational glycosylation requires two steps: synthesis of a dolichol-linked oligosaccharide core precursor and transfer of this precursor by oligosaccharide transferase to the asparagine residue in the sequence Asn-X-Ser/Thr, where "X" is any amino acid except proline. Synthesis of the *N*-linked oligosaccharide core structure starts on the cytoplasmic side of the ER membrane and finishes in the ER lumen. This involves the stepwise addition of monosaccharide units onto a lipid-linked precursor, dolichol pyrophosphate. Each monosaccharide is transferred from a sugar nucleotide donor to the growing dolichol-PP-oligosaccharide by a unique glycosyl transferase. The most common sugar donors are UDP-N-acetylglucosamine (UDP-GlcNAc), UDP-galactose, UDP-glucose, GDP-fucose, GDP-mannose, and CMP-sialic acid. The first two monosaccharides that are transferred onto dolichol-P are *N*-acetylglucosamine, resulting in dolichol-PP-$GlcNAc_2$. Next, five mannosyl residues are transferred from five GDP-mannose onto the dolichol-PP-$GlcNAc_2$ by five different mannosyl transferases, resulting in dolichol-PP-$GlcNAc_2Man_5$. This structure is "flipped" from the outer face to the lumen face, still attached to dolichol. Then four mannosyl residues are transferred from dolichol-P-mannose onto the growing oligosaccharide chain, resulting in dolichol-PP-$GlcNAc_2Man_9$. Addition of three glucosyl residues result in the final core structure, $GlcNAc_2Man_9Glc_3$, which is co-translationally transferred to asparagine residues contained in the *N*-linked consensus sequence. This oligosaccharide transfer to the *N*-linked sites is not specific for a particular protein, nor is it always transferred to all the potential *N*-linked sites. Gavel and von Heijne (1990) have estimated that approximately 10 to 30% of potential *N*-linked sites are not glycosylated. Thus, there must be some restrictions as to which sites are glycosylated. For example, the *N*-linked sequence must be more than 10 amino acids from the membrane in order to have efficient transfer (Kornfeld and Kornfeld, 1985). *N*-linked sequences close to either the amino or carboxyl terminus are also less efficiently glycosylated (Gavel and von Heijne, 1990). Proline residues immediately following

Asn-X-Ser/Thr actually inhibit glycosylation (Bause, 1983). It is interesting that *O*-linked glycosylation, which occurs on serine or threonine residues, occurs more efficiently if proline occupies positions -1 and +3 relative to the glycosylated residue (Wilson et al., 1991). The most important determinant for the efficiency of *N*-linked glycosylation, however, appears to be the X-position of Asn-X-Ser/Thr. Using site-directed mutagenesis, Shakin-Eshleman et al. (1996) have shown that proline completely blocks glycosylation. They have also shown that large hydrophobic amino acids (i.e., tryptophan) cause inefficient (5%) oligosaccharide transfer. Negatively charged amino acids, aspartic and glutamic acids, were also inefficiently glycosylated, 19% and 24%, respectively. Other amino acids show more efficient glycosylation, ranging from 70% (phenylalanine) to 97% (serine). The structure and enzymatic mechanism of oligosacharyl-transferase are not well characterized, and thus, the mechanism by which individual amino acid influence core glycosylation is uncertain. However, Shakin-Eshleman et al. have hypothesized that large hydrophobic residues (i.e., tryptophan) may produce unfavorable local protein conformation and that positively charged amino acids are favored over negatively charged amino acids because the oligosaccharyltransferase needs to bind to both the Asn-X-Ser/Thr sequence and the negatively charged dolichol-PP-oligosaccharide precursor.

Oligosaccharide processing continues in the ER and finishes in the Golgi apparatus. In the ER lumen, the first glucose residue is removed within 30 seconds by α-glucosidase I (Rudd and Dwek, 1997). The second glucose residue is cleaved by α-glucosidase II within 30 minutes. The final glucose residue is removed more slowly allowing interaction with calnexin or calreticulin, ER molecular chaperones which specifically interact with all oligosaccharide structures containing the monoglucosylated Glcα1-3Man motif. Because calnexin and calreticulin bind to the oligosaccharides rather than to the polypeptide, like GRP78 (glucose-regulated protein), they will be briefly addressed in this section, whereas the role of GRP78 in protein folding will be addressed in the following section.

As mentioned above, all *N*-linked glycoproteins acquire a common core precursor, $GlcNAc_2Man_9Glc_3$, to the nitrogen in the side chain of an asparagine residue. Glycosylation is known to affect protein folding. Imperiali and Rickert (1995) have demonstrated that glycosylation can alter the conformation of oligopeptides to allow them to take up conformations not accessible to unglycosylated peptides. This implies that glycosylation provides a structural nucleation element that can direct a protein towards a particular folding pathway, thus increasing efficiency of the folding process. Complementary to this prediction is that site-directed mutations of certain *N*-linked sites on the insulin proreceptor prevent processing and/or function. There are several other potential roles that protein glycosylation may play. Due to the size and hydrophilicity of the oligosaccharide core structures, they may prevent non-specific aggregation of newly synthesized proteins and prevent hydrophobic areas of a protein that would normally be on the surface of a protein from collapsing inward. They also increase solubility of proteins within the highly concentrated protein environment of the ER lumen. Since all *N*-linked glycoproteins acquire the same oligosaccharide core structure, specific sugar residues are not thought to be required for any of the roles mentioned above.

Understanding of the calnexin and calreticulin-folding pathways have demonstrated that glycosylation plays an important role in protein folding and assembly. Upon glycosylation, *N*-linked glycoproteins undergo the same oligosaccharide trimming independent of the protein to which it is attached. In addition, trimming of sugar residues is followed by the addition of more sugars forming high-mannose, complex, and/or hybrid-type structures in the Golgi network (see below). The exact role of this oligosaccharide trimming is unknown. However, the Glcα1-3Man motif, which results from trimming of the first two glucose residues from the core structure, is known to modulate interactions with the molecular chaperones, calnexin and calreticulin (Rudd and Dwek, 1997).

Calnexin and calreticulin are hypothesized to be ER molecular chaperones which bind transiently to monoglucosylated structures in the ER lumen. Although both are ER localized proteins, calnexin is an integral membrane glycoprotein whereas calreticulin is soluble and retained in the ER through the KDEL motif at the carboxy terminus. The chaperone function of calnexin and calreticulin appears to be very similar. Both bind to the Glcα1-3Man motif. However, because calnexin is better understood, calnexin will be addressed in more detail. The interaction of these chaperones to the Glcα1-3Man motif of a glycoprotein is coupled to protein folding. Protein folding intermediates are usually monoglucosylated and bound transiently to calnexin (Ou et al., 1993). Furthermore, calnexin only recognizes glycoproteins that are incompletely folded. Because this interaction is transient, α-glucosidase II has the opportunity to bind and cleave off the last glucose residue, resulting in a deglucosylated glycoform. If folding is complete, then the glycoprotein proceeds to the Golgi for further oligosaccharide processing. If folding is incomplete, then a glucosyl transferase reglucosylates the $GlcNAc_2Man_9$ structure at the same position (Glcα1-3Man) using UDP-glucose as a donor species (Rudd and Dwek, 1997). This results in rebinding of calnexin to the monoglucosylated glycoprotein. This cycle is repeated until the protein achieves proper folding. Thus, the role of calnexin (or calreticulin) supports a conventional chaperone function of preventing aggregation and/or stabilizing folding or assembly of intermediates. At present, there are no rules to guide our predictions of which glycoproteins will bind calnexin and/or calreticulin. One postulated difference between calnexin and calreticulin binding arises from their structure. The lectin binding domain (proline-rich P-domain) of calnexin is located next to the single transmembrane domain. Therefore, it is hypothesized that calnexin binds to the Glcα1-3Man motif close to the ER membrane, whereas, the soluble calreticulin may bind at sites further from the ER membrane. In some instances, both calnexin and calreticulin will interact with the same glycoprotein, such as transferrin (Wada et al., 1997) and the insulin proreceptor (Bass et al., 1998). Castanospermine, an inhibitor of α-glucosidase which "trims" glucose, causes a prolonged and stable interaction of these chaperones with transferrin and insulin proreceptor. Other examples of ways in which calnexin interacts with its substrate include a sequential action in which GRP78 interacts first with newly synthesized thyroglobulin, followed by interaction with calnexin (Kim and Arvan, 1995).

Oligosaccharide processing continues in the Golgi apparatus. Protein folding as well as assembly of multimeric units occurs during passage from the ER to an ER-Golgi intermediate compartment. Once properly folded and/or assembled, glycoproteins enter the cis Golgi, where they undergo further oligosaccharide trimming and addition of new sugars. The Golgi apparatus, which is composed of several membranous sacs, is classified as cis, medial, and trans Golgi in order of processing. From cis to the trans Golgi, mannose residues are trimmed and new mannose, GlcNAc, galactose, fucose, or sialic acid residues are added to complete the oligosaccharide processing. These different sugar residues are added in a way which gives rise to an enormous heterogeneity among *N*-linked glycoproteins. These proteins are classified into three groups. The high mannose oligosaccharides contain 2 to 9 more mannose residues apart from the remaining oligosaccharide core structure, $GlcNAc_2Man_5$ (Kornfeld and Kornfeld, 1985). Complex oligosaccharides contain variable numbers of GlcNAc, sialic acid, and/or fucose residues linked to the pentasaccharide core structure. Hybrid oligosaccharides contain elements of both high mannose and complex oligosaccharides.

Once glycoproteins have completed maturation, they are sorted in the trans Golgi network and targeted to their appropriate compartments. One example of sorting involves another extensively examined oligosaccharide motif. All glycoproteins destined for the lysosome are tagged with mannose-6-phosphate (Kornfeld, 1992). Thus, phosphorylation of a mannose residue directs targeting to the lysosome. Cell surface membrane proteins and secreted proteins are transported to their proper compartment through a constitutive pathway.

GRP78 and "Quality" Control

The endoplasmic reticulum (ER) is one of the major sites for the folding and assembly of newly synthesized glycoproteins. Studies with a select set of purified proteins suggest that the primary sequence contains sufficient information to give rise to the final, functional conformation of a protein (Anfinsen et al., 1961). However, the refolding of purified proteins *in vitro* is different from *in vivo* folding. Specifically, a nascent polypeptide has an opportunity to initiate folding as soon as it emerges from cytoplasmic ribosomes or as soon as it translocates into the ER lumen. In addition, protein folding must be accomplished in a highly crowded macromolecular environment. One might suggest that these two conditions would interfere with productive protein folding in the cell. Yet, refolding of a protein *in vitro* rarely occurs at the efficiency observed *in vivo*. Therefore, it is predicted that the folding and assembly of peptides *in vivo* often involve molecular chaperones (Gething and Sambrook, 1992; Ellis, 1987; Hendrick and Hartl, 1993).

Molecular chaperones were originally defined as proteins which mediate the correct folding (defined as the acquisition of tertiary structure) and assembly (defined as the acquisition of oligomers) of other proteins. Currently, molecular chaperones are characterized by several properties: (1) ability to recognize and bind unfolded protein; (2) ability to suppress aggregation during protein unfolding and folding; and (3) ability to influence the yield of folding (Lee, 1995; Hartl, 1996). However, molecular chaperones do not contain steric information for specifying proper folding. Rather they increase the yield of protein assembly by suppressing their aggregation and not by increasing the rate of folding reactions. Thus, molecular chaperones are different from enzyme catalysts, such as protein disulfide isomerase (PDI) and peptidyl-prolyl isomerase (PPIase) which accelerate intrinsically slow steps in the folding of some proteins. PDI catalyzes the rearrangement of disulfide bonds while PPIase catalyzes the cis-trans isomerization of peptide bonds preceding proline residues.

Studies focused on the 70 kDa heat-shock protein (Hsp70) family have increased our understanding of the role of molecular chaperones in protein folding. Members of the Hsp70 family interact with their substrates by binding to unfolded regions of a polypeptide. They have two functional domains: a highly conserved amino-terminal adenosine triphosphatase (ATPase) domain which facilitates substrate exchange and a variable carboxyl-terminal peptide-binding domain which binds hydrophobic stretches of amino acid residues. The three-dimensional structures of a 44kDa fragment from the ATPase domain of bovine Hsc70 (heat-shock cognate) and a 27kDa fragment from the peptide-binding domain of *E.coli* DnaK have been determined at 2.2 and 2.0 angstroms, respectively (Flaherty et al., 1990; Zhu et al., 1996). The ATPase fragment has two structural lobes with a deep cleft between them to which ATP binds. The peptide-binding fragment consists of a compact β-sandwich followed by helical elements which appear to stabilize the β-domain. These structural data predict a model in which the two domains communicate to regulate the affinity and duration of polypeptide binding. For example, the affinity of a substrate for the peptide-binding domain is greater when ADP (rather than ATP) is bound within the ATPase domain. Furthermore, the binding of a substrate in the peptide-binding domain stimulates ATP hydrolysis within the ATPase domain (Gething, 1996).

GRP78 (a resident ER protein) exhibits many of the properties which define a molecular chaperone. GRP78 binds many misfolded proteins (see below). It prevents aggregation of denatured lysozyme *in vitro* (Puig and

Gilbert, 1994) and is required to prevent aggregation of carboxypeptidase Y in the ER (Simons et al., 1995). In addition, reduction of GRP78 expression in *Saccharomyces cerevisiae* diminishes the secretion of several proteins including colony-stimulation factor, acid phosphatase, and bovine pancreatic trypsin inhibitor (Robinson et al., 1996). There is no evidence to support a direct role for GRP78 in the *in vitro* refolding of a protein as there is for other Hsp70 homologues (Kang et al., 1990; Skowyra et al., 1990; Schroder et al., 1993).

The glucose-regulated proteins (GRPs), which include GRP78 and GRP94, were first observed as proteins whose synthesis was increased upon transformation of rat and chick embryo fibroblasts with avian sarcoma viruses (Stone et al., 1974; Isaka et al., 1975). However, subsequent studies showed that the increase in synthesis of these proteins was correlated to glucose deprivation rather than infection (Pouyssegur et al., 1977; Shiu et al., 1977). A few years after this discovery, Haas and Wabl independently discovered a protein (immunoglobulin heavy-chain binding protein, BiP) which binds to free immunoglobulin heavy chain, but not to the immunoglobulin heavy chain associated with its light chain (Haas and Wabl, 1983). When the cDNAs of GRP78 and BiP were compared, 100% identity was revealed

(Munro and Pelham, 1986; Hendershot et al., 1988). Intense investigation has led to a better understanding of the functional role of GRPs, especially GRP78 in protein maturation in the ER.

Like other Hsp70 homologues, GRP78 binds ATP with a K_d of 0.2-0.4 μM (Blond-Elguindi et al., 1993; Wei and Hendershot, 1995) and possesses a weak ATPase activity, turnover time of 0.2/min (Flynn et al., 1989). ATP hydrolysis is required for the dissociation of a substrate from GRP78 because the addition of ATP, but not ADP or nonhydrolyzable ATP, can dissociate the substrate complex (Gething and Sambrook, 1992; Flynn et al., 1989; Toledo et al., 1993). However, in recent studies, Wei et al. (1995). have characterized GRP78 mutants that are defective in ATP hydrolysis (T229G), ATP binding (G226D, G227D), and ATP-induced conformation (T37G). All mutants were able to bind to a peptide substrate and both the wild type and ATP hydrolysis mutant were able to release the peptide upon addition of ATP. Thus, Wei et al. concluded that an ATP-induced conformational change is necessary for the dissociation of the complex, but not ATP hydrolysis.

GRP78 is posttranslationally modified by ADP-ribosylation and phosphorylation. Under normal conditions, it has been suggested that approximately 60% of GRP78 exists as inactive modified dimers while 40% of the pool is unmodified and active (Vidal et al., 1996). GRP78 is mono-ADP-ribosylated as shown by the incorporation of [^{3}H]adenosine (Hendershot et al., 1988; Leno and Ledford, 1989; Welch et al. , 1983). Phosphorylation occurs on Thr37 and Thr229 of mouse GRP78 *in vitro* and on an unidentified serine and threonine residue *in vivo*, as revealed by phosphoamino acid analysis (Hendershot et al., 1988; Leno and Ledford, 1990).

The importance of GRP78 in biological function is supported by several lines of evidence. First, deletion of Kar2p (the yeast homologue of GRP78) in *S. cerevisiae* results in loss of cell viability (Vogel et al., 1990). Second, the evolutionary conservation of GRP78 predicts its importance in biological function. Rat GRP78 shows 57% identity with *Drosophila* Hsp70 (Munro and Pelham, 1986), 61% identity with human Hsp70 (Hunt and Morimoto, 1985), and 99.4% identity in amino acid sequence with hamster GRP78 (Ting et al., 1987). Finally, several molecular chaperones have been implicated in human diseases related to defective protein folding. The clinical relevance of molecular chaperones has only been realized in recent years. GRP78 has been implicated in the retention of several type I procollagen mutants that are defective in folding and assembly in osteogenesis imperfecta (Chessler and Byers, 1993). GRP78 has also been implicated in cancer. It is the major protein induced in solid tumors (Little et al., 1994). Interestingly, based on the inducibility of the grp78 promoter, it may be used in gene therapy to allow overexpression of foreign proteins in tumor cells. Other compelling evidence that abnormal protein folding can lead to disease states concerns the ER chaperone, calnexin. The most common cause of cystic fibrosis is the deletion of Phe-508 (F508) from the cystic fibrosis transmembrane conductance regulator, CFTR (Yang et al., 1993). In epithelial cells, CFTR is transported to the apical membrane where it forms a chloride channel. F508 CFTR has a folding defect in a portion of the amino-terminal nucleotide-binding domain. It is stably bound to calnexin and retained in the ER where it is degraded in a pre-Golgi nonlysosomal compartment. Because the folding defect only affects its targeting to the plasma membrane and not its function, manipulation of calnexin expression may allow a bypass of this retention system. Other human diseases associated with defective protein folding include Marfan syndrome, amyotrophic lateral sclerosis, scurvy, Maple syrup urine disease, scrapie, Alzheimer’s disease, familial amyloidosis, familial hypercholesterolemia, α_1-antitrypsin deficiency, and Tay-Sach's disease (Little et al., 1994; Macario, 1995; Thomas et al., 1995; Choudhury et al., 1997). This list will continue to grow as more diseases are characterized. The protein folding diseases emphasize the importance of molecular chaperones and the stringent conformation-based "quality control" in the secretory pathway to prevent the transport of misfolded or partially assembled proteins beyond the ER.

Besides its role in protein folding, GRP78 has also been implicated in the translocation of newly synthesized proteins and retention and retrieval of misfolded proteins. GRP78, as well as GRP94, possesses an ER retention motif, KDEL (lys-asp-glu-leu), at the C-terminus which allows recycling back to ER via KDEL sequence interacting receptors (Munro and Pelham, 1987; Hammond and Helenius, 1994). GRP78 is also required for translocation of proteins into the ER in *S. cerevisiae*. A KAR2 gene mutation blocks translocation of secretory proteins in yeast (Vogel et al., 1990; Sanders et al., 1992). Kar2p, the yeast homologue of GRP78, binds to Sec63p, an ER membrane protein associated with the translocation complex (Brodsky and Schekman, 1993; Scidmore et al., 1993). Furthermore, Kar2p can be crosslinked to partially translocated substrates (Brodsky and Schekman, 1993).

Other Hsp70 homologues in the cytoplasm, mitochondria, and chloroplast also bind to nascent peptides as they emerge from ribosomes or membranes and assist in protein translocation across membranes, suggesting a common function for members of the Hsp70 family (Wild et al., 1992; Tsugeki and Nishimura, 1993; Stuart et al., 1994).

Under normal growth conditions, GRP78 binds transiently to nascent peptides and assists in protein folding and assembly. Included among these are membrane proteins, like the acetylcholine receptor (Blount and Merlie, 1991), T-cell receptor (Suzuki et al., 1991), EGF receptor (Fiege et al., 1988), transferrin receptor (Williams and Enns, 1991), and insulin receptor (Accili et al., 1996), and secreted proteins such as immunoglobulins (Haas and Wabl, 1983). In contrast, GRP78 binds stably to misfolded or incompletely assembled multimeric proteins and prevents their exit from the ER. GRP78 is constitutively expressed under normal conditions, but can be transcriptionally induced under a variety of stress conditions (such as glucose or amino acid deprivation, 2-deoxyglucose, tunicamycin treatment, sulfhydryl-reducing agents, and low extracellular pH) which affect protein folding. In addition, GRP78 is also induced by agents such as Ca^{2+} ionophores and thapsigarin which disturb the integrity of the ER, and thus, its function in providing an enviroment for protein folding (Lee, 1987). Conditions which denature proteins induce both GRPs and Hsps. However, unlike other Hsp70s, the GRPs (GRP78 and GRP94) are not significantly induced by heat-shock, but are specifically induced by glucose deprivation (Gething and Sambrook, 1992). One of the effects of glucose deprivation is aberrant glycosylation of proteins due to the lack of glucose as substrate for the synthesis of oligosaccharide chains. There are several pieces of evidence to support the notion that aberrant glycosylation induces GRP78. 3T3 fibroblast mutants (AD6) which are defective in glycoprotein synthesis show an elevated level of GRP78 which can be reduced to normal levels with the addition of *N*-acetylglucosamine (Pouyssegur et al., 1977). Chang et al. (1987) demonstrated an inverse relationship between the rate of glycosylation and steady-state level of GRP78 transcripts. More importantly, drugs that interfere with oligosaccharide processing in the ER induce GRP78. Such drugs include castanospermine which inhibits ER resident glucosidase I and II, 1-deoxynojirimycin which inhibits ER resident glucosidase I and II, and tunicamycin which inhibits *N*-linked glycosylation. However, drugs that interfere with oligosaccharide processing in the Golgi (i.e., swainsonine which inhibits Golgi mannosidase II and 1-deoxymannojirimycin which inhibits Golgi mannosidase IA/B) do not induce GRP78 (Kozutsumi et al., 1988).

GRP78 is also involved in the "quality control" of proteins which move through the secretory pathway. A "quality control" system in the ER to Golgi transit ensures that misfolded or unassembled oligomers do not proceed past the cis Golgi. "Quality control" was coined by Hammond and Helenius in 1994 to refer to the retrieval of a misfolded glycoprotein from the cis Golgi back to the ER where it is retained (Hammond and Helenius, 1994). In addition, it was observed that GRP78 remained bound to the misfolded protein and accompanied it from the ER to cis Golgi and back to the ER. Retention of misfolded proteins appears to be a general process as other ER chaperones such as calnexin retains the most common mutant form CFTR in the ER, as mentioned previously (Yang et al., 1993). Furthermore, misfolded proteins that are retained in the ER are degraded in a pre-Golgi nonlysosomal compartment which has been termed "ER degradation" (Klausner and Sitia, 1990; Kopito, 1997).

A model for the interaction of GRP78 with newly synthesized proteins in the ER is represented in Figure 1-3. GRP78 binds to nascent peptide as it translocates into the ER lumen via its interaction with Sec63p, which is an essential component of the translocation complex. The binding of a newly synthesized peptide converts the modified dimer (Blond-Elguindi et al., 1993; Carlsson and Lazarides, 1983), as represented by an asterisk to active monomers to which ADP is bound (Flynn et al., 1989; Brot et al., 1994). In addition, the binding of the peptide to the C-terminal peptide-binding domain induces a conformational change in the N-terminal ATPase domain such that it stimulates the exchange of ADP for ATP. The binding of ATP induces a conformational change, releasing the substrate from GRP78. Then ATP is hydrolyzed, returning GRP78 to an ADP-bound form that is capable of binding to another or same substrate or undergo phosphorylation and ADP-ribosylation which would then trigger dimerization into the inactive dimeric form. However, a newly synthesized protein may fail to fold properly even in the presence of GRP78, for example, due to aberrant glycosylation (Gibson et al., 1979; Gallagher et al., 1988; Machamer and Rose, 1988; Ng et al., 1990; Melnick et al., 1992). Under these conditions GRP78 will bind stably to the substrate and retain it in the ER until the substrate is released and degraded in a pre-Golgi nonlysosomal compartment.

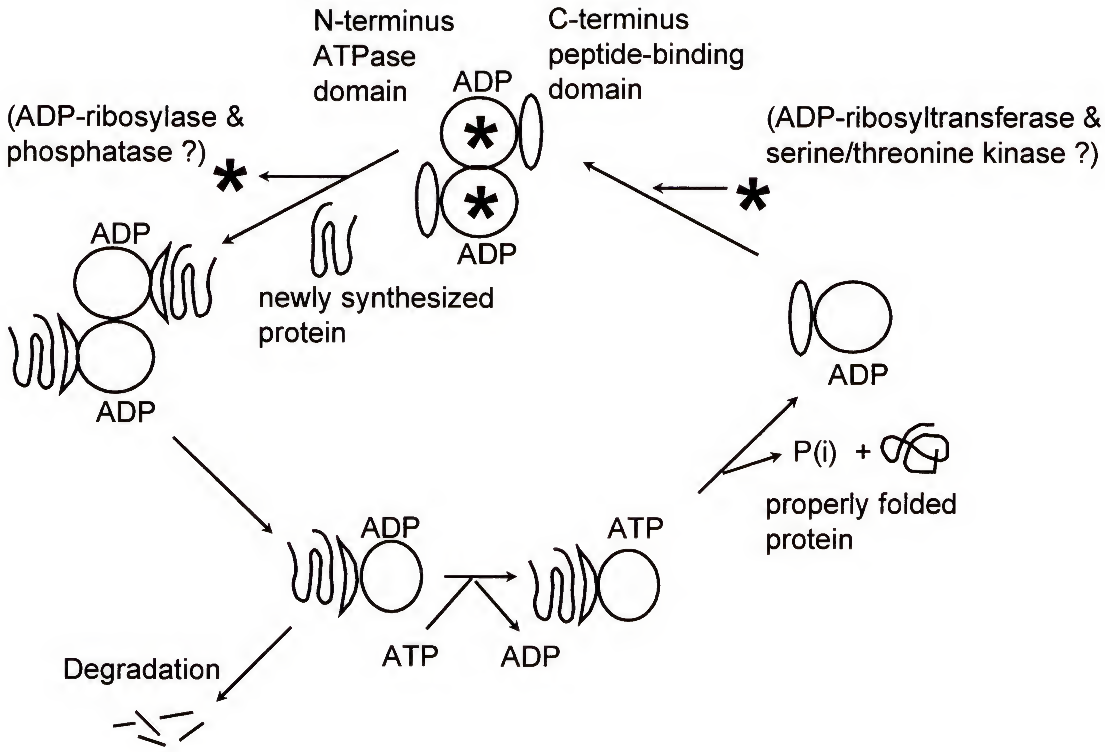

Figure 1-3 - A Model of GRP78 Interacting with Newly Synthesized Proteins This model is modified from Blond-Elguindi et al. (1993). See text for explanation.

As a result of greater understanding of the machinery involved in "quality" control of protein processing in the ER, the mechanism of protein folding and its influence by glycosylation has become more apparent. The goal of this research is to understand further the processing pathway using glucose deprivation as a reversible tool to alter normal processing of the insulin proreceptor.

CHAPTER 2
MATERIALS AND METHODS

Materials

Dulbecco's modified Eagle's medium (DMEM) and glutamine, glucose-free DMEM were purchased from Life Technologies, Inc (Gaithersburg, MD). Calf serum (lot#S11450) was purchased from Atlanta Biologicals (Norcross, GA). Fetal bovine serum (lot#1020-90) was purchased from Intergen (Purchase, NY). *N*-glycosidase F and endoglycosidase H were purchased from New England Biolabs (Beverly, MA). Promix containing [^{35}S]methionine and cysteine was purchased from Amersham (Piscataway, NJ). Enhanced chemiluminescence (ECL) detection system was also purchased from Amersham (RPN 2105). The affinity-purified rabbit polyclonal antibody against a peptide (CGRVLTLPRSNPS; each letter represents an amino acid) corresponding to the last 12 amino acids of the IRβ-subunit(SC-711) was purchased from Santa Cruz Biotechnology, Inc. (Santa Cruz, CA). Rabbit polyclonal antibody against this same peptide that was synthesized by the Protein Core Facility at University of Florida was also generated in rabbits (Cocalico). For immunoblot analysis of GRP78, we generated a rabbit polyclonal antibody against a peptide corresponding to the first twelve amino acids from the N-terminus. For immunoprecipitation of GRP78, we purchased a polyclonal antibody generated against the C-terminus of GRP78 (PA1-014) from Affinity BioReagents (Golden, CO).

Methods

Cell Culture

3T3-L1 fibroblasts were grown and differentiated in 100mm plates according to the procedure of Frost and Lane (1985). Adipocytes derived from fibroblasts that were passed eight times or less were used in all the experiments. Briefly, fibroblasts were cultured in DMEM containing 10% calf serum, refeeding every other day until confluence. Two days post confluence, the fibroblasts were induced to differentiate into adipocytes by incubation in DMEM containing 10% fetal bovine serum (FBS), 1μg/mL insulin, 0.5mM methylisobutylxanthine, and 0.25mM dexamethasone. Two days later, medium was replaced with DMEM containing 10% FBS and insulin. Two days later, medium was replaced with DMEM containing 10% FBS only and every two days hence. Twenty-four hours prior to the start of any protocol, 3T3-L1 adipocytes were provided with fresh DMEM containing 10% FBS (complete medium). This brings cells to a common starting point and provides the basis for reproducible data. Cells were then either fed with complete medium (containing 25mM glucose) or incubated in glucose-free DMEM containing 10% dialyzed FBS (glucose-free medium) for the times indicated.

Antibody Production

A rabbit polyclonal antiserum against a peptide corresponding to the carboxyl terminus of the IR β-subunit (GRVLTLPRSNPS) of mouse origin was generated for the detection of the insulin receptor. Our purpose for generating antibodies against IR was to replace the high cost and shipping delays imposed by the company which supplies the IRβ antibody (Santa Cruz Biotech). The same carboxy terminus sequence was used to generate our polyclonal antiserum as that used by Santa Cruz.

Antibodies generated against synthetic peptides have several advantages over antibodies generated against native proteins (Harlow and Lane, 1998). First, anti-peptide antibodies can be generated without knowing the entire sequence of the protein. While the complete sequence of the mouse insulin receptor is known, tedious purification of the insulin receptor was avoided. Second, peptides can be easily synthesized and purified. Finally, antibodies can be generated against peptides that are specific for a sequence or conformation of interest. However, there is clearly one major disadvantage in choosing a peptide over a native protein in generating antibodies. Antibodies generated against a peptide may not recognize the native protein of interest. Thus, the anti-peptide antibody may bind to denatured proteins as in Western analysis, but may not bind to the native or semi-native protein by immunoprecipitation or immunofluorescence. To avoid this problem, it is imperative to choose a peptide sequence in a region of the protein that is predicted to lie on the surface of the native protein. Several investigators have shown that the carboxyl termini of proteins are often exposed (Harlow and Lane, 1988). Thus we selected a peptide sequence (GRVLTLPRSNPS) which corresponds to the last twelve amino acid residues of the IR (1361 - 1372). Furthermore, the presence of prolines are also predictors of surface exposure. Note that the IR peptide has two prolines.

The IR peptide was synthesized by the Protein Chemistry Core facility group at the University of Florida and purified by HPLC (high-performance liquid chromatography). A cysteine residue was attached to the *N*-terminus of the peptide to facilitate covalent coupling to an immune carrier and affinity matrix. Small peptides are poor immunogens and, therefore, are coupled to larger proteins, termed immune carriers, in order to ensure immunogenicity (Harlow and Lane, 1988). A good antigen must be able to bind to the B-cell cell-surface antibody which then presents the antigen to the MHC II T-cell receptor. The antigen/MHC II T-cell receptor binding site imploses a minimum size limitation on the antigen (must be larger than 3-5kDa). Therefore, an immune carrier such as Keyhole limpet hemocyanin (KLH), ovalbumin, or BSA is coupled to small peptides to elicit an immune response.

IRβ-peptide was conjugated to KLH using a cross-linking reagent, sulfo-m-maleimidobenzoyl-N-hydroxysuccinimide ester (sulfo-MBS). Sulfo-MBS links via the free sulfhydryl cysteine residue. Sixty mg of KLH were dissolved in 10mL of 10mM KH_2PO_4, pH7.3, and placed in dialysis tubing with a molecular weight cut off of 12 - 14kDa. KLH was dialyzed against 500mL of the same buffer for 48h at 4°C with two changes of buffer. The dialysate was concentrated to approximately 4mL by completely covering the dialysis bag with Aquacide and then wrapping it in aluminum foil for 30min at room temperature. The concentrated dialysate was divided into microcentrifuge tubes. Protein aggregates were removed by centrifugation at 12,000 x g for 10min in a microcentrifuge. The concentration of KLH in the supernatant was determined by measuring the absorbance at 280nm and multiplying by the milligram extinction coefficient for KLH (1.6). A volume equivalent to 6mg of KLH in 10mM KH_2PO_4, pH7.3, was reacted with 0.6mg of sulfo-MBS for 45min at room temperature. The KLH-MBS conjugate was separated from free sulfo-MBS by passing the reaction mixture over a 10mL Sephadex G-100 column, pre-equilibrated in 50mM KH_2PO_4, pH6.0. The KLH-MBS conjugate was eluted with the equilibration buffer in the flow-through volume, whereas the free sulfo-MBS was retarded in the column. Twenty-four fractions (500μL each) were collected and absorbance measured at 280nm. The fractions from the first peak containing the KLH-MBS conjugate were pooled (total volume of 1.5mL) and reacted with 6mg of IRβ-peptide dissolved in 500μL of 50mM KH_2PO_4, pH6.0. The pH of the reaction mixture was adjusted to pH7.4 with 0.1N NaOH in order to maximize solubilization. The reaction mixture was incubated at room temperature for 3h with end-over-end rotation before transferring to the cold room (4°C) for an overnight incubation with end-over-end rotation. The KLH-peptide conjugate was shipped to Cocalico Biological Inc. for the generation of rabbit polyclonal antiserum to this conjugate.

The IRβ prebleed and the first bleed were tested on a dot blot. One μL of various amounts (0.001, 0.01, 0.1, and 1.0μg) of the IRβ peptide to which the antibody was raised was spotted onto a strip of nitrocellulose membrane. The membrane was allowed to air dry for 30min before applying either the prebleed antibody or the test bleed antibody (1:1000 dilution in TBS-T containing 5% milk). Immunoblot analysis was performed as described in the Immunoblot analysis section below. Results are shown in Figure 2-1. The first test bleed was able to detect 0.001μg of the IRβ peptide with a 1min exposure time.

Peptide Purification of Anti-IRβ Antibody

The antiserum generated against the IRβ peptide recognized the normal and alternative proreceptor as well as the β-unit by an immunoblot analysis (data not shown). However, it also detected several other nonspecific bands. Therefore, the IRβ antibody was purified from total IgG in the serum using a method described by Dankert et al.(1985). The first step in this process was to prepare an IgG

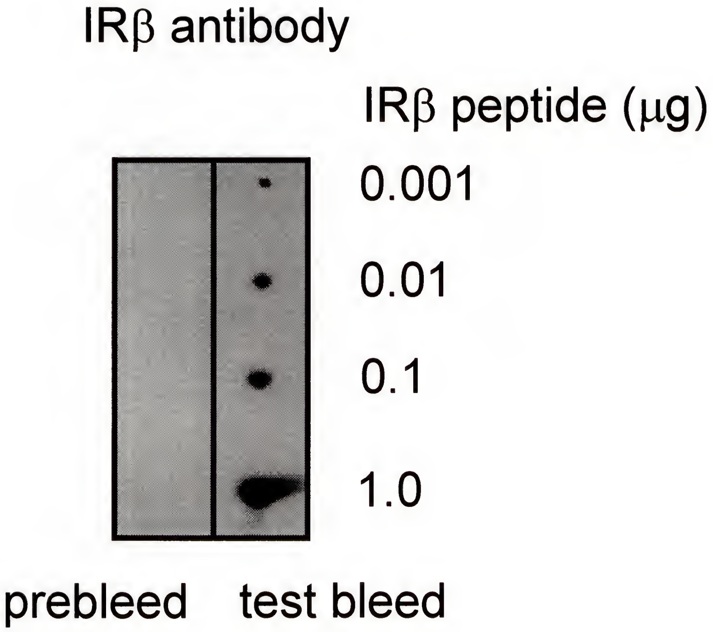

Figure 2-1 - Dot Blot Analysis of IRβ Prebleed and Test Bleed Various amounts (0.001, 0.01, 0.1, and 1.0μg) of the IRβ peptide were spotted onto two strips of nitrocellulose membranes. Immunoblot analysis was performed using 1:1000 dilution of either the prebleed or test bleed.

fraction from immunoreactive serum. In this method, the IRβ serum, treated with caprylic acid, is passed through a column that is coupled to the IRβ peptide using a SulfoLink Kit (Pierce), which couples peptides to the gel column through sulfhydryl groups. In a glass container, 6ml of the IRβ serum were adjusted to a pH of 5.0 with 3.0M acetic acid (approximately, one drop/mL of serum). One part caprylic acid was slowly added to twenty parts serum which were stirred vigorously for 30 min. at room temperature. The sample was transferred to a glass Corex tube and the precipitate collected by centrifugation for 30 min. at 20,000rpm at 4°C using an SS34 Sorvall rotor. The clear brown colored supernatant was transferred to a glass beaker and its volume measured. An equal volume of saturated ammonium sulfate was added to the supernatant in the glass beaker and stirred for 2h at room temperature. The solution was subjected to centrifugation for 30min at 20,000rpm at 4°C. The resulting tan-colored pellet was resuspended in 2mL of phosphate buffered saline solution, PBS (120mM NaCl, 2.7mM KCl, and 5mM Na_2HPO_4, and 5mM NaH_2PO_4, pH 7.4) containing 0.1% sodium azide. The solution was placed into dialysis tubing (molecular weight cut off of

13,000Da) and dialyzed against 250mL of PBS containing 0.1% sodium azide for 2 days at 4°C with two changes of buffer.

The IRβ peptide was coupled to a SulfoLink column using the SulfoLink Coupling kit by Pierce. The 2mL SulfoLink Coupling Gel column was warmed to room temperature. The column caps were removed and the storage buffer was released. The column was then equilibrated with 12mL of SulfoLink Coupling Buffer. The bottom cap was replaced on the column. The IRβ peptide (2mg) was dissolved in 2-3mL of SulfoLink Coupling Buffer. The absorbance at 280 was measured before adding the peptide to the column. The top cap was replaced and the column was mixed on a rotator at room temperature for 15min. The column was clamped upright and the matrix allowed to settle at room temperature for 30min. The caps were removed in order to drain the buffer into a 15mL plastic tube. The absorbance of the drained buffer was measured at 280nm. The column was washed twice with 3mL of SulfoLink Coupling Buffer. The coupling efficiency was determined by multiplying the ratio of A_{280} of the drain buffer divided by the A_{280} of the starting peptide solution times 100%. The bottom cap was replaced and nonspecific binding sites on the peptide column were blocked with the addition of 2mL of 0.05M L-cysteine-HCl (15.8mg in 2mL of SulfoLink Coupling Buffer). The top cap was replaced and the column was mixed for 15min at room temperature. Then the column was fixed in the upright position at room temperature for 30min. The caps were removed to drain the column. The column was washed four times with 4mL of SulfoLink Wash Buffer and three times with 4mL of PBS containing 0.05% sodium azide. The column was capped and stored at $4^{O}C$.

Once the peptide affinity column was ready for use, the IgG containing solution was applied to the column. The affinity column was brought to room temperature. The caps were removed to drain the storage buffer. The column was equilibrated by washing twice with 3mL of PBS. The bottom cap was replaced and 2-3mL of the IgG solution were added to the column. The top cap was replaced and the column was rotated for 3h at room temperature. The caps were removed to release the solution from the column. The column was washed four times with 4mL of PBS. To elute the bound IgG, the column was sequentially washed four times with 4mL of 0.1M of glycine (pH 3.0). One mL fractions were collected into glass tubes containing 100μL of 1M Tris-base (to neutralize the acidic pH). The absorbance was measured at 280nm for each fraction. The extinction coefficient of IgG at A_{280} is 0.014 (assuming that there are 10.15mg IgG/mL serum). The appropriate fractions were pooled (fractions

3-5) and the absorbance remeasured. To regenerate the column, it was washed four times with 4mL of PBS and then stored in 2mL of PBS containing 0.05% sodium azide at 4°C.

The affinity purified IRβ antibody was tested on immunoprecipitation of radiolabeled total membrane proteins (for procedures, see below). Ten μg of this affinity purified IRβ antibody were used to immunoprecipitate IR from glucose-fed or glucose-deprived cells (Figure 2-2).

Total Membrane Isolation

The insulin receptor is an integral membrane protein that is processed from the endoplasmic reticulum to the Golgi complex and then to the plasma membrane, where it binds to extracellular insulin. When the total pool of insulin receptor (i.e., proreceptor and mature receptor) is to be examined, it is beneficial to separate a total membrane fraction from the cytosolic and nuclear fractions. This procedure reduces non-specific interactions that can occur in procedures involving protein-protein interactions, such as immunoblot analysis and immunoprecipitation. As well, it provides a means of concentrating the IR.

Plates containing 3T3-L1 adipocytes (~12×10^6 cells/10cm plate) were incubated in complete or glucose-free medium

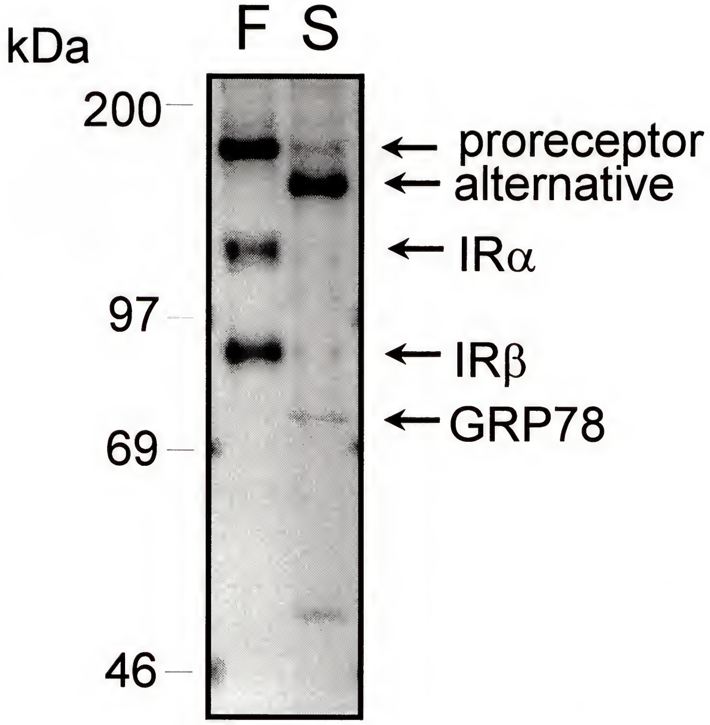

Figure 2-2 - Immunoprecipitation of IR Using Affinity Purified IRβ Antibody Glucose-fed or glucose-deprived cells were radiolabeled for 3h. IR was immunoprecipitated from total membrane proteins using 10μg of the affinity purified IRβ antibody. Immunoprecipitates were resolved by 7.5% SDS-PAGE, followed by autoradiography.

for the indicated times, typically 24h. The culture medium was aspirated and the cell monolayer was rinsed four times with 4mL Krebs-Ringer phosphate (KRP) buffer (128mM NaCl, 4.7mM KCl, 1.25mM $MgSO_4$, 1.25mM $CaCl_2$, 5.0mM Na_2HPO_4, and 5.0mM NaH_2PO_4, pH7.4) at 37°C. Cells were collected in 4mL Tris/EDTA/Sucrose (TES) buffer (20mM Tris, 1mM EDTA, and 255mM sucrose, pH 7.4) containing 1mM phenylmethylsulfonyl-fluoride (TES-P) on ice and homogenized in a 10mL Potter-Elvejhem homogenizing flask with 20 strokes using a motor-driven teflon pestle. The cell homogenate was transferred into a 15mL polypropylene tube. Unbroken cells and nuclei were removed by centrifugation at 1,300 x g for 5min in a clinical centrifuge at room temperature. The supernatant was transferred to a polycarbonate tube or tubes and total membranes were collected by centrifugation at 212,000 x g (55K spin in Ti70 rotor) for 1h at 4°C. The supernatant containing the cytosolic fraction was discarded while the pellet was resuspended in 300μL TES-P buffer. Twenty five μL of each sample were set aside for protein concentration determination. Samples were stored at -20°C until all samples were collected. It is important to point out that towards the latter part of my research, the low spin (1,300 x g for 5min in a clinical centrifuge) was omitted due to the loss of some IR in this discarded pellet.

Subcellular Fractionation

To examine the subcellular localization of IR and GRP78, plasma membrane (PM), high density membranes (HDM), and low density membranes (LDM) were isolated from cell homogenates (H) using a technique described by Fisher and Frost (1996) [Figure 2-3]. This technique provides a reproducible method for fractionating 3T3-L1 adipocytes. The general procedure follows that of Weber et al. (1988) which used a combination of differential and equilibrium centrifugation for isolating membranes from rat adipocytes. Fisher and Frost applied the use of a steel block homogenizer, originally designed by Balch and Rothman (1985), to provide reproducible sheering. This homogenizer is composed of a steel block with a cylindrical chamber of 0.5 inches in which a tungsten ball of diameter 0.4975 inches slides to provide a fixed clearance of 0.0025 inches. The plasma membrane of cells is fractured as the cells pass over the bearing under pressure. Specifically, five 10cm plates, representing a total of 60 million 3T3-L1 adipocytes, were used for each metabolic condition (as described under cell culture). Cells were washed three

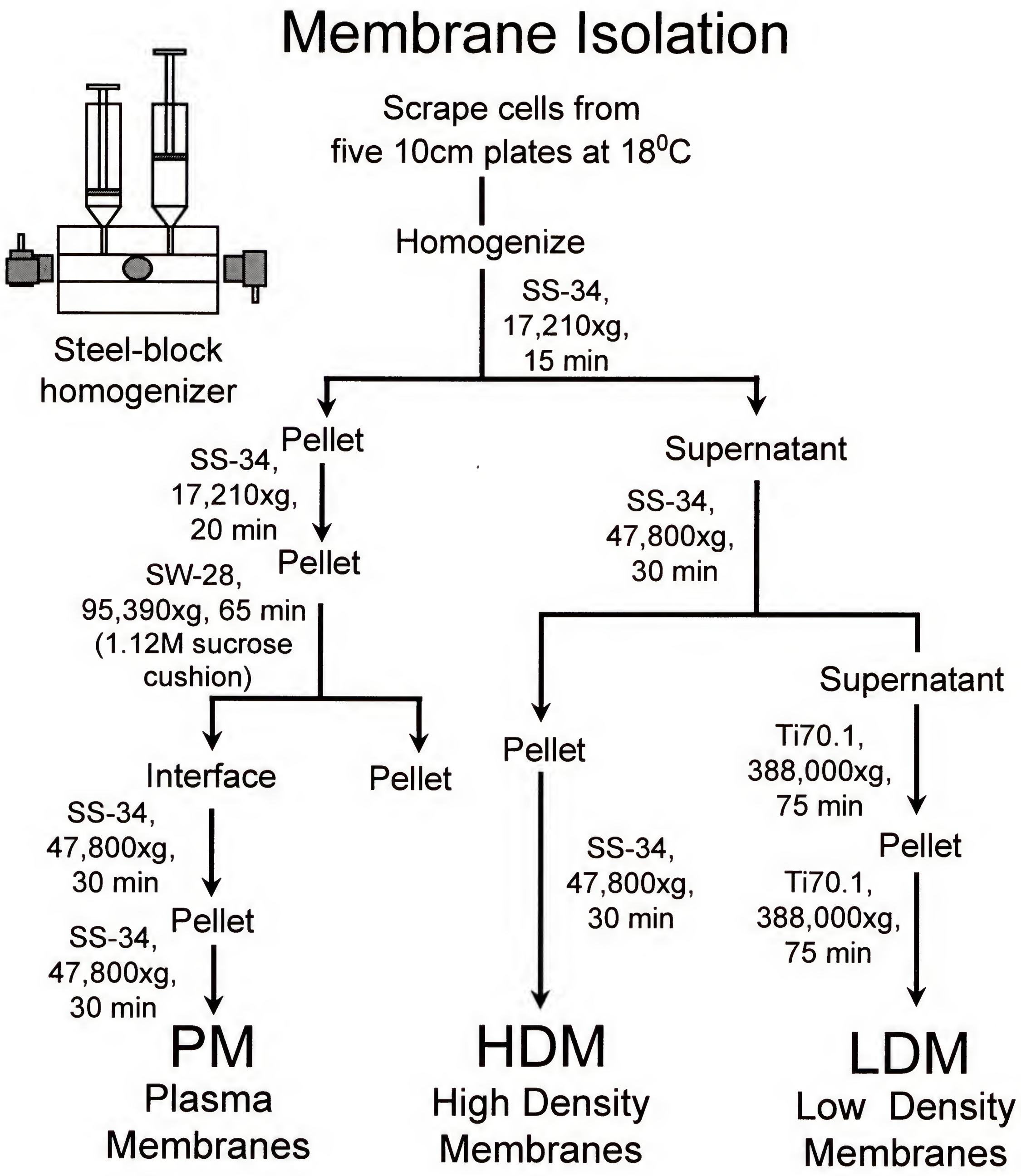

Figure 2-3 - Subcellular Fractionation of 3T3-L1 Adipocytes
Cell homogenates were subfractionated into plasma membranes (PM), high density membranes (HDM), and low density membranes (LDM) according to procedures by Fisher and Frost (1996). Refer to text for description.

times with 4mL of KRP at 37°C and collected in 4mL TES-P per plate (total of 20mL for the five plates) at 18°C. The cells were loaded into a syringe that was attached to the pre-cooled steel block homogenizer and then passed through the chamber 10 times at 18°C. PM, HDM, and LDM fractions were then collected by a combination of steps as shown in Figure 2-3. Each membrane fraction was resuspended in 0.3mL of TES-P. Twenty five μL of each sample were set aside for protein concentration determination. Samples were then stored at -20°C.

Markwell Assay for Protein Concentration Determination

Protein concentration was determined using a modified Lowry assay (1978). The Lowry assay is a standard and quantitative method for determining concentration of soluble proteins. This assay involves a colorometric reaction produced by the coupling of Folin-Ciocalteu phenol reagent to tyrosyl residues of proteins by copper. The Lowry assay has advantages over other assays. Nucleic acids do not interfere with the Lowry assay as does determining protein concentration by measuring the absorbance of protein solution at 280nm. In the Bradford assay, a blue dye interacts with different proteins to various degrees, and thus, is not strictly quantitative.

One major disadvantage of the standard Lowry assay is the lack of reliability in determining the concentration of protein in membrane preparations. Sucrose and EDTA, which are commonly used to isolate membrane fractions, interfere with the Lowry assay. Markwell et al. (1978) modified the Lowry assay for the use in determining the concentration of membrane proteins by the addition of SDS and an increase in the copper tartrate reagent.

The concentration of proteins in membrane fractions was calculated by comparison of their absorbance against a standard curve. The standard curve was prepared in duplicate using bovine serum albumin (BSA) ranging from 0 to 100µg. These standards were brought to 100µL with H_2O. Then, 10µL of TES-P were added to each standard to reflect the buffer in which membranes were suspended. For the unknown membrane samples, 10µL of sample were added to 100µL of H_2O so that the volumes in all the samples were equal. To all the samples, 1mL of a mixture of 100 parts solution 1 (2.0% Na_2CO_3, 0.4% NaOH, 0.16% NaKtartrate, 1.0% SDS) and 1 part solution 2 (4% $CuSO_4$) was added and incubated at room temperature for 10min. Folin and Ciocalteu's phenol reagent (0.1mL of 1N) was added to each sample and incubated for 45min at room temperature. A spectrophotometer (LKB 4053 Ultraspec K) was used to measure the absorbance of the samples for the standard curve and the unknowns at 650nm. The absorbance of the standards were plotted against the amounts of BSA. A second order regression of the standard curve was calculated using a SigmaPlot graphics computer program. The correlation coefficient value (r^2) was always greater than 0.99. The unknown protein concentrations were calculated using the quadratic equation defined by the standard curve.

Metabolic Radiolabeling

[^{35}S]methionine/cysteine

Immunoblot analysis is useful for determining the effect of stimuli on the steady-state level of the protein of interest. However, it cannot be used for examining the life cycle (synthesis and degradation) of a specific protein. To study the course of a newly synthesized pool of proteins, the protein must be tagged or labeled. A common method used to examine the life cycle of a protein is to radiolabel newly synthesized proteins with [^{35}S]methionine, [^{35}S]cysteine, or both. Radiolabeled proteins can be immunoprecipitated with a specific antibody against that protein, resolved by SDS-PAGE, and then examined by autoradiography (see below). This same strategy can be used to examine the maturation of a protein (i.e., glycosylation and proteolytic cleavage) and processing using a "pulse" of labeled amino acids followed by a chase in the presence of unlabeled amino acids. Optimal conditions for metabolic labeling and immunoprecipitation of insulin receptor expressed at endogenous levels in 3T3-L1 adipocytes were determined empirically.

3T3-L1 adipocytes were incubated in 8mL of complete medium or glucose-free medium for appropriate times. Cells were then incubated in 8mL of methionine- and cysteine-free DMEM with or without 25mM glucose for 1h to deplete intracellular pools of sulfur-containing amino acids. The depletion medium was replaced with 2mL of methionine- and cysteine-free DMEM containing 400μCi of [^{35}S]methionine/cysteine with or without 25mM glucose for specific times (10-180min). For chase periods, the labeling medium was replaced with 8mL of complete medium or glucose-free medium for the indicated times. This contains 200μM of methionine and 100μM of cysteine.

[^{3}H]mannose

Metabolic labeling with [^{3}H]mannose was used to specifically label the oligosaccharide moiety of the IR. [^{3}H]mannose was chosen over [^{3}H]glucose because Panneerselvam et al. (1997) have shown that 90% of the trichloroacetic acid-precipitable [2-^{3}H]mannose label is released by *N*-glycosidase (which cleaves all *N*-linked oligosaccharides), while only 10% of the trichloroacetic acid-precipitable [1,5,6-^{3}H]glucose label was released by the same digestion. In addition, while 7-14% of the [2-^{3}H]mannose is used for glycosylation, only 1-2% of [1,5,6-^{3}H]glucose is used for glycosylation. Furthermore, there are nine mannose residues on the normal insulin proreceptor and five mannose residues on the alternative proreceptor which may increase the specificity of labeling of IR.

To label glycoproteins with [2-^{3}H]mannose, 3T3-L1 adipocytes (10cm plates) were glucose-fed or glucose-deprived for a total of 24h. For glucose-fed cells, 4h prior to the end of the 24h feeding period, the cells were placed in 8mL of glucose-free DMEM containing 10% dialyzed FBS for 1h to deplete the intracellular pool of free sugar residues. The sugar depletion medium was then replaced with 2mL glucose-free DMEM containing 420μCi of [2-^{3}H]mannose (10μM final concentration) and incubated for 3h.

For glucose-deprived cells, cells were incubated in 2mL glucose-free DMEM containing 420μCi of [2-^{3}H]mannose for the last 3h of the 24h deprivation period. For chase periods, the labeling medium was replaced with 8mL complete or glucose-free medium for the indicated times.

Immunoprecipitation

A specific protein of interest can be isolated from other newly synthesized proteins that have been radiolabeled by interaction with an antibody against that specific protein. The immune complex (IgG/protein) can then be separated from the bulk solution of proteins by centrifugation with protein A conjugated to Sepharose beads (protein A-Sepharose or PAS). This immune complex can be washed with increasing stringency (i.e., 1M NaCl) to remove proteins that associate non-specifically. The immunoprecipitated protein can be released from its interaction with the antibody (bound to PAS) by treatment with solutions which break protein-protein interactions, such as SDS, urea, low pH, or a combination (Harlow and Lane, 1988) and detected by autoradiography.

To analyze IR and GRP78, radiolabeled membrane proteins (2.5 - 3.5mg) were solubilized in 1mL of radioimmune precipitation (RIPA) buffer (150mM NaCl, 9.1mM

Na_2HPO_4, and 1.7mM NaH_2PO_4, 0.5% deoxycholate, 1% Nonidet P-40, and 0.1% SDS, pH 7.4) with 1mM PMSF. Insoluble materials were remove by centrifugation at 1,300 x g for 5min. Solubilized proteins were then pre-cleared with 25μL of Protein-A Sepharose (50% suspension) and 5μL of preimmune serum for 1h at 4°C with rotation in order to remove any non-specific binding of proteins to either pre-immune IgG or PAS. Protein-A Sepharose (PAS) was collected by brief centrifugation and the supernatant was transferred to a new centrifuge tube. This process was repeated. The two preclear steps do not result in any detectable loss of the insulin receptor as visualized by autoradiography (data not shown). The final supernatant was transferred to a new tube containing 5μg of anti-IRβ or GRP78 antibody and incubated overnight at 4°C with rotation. The immune complex was collected with 25μL PAS by incubation for 2h followed by brief centrifugation. The immunoprecipitated complex was washed twice with 1mL RIPA buffer, four times with 1mL RIPA containing 1M NaCl, and once with 1mL TES. The high salt wash were necessary to remove nonspecific interactions with the insulin receptor. Immunoabsorbed proteins were released in 50μL of 2X sample dilution buffer (SDB, 4% SDS, 10% β-mercaptoethanol, 40% glycerol, 0.15

mg/mL bromophenol blue, and 20mM Tris-base, pH 6.6) containing 6M urea, boiled for 5min, and separated on a 7.5% SDS-PAGE gel run overnight at 30-40V (see below). For fluorography, the gels were fixed in 10% trichloracetic acid, 40% MeOH for 30min, soaked in water for 30min, and then soaked in 1M sodium salicylate for 1h before drying at 60°C under vacuum. Dried gels were exposed to Amersham Hyperfilm for 1 day to 1 month, depending on the radioisotope ([^{35}S] or [^{3}H]) used. Densitometry was performed in the linear range of the film.

SDS-Polyacrylamide Gel Electrophoresis

One-dimensional gel electrophoresis

Proteins were separated by molecular weight using SDS-polyacrylamide gel electrophoresis (SDS-PAGE) as described by Laemmli (1970). Protein samples in TES-P buffer were dissolved in an equal volume of 2X SDB and resolved on 7.5% gels. Gels were typically run overnight at room temperature at 30-40V.

Two-dimensional gel electrophoresis

Two-dimensional (2-D) gel electrophoresis is a high-resolution separation technique designed to resolve proteins based on their isoelectric point (pI) and molecular weight. The pI of a protein is defined as the pH at which its net charge equals zero. Once a protein reaches its pI, it becomes immobile in an electric field. The first dimension of the 2-D gel electrophoresis system allows isoelectric focusing (IEF) of proteins along a stable pH gradient established by small carrier ampholytes. The second dimension consists of the standard SDS-PAGE. The following procedure was performed as previously described by Semple-Rowland et al. (1991).

First dimension. Membrane fractions in TES buffer were isolated as before or radiolabeled IR or GRP78 was immunoprecipitated as described above. Membrane fractions (200-400μg in 110μL TES) were solubilized in an equal volume of IEF sample buffer (6.4% NP-40, 6.5mM DTT, and 0.1% SDS). Insoluble material was removed by centrifugation at 13,300 x g for 5min at 4°C in a microcentrifuge. The supernatant (200μL) was transferred to a glass tube. For immunoprecipitated samples, IR or GRP78 were released from the PAS/IgG complex with 100μL of 0.1M glycine, pH 2.8, containing 0.5% Triton X-100 for 30min at room temperature. The samples were neutralized with 10μL of 1M Tris-base. The IgG/PAS complex was removed by centrifugation. The eluates (100μL) were transferred to glass tubes containing 100μL of isoelectric focusing (IEF) sample buffer. All samples were then mixed with 4% acrylamide, 9M urea, 2% NP-40, and 2% carrier ampholytes (pH3.5-10). Polymerization of the gel was initiated with the addition of 2μL TEMED (N,N,N',N'-tetramethylethylenediamine) and 2μL of 30% APS (ammonium persulfate). Gels were cast in 11cm (length) by 3.4mm (inner diameter) glass tubes and were polymerized for 1h. The gel rods were placed in the IEF gel apparatus and the upper and lower reservoirs were filled with the cationic buffer (20mM sodium hydroxide, degassed) and anionic buffer (10mM phosphoric acid), respectively. The first dimension (IEF) was run at 350V for 18h, followed by 800V for 2.5h. The gel rods were extruded from the glass tubes and equilibrated in IEF equilibration buffer [5% β-ME, 62.5mM Tris-HCl, pH6.8, 2.3% SDS, and 10% glycerol] for 30min before loading onto a 7.5% SDS-PAGE for protein separation by mass (second dimension). For pH gradient determination, an identical gel with 200μL TES:IEF sample buffer (no protein) was run along with the samples. The gel was extruded, cut into 0.5cm pieces and each piece was soaked in 1mL distilled water for 2h before measuring each pH.

Second dimension. One SDS-PAGE gel, composed of a stacking gel on top of a running gel, was prepared for each tube gel. Melted agarose embedding solution (1% agarose in

SDS-PAGE stacking gel buffer) was layered on top of the stacking gel. The tube gel was placed on top of the embedding layer, next to a smaller (~1cm) tube gel composed of either 5µL of molecular weight standards (Biorad) or 2µCi [^{14}C]methylated standards (Amersham) in 150µL 1% agarose in equilibration buffer. The tube gels were then overlaid with more melted embedding agarose that contains bromophenol blue (<0.01%). Once solidified, the gels were placed in the gel apparatus and run overnight at 30-40V. Non-radioactive samples were electrotransferred to nitrocellulose membrane and immunoblot analysis performed (see below), whereas radioactive samples were enhanced, dried and exposed to film for autoradiography.

Electrotransfer and Immunoblot Analysis

To detect proteins by immunoblot analysis, proteins that were separated by SDS-PAGE first need to be transferred onto a membrane, usually nitrocellulose. The following procedure describes a method for electrotransfer of proteins onto a nitrocellulose membrane followed by immunoblot analysis (Towbin et al., 1979). After running a gel overnight, the gel was removed from the gel apparatus and juxtaposed to a nitrocellulose membrane (equilibrated for 30min in transfer buffer) sandwiched between two pieces of 3M Whatman paper. This sandwich was then placed in an electrotransfer apparatus filled with transfer buffer (25mM Tris-base, unadjusted pH, 192mM glycine, and 20% methanol). Proteins were transferred from the gel to the nitrocellulose membrane at 250mA for 2.5h or overnight at 30V at 4°C. The membrane was removed from the transfer apparatus and stained with amido black solution (0.2% amido black, 40% methanol, and 10% acetic acid) for 1min and then destained in a solution containing 40% methanol and 10% acetic acid for 1 to 5min. For immunoblot analysis, the membrane was blocked in Tris-buffered saline/0.1% Tween-20 (TBS-T, 20mM Tris-base, pH7.4, 0.137M NaCl, and 0.1% Tween 20) containing 5% non-fat dry milk for 30 to 60min. All subsequent steps were performed at room temperature on an orbital shaker with constant speed. The blot was then washed three times (1min each) with TBS-T. The blot was incubated with the primary antibody (1:1,000 dilution of anti-serum in 10 to 20mL TBS-T containing 5% milk) for 1 to 2h. The blot was then washed three times for 1min each, followed by two times for 5min each in TBS-T before applying the secondary antibody (10 to 20mL, 1:100,000 dilution of anti-rabbit antibody coupled to horseradish peroxidase in TBS-T containing 5% milk) for 1 to 2h. The blot was washed four times for 1min each followed by three times for 5min each in TBS-T before applying Amersham's Enhanced Chemiluminescence (ECL) detection reagents to the blot. ECL couples the reduction of hydrogen peroxide by peroxidase (cross-linked to the secondary antibody) to the oxidation of luminol, which produces blue light that can be captured on film. Bands on the film were quantified by video densitometry on a Visage bioscan (Millipore) in the linear range of the film.

Glycosidase Digestions

N-glycosidase F and endoglycosidase H digestion were used as tools to examine the oligosaccharide structures of the insulin proreceptor isoforms. *N*-glycosidase F is an enzyme that cleaves all *N*-linked oligosaccharides attached to an asparagine residue contained within the amino acid sequence, N-X-T/S (single letter amino acid abbreviation) where X represents any amino acid except for proline. As shown in Figure 2-4, *N*-glycosidase F specifically cleaves in between the first *N*-acetylglucosamine (GlcNAc) and the asparagine residue. Endoglycosidase H is an enzyme which cleaves oligosaccharide structures that contain high mannose residues. It specifically cleaves in between the first and second GlcNAc residues. Neither of these two

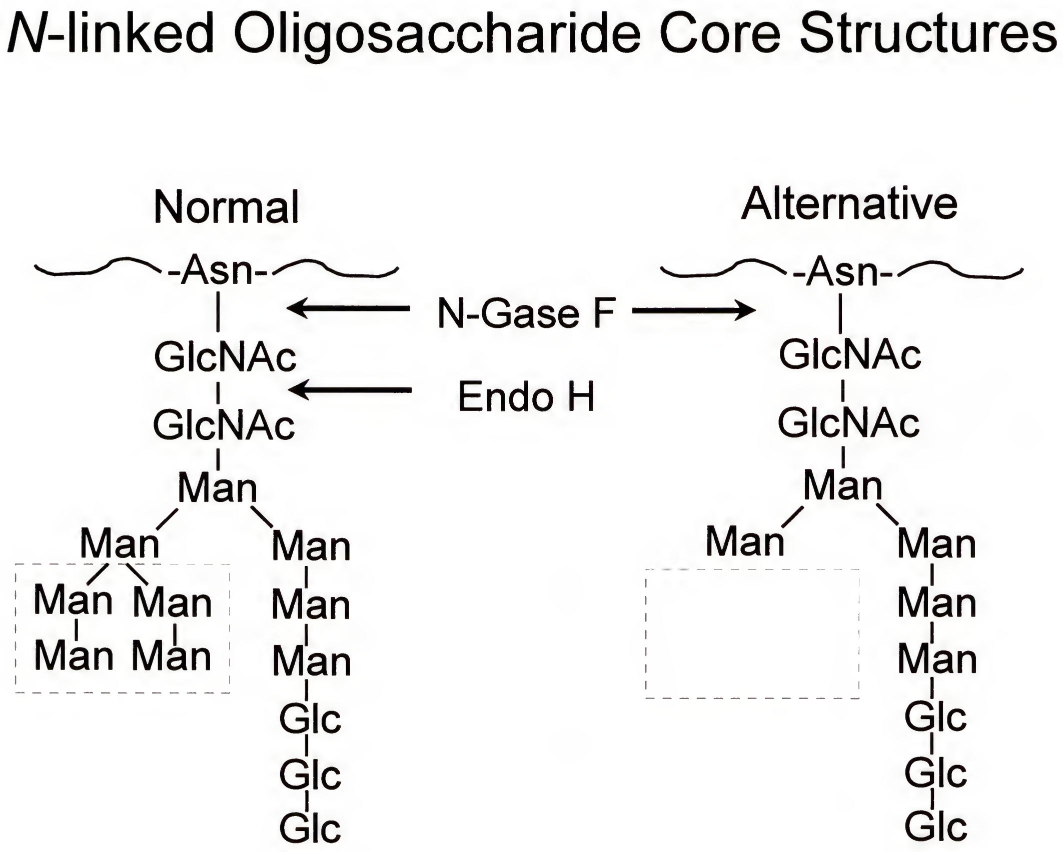

Figure 2-4 - *N*-glycosidase F and Endoglycosidase H Digestions Two different *N*-linked core oligosaccharide structures are represented. Under normal conditions, a nine-mannose structure is attached to the *N*-linked consensus sequence, Arg-X-Ser/Thr, of a protein. Under glucose-deprivation, an alternative core structure containing five mannose residues is attached. *N*-glycosidase F cleaves all *N*-linked oligosaccharide structures in between the first GlcNAc residue and the arginine residue of the protein (as represented by an arrow). Endoglycosidase H cleaves high mannose containing oligosaccharide structures in between the first and second GlcNAc residues (as represented by an arrow).

enzymes cleave *O*-linked oligosaccharides that are attached to either threonine or serine residues.

Fifty μg of membrane protein or radiolabeled IR immunoprecipitated from 2.5 to 3.5mg of membrane protein were digested with *N*-glycosidase F or endoglycosidase H. Specifically, samples were incubated in denaturing buffer (0.5% SDS and 1% β-mercaptoethanol) for 10min at 100°C. For *N*-glycosidase F digestion, samples were brought to 50mM sodium phosphate, pH 7.5, and 1% NP-40. For endoglycosidase H digestion, samples were brought to 50mM sodium citrate, pH 5.5. Then, 1μL (500U) of either *N*-glycosidase F or endoglycosidase H was added and incubated for 1 to 2h at 37°C. Following incubation, 2X SDB containing 6M urea was added and proteins separated on a 7.5% SDS-PAGE gel. Gels were either dried for autoradiography or proteins in the gels were electrotransferred onto nitrocellulose for immunoblot analysis.

Furin Digestion

Furin is a member of a family of subtilisin-like proprotein convertases. It is a calcium-dependent serine endoprotease that is responsible for the proteolytic cleavage of proproteins in the secretory pathway. Furin recognizes the motif, RXK/RR (each letter represents an amino acid, where X is any amino acid). In the mouse or human insulin proreceptor, furin cleaves after the amino acid sequence, RKRR, which lies between the α- and β-domains (Barbara Robertson et al., 1993; Bravo et al., 1994). Thus, furin, which is localized to the trans Golgi network (Zhou et al., 1999), proteolytically cleaves the proreceptor dimer into a heterotetramer composed of two α-subunits and two β-subunits.

In vitro digestion of the alternative proreceptor with furin was performed in order to determine whether both the α- and β-subunits were glycosylated. Cells that were glucose-deprived for 21h were radiolabeled with [^{3}H]mannose (420μCi/10cm plate) for 3h. A total membrane fraction was collected and used in immunoprecipitation of IR. IR was immunoprecipitated using RIPA buffer without 1mM PMSF (a serine protease inhibitor) as described above. For the wash step, the immune complex was washed twice with 1mL RIPA buffer, four times with 1mL RIPA buffer containing 1M NaCl, and twice with 1mL HEPES buffer (100mM HEPES, pH 7.6, 1mM $CaCl_2$, 0.5% Triton X-100). For furin digestion, 35μL HEPES buffer with 1mM β-ME and 1μL (60U) furin (received as a gift from Dr. Richard Leduc) were added to the immune complex and incubated for 2h at 37°C. The reaction was quenched with 40μL 2X SDB and incubated for 5min at 95°C before separating proteins by SDS-PAGE. Gels were then processed for autoradiography as before.

Glycogen Assay

Glucose is stored in most cells as glycogen (Voet and Voet, 1990). The breakdown of glycogen into glucose (i.e., during starvation) provides cells with energy through glycolysis, and with substrates for glycosylation and other important precursors necessary to sustain life. Therefore, intracellular storage of glycogen provides a limited source of glucose during times of glucose stress. In order to determine the length of time that the breakdown of glycogen can provide glucose for the cell, a procedure described by Pfleiderer (1963) for the isolation of glycogen was used. In this procedure, glycogen, isolated from 3T3-L1 adipocytes, was hydrolyzed with acid to produce free glucose which is assayed using a hexokinase kit from Sigma Diagnostics. This assay does not directly measure glycogen content; however, it does represent the amount of glucose contained in glycogen.

Glycogen was isolated from 3T3-L1 adipocytes (12 million cells/10cm plates) that were glucose-fed or glucose-deprived for specific times. Cells were washed four times with 4mL of PBS, pH 7.2 at 4°C. One mL of PBS was added to each plate and scraped into 15mL polypropylene tubes. The cells were sonicated for 10sec on 50% duty cycle with power setting of 2 using a Branson Sonifier 450. KOH (2.0mL, 30% w/v) was added to the lysate and mixed vigorously. The samples were boiled for 15min in a water bath. The samples were then allowed to cool for 5min before adding 3.5mL of 95% ethanol. The samples were again mixed vigorously and boiled for 2 to 3min. The samples were cooled to room temperature before collecting the precipitates by centrifugation at 1,300 x g for 5min at room temperature. The clear supernatant was removed by aspiration while the pellet was resuspended in 1mL of 95% ethanol using a Pasteur pipette. The suspension was transferred into a microcentrifuge tube and subjected to centrifugation at 12K for 5min to recollect the glycogen. The supernatant was aspirated and the glycogen pellet was stored at -20°C. Glucose was released from glycogen by hydrolysis in 0.2mL of 2N H_2SO_4. The samples were boiled for 2h and then allowed to cool to room temperature. The solution was neutralized with 0.15mL of 2N NaOH and the volume was adjusted to 1mL with 0.65mL of H_2O. The hydrolysates were used to determine glucose concentration as described below.

The glucose assay involves the phosphorylation of glucose on the 6th carbon position by hexokinase. Glucose-6-phosphate (G6P) is then oxidized to 6-phosphogluconate while NAD^+ is reduced to NADH in a reaction catalyzed by G-6-P dehydrogenase. The production of NADH, which is in direct proportion to the initial concentration of glucose, is measured at an absorbance of 340nm (millimolar extinction coefficient of NADH at 340nm is 6.22). For this assay, 0.1mL hydrolysate (from above) was diluted with 0.4mL $H_2SO_4/NaOH/H_2O$ mixture (2/1.5/6.5 ratio). An aliquot (0.1mL) of this solution was placed into borosilicate tubes (all samples were performed in triplicate). The samples and the assay reagents were warmed to 37°C. To each tube, 1mL of the assay mixture was added and mixed gently. The samples were incubated for 30min at 37°C. The absorbance at 340nm was measured for each sample.

Glucose Transport

In 3T3-L1 adipocytes, extracellular glucose is transported into the cell via the constitutive glucose transporter (GLUT1) and/or the insulin-stimulated glucose transporter (GLUT4). The following procedure for the glucose transport assay described by Frost and Lane (1985) uses a tritiated glucose analog (2-deoxy-2-[2,6-^{3}H]glucose) to determine the rate of glucose uptake into cells. The analog is phosphorylated by hexokinase but not further metabolized. Cells (2.1 million cells/35mm plate) were washed three times with 3mL KRP at 37°C. Then, 0.95mL KRP was added to the cells and allowed to incubate for 10min at 37°C. Insulin (at specific concentrations) was added (or not) to each plate and incubated for 10min at 37°C. To each sample, 50μL of a mixture of 2-deoxyglucose (final concentration of 0.2μM) and 2-deoxy-d-[2,6-^{3}H]glucose (0.2μCi/plate) in KRP were added and incubated for 10min at 37°C. The cells were washed three times with 3mL ice-cold PBS, pH7.4. The plates were air-dried for 1h at room temperature. The cells were extracted with the addition of 1.0mL of 0.1% SDS. The cells were lysed by passing the cells through a Pasteur pipette several times. An aliquot (0.3ml) of the cell lysate was added to 3.7mL of scintillant (ScintiSafe, 30%) and radioactivity was determined using a liquid scintillation counter (Beckman LS 5000TD). All samples were performed in duplicate.

Autophosphorylation Assay

The binding of insulin to the IR α-subunit induces autophosphorylation on several tyrosine residues located within the intracellular domain of the β-subunit. Thus, autophosphorylation provides an assay to determine the functional status of the IR. An *in vitro* autophosphorylation assay was performed using a procedure described by van der Vorm et al. (1994). First, cells were glucose-fed or glucose-deprived for 24h and total membranes were collected for immunoprecipitation of IR as before with the following modifications. The immunoprecipitation buffer was changed to PBS, pH7.4, with 1% Triton-X-100 (PBS-T) and the immune complex was washed twice with 1mL PBS-T, four times with 1mL PBS-T containing 1M NaCl, and twice with 1mL HEPES buffer (50mM HEPES, pH 6.9, and 1mM EDTA). After aspiration of the last wash buffer, 30μL HEPES buffer and 4μL 1% Triton-X-100 were added to the immune complex and allowed to incubate for 30min at room temperature. Then, 2μL of 100mM $MnCl_2$ (5mM), 0.8μL of 1mM ATP (20μM), 2μCi/tube [γ^{32}P]ATP were added with or without 0.4μL of 100μM insulin (1μM) were added to each sample and incubated for 15min at room temperature. The reaction was quenched with 10μL of 5X SDB. The samples were heated to

95-100°C for 5min before loading onto a 7.5% SDS-PAGE gel. Gels were typically run overnight at 30-40V and then processed for autoradiography as described above.

CHAPTER 3

GENERAL CELLULAR CHANGES IN RESPONSE TO GLUCOSE DEPRIVATION

Introduction

Glucose is required to maintain metabolic processes that are essential for life. Glucose provides a major source of energy for all mammalian cells. One of the primary products of glucose metabolism is adenosine triphosphate (ATP). Large amount of free energy is stored in the phosphoanhydride bonds of ATP. Free energy released from ATP hydrolysis is coupled to endergonic reactions, driving all essential biological systems necessary to maintain life. However, in order for the cells to utilize glucose, glucose must be transported into the cell which is, in many cases, the rate limiting step.

Due to the impermeability of plasma membranes toward small polar molecules, glucose is transported into cells via transport proteins (GLUTs) which exhibit tissue-specific expression. In 3T3-L1 adipocytes, two isoforms of the glucose transporters, GLUT1 and GLUT4, transport glucose across the lipid bilayer by facilitative transport. GLUT1, which is known as the constitutive glucose transporter, is localized mainly at the plasma membrane. GLUT4, which is known as the insulin-dependent glucose transporter, is translocated from intracellular vesicles to the plasma membrane in response to insulin stimulation. Although they share 62% amino acid identity, they display different kinetics and regulation.

Glucose deprivation increases the rate of glucose transport by a protein synthesis-dependent process in 3T3-L1 adipocytes (van Putten and Krans, 1985). Van Putten and Krans (1985) have shown that the time- and protein synthesis-dependent increase in 2-deoxyglucose uptake was due to an increase in the apparent Vmax. An increase in Vmax can be attributed to an increase in the level of glucose transporters at the cell surface (i.e., due to an increase in rate of synthesis or decrease in rate of degradation, or both, or due to translocation from an intracellular compartment). Alternatively, an increase in Vmax could occur because of transport activation or release from inhibition of GLUT1. In 3T3-L1 adipocytes, the increase in glucose transport is predicted to be caused by a newly synthesized protein, TAP (transporter activating protein), that activates GLUT1 rather than by an increase in levels of either GLUT1 or GLUT4 at the cell surface (Kitzman et al., 1993; Fisher and Frost, 1996).

In times of surplus energy, glucose is stored in all mammalian cells as glycogen. In times of glucose stress, glucose from glycogen breakdown provides the cell with a limited supply of energy. Depletion of the intracellular pools of glucose, including glycogen, has a pronounced effect on protein glycosylation and the expression of ER molecular chaperones as is discussed below.

Glucose provides substrates for protein glycosylation. Glucose, mannose, or fructose can be used interchangeably in providing substrates for the synthesis of the core dolichol-linked oligosaccharide structure (Figure 3-1). The core oligosaccharide structure, composed of two *N*-acetylglucosamine (GlcNAc), nine mannose (Man), and three glucose (Glc) or $(GlcNAc)_2(Man)_9(Glc)_3$, is transferred from dolichol to an asparagine residue contained within the *N*-linked consensus site (Asn-X-Ser/Thr; where X is any amino acid except proline) of a protein (see Figure 2-4). Glucose deprivation alters the synthesis of this normal core structure and causes aberrant glycosylation of the constitutive glucose transporter, GLUT1 (Kitzman et al., 1993). Aberrant glycosylation has been known to cause misfolding of glycoproteins which in turn induces the expression of ER molecular chaperones.

Sugars Used to Make Dolichol-linked Core Oligosaccharides

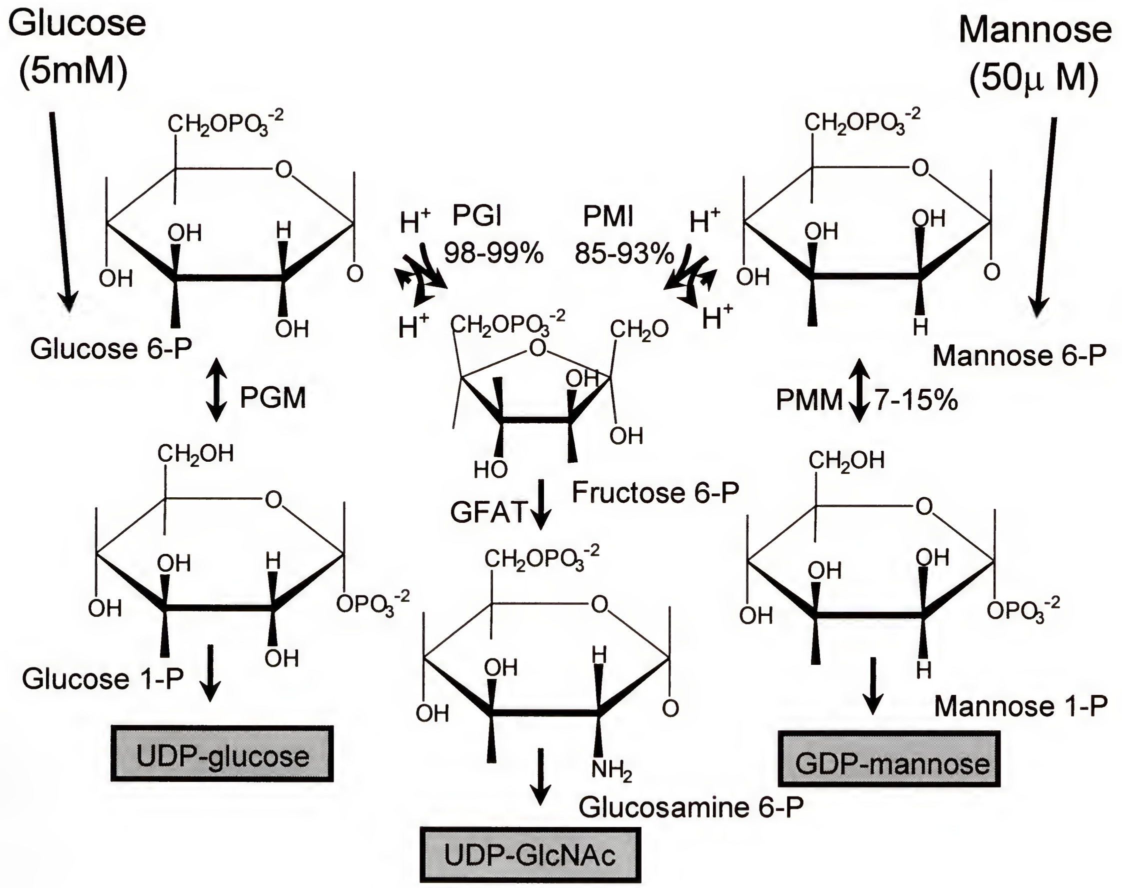

Figure 3-1 - Sugars Used for Dolichol-linked Core Oligosaccharides Refer to text for description. Abbreviations include PGI, phosphoglucose isomerase; PMI, phosphomannose isomerase; PGM, phosphoglucose mutase; PMM, phosphomannose mutase; and GFAT, glucosamine:fructose 6-P aminotransferase.

Cells respond to stress in a number of ways. One of the ways that the cell responds to glucose deprivation or glycosylation inhibitors is called the unfolded protein response (UPR). Glucose deprivation or glycosylation inhibitors, such as tunicamycin, castanospermine (ER glucosidase inhibitor) but not swainsonine (Golgi mannosidase inhibitor), have been known to affect folding and/or assembly of glycoproteins in the ER (Kozutsumi et al., 1988). Misfolded proteins are prevented from exiting the ER by virtue of their stable interaction with ER molecular chaperones, like GRP78. The accumulation of misfolded proteins bound to GRP78 in the ER causes activation of IRE1p, an integral membrane endonuclease that is localized to both the ER and nuclear membrane (Pahl and Baeurerle, 1997). Only free GRP78, and not GRP78 bound to its substrate, binds to IRE1p. Thus, it is hypothesized that the loss of GRP78 interaction with IRE1p during ER stress activates IRE1p. In the nucleus, IRE1p alternatively splices the unstable form of Hac1 mRNA into a stable form, allowing translation of Hac1 mRNA into an active transcription factor. Hac1p binds to UPR elements and enhances transcription of UPRE (unfolded protein response element) containing genes, such as the ER molecular chaperones (Sidrauski et al., 1998; Chapman et al., 1998).

Results

Glucose Transport

Glucose deprivation has been shown to increase glucose transport in 3T3-L1 adipocytes (Kitzman et al., 1993). To confirm this phenomenon, the rate of $[^3H]$-deoxyglucose uptake was measured in 3T3-L1 adipocytes. Glucose deprivation led to an increase in transport activity by 3h and resulted in a nine-fold increase in transport activity by 24h (Fig. 3-2) as compared to cells that were maintained in complete medium containing 25mM glucose (controls). Fructose, which can provide substrate for protein glycosylation, is not able to prevent this glucose-induced increase in transport activity. Pretreatment of cells with 1μM insulin for 10min before measuring 2-deoxyglucose uptake resulted in a 6 - 8 fold increase in transport in glucose-fed controls (+glucose/-fructose) at each time point over a 24h time interval. Over time, both glucose-deprived and glucose-deprived cells fed with fructose showed diminished response to insulin (compare 0 vs 24h time points). These data confirm earlier works by van Putten and Krans (1985).

Figure 3-2 - Effect of Glucose or Fructose on Insulin-stimulated Glucose Uptake 3T3-L1 adipocytes were maintained in medium containing 25mM glucose (○,●), 25mM fructose (Δ,▲), or no sugars (□,■) for specific times (0, 3, 6, 9, 12, and 24h). At each time point, cells were washed and glucose transport activity was measured in the absence or presence of 1μM insulin. Data represents the average ± SD of two independent experiments (n=4).

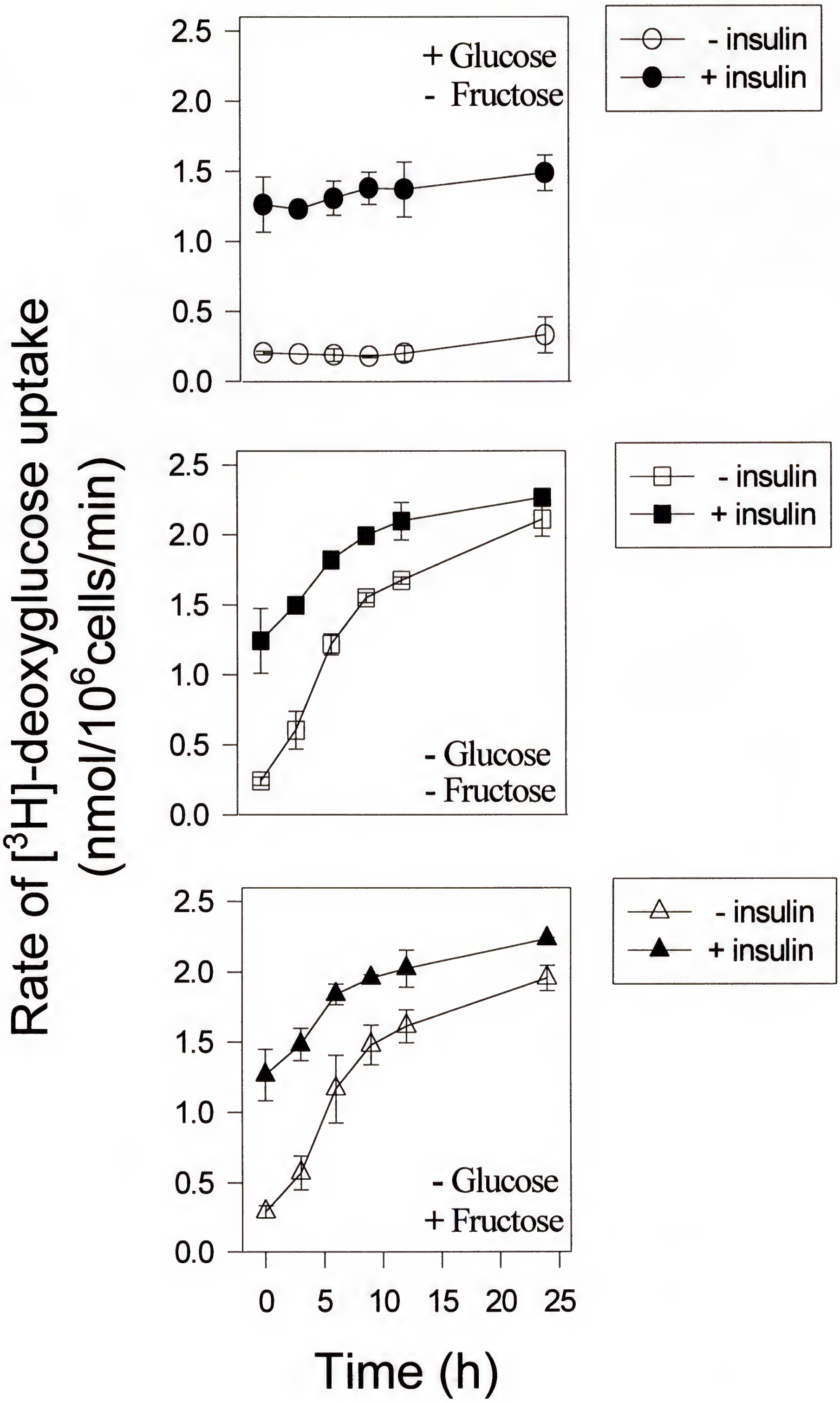
+ Glucose
- Fructose
- insulin
+ insulin
- Glucose
- Fructose
- insulin
+ insulin
- Glucose
+ Fructose
- insulin
+ insulin
Rate of [³H]-deoxyglucose uptake (nmol/10⁶cells/min)
0.0
0.5
1.0
1.5
2.0
2.5
0
5
10
15
20
25
Time (h)

Glycogen Content

3T3-L1 adipocytes (and adipose tissue) store relatively small amounts of glycogen relative to liver and muscle (McMahon and Frost, 1996). However, during glucose deprivation this pool acts as a source of glucose for metabolism and protein glycosylation. As shown in Figure 3-3, glucose deprivation led to a time-dependent loss of glycogen. The decrease in glycogen content at 3 and 6h time points for the glucose-fed cells may be attributed to the replacement of old with fresh new medium. This first order process led to greater than 90% depletion of the glycogen pool by 24h. Glucose, but not fructose, was able to prevent glycogen depletion.

Glycosylation of GLUT1 and GLUT4

Prior to the glycogen depletion, protein glycosylation occurs normally, as analyzed by examining the migration pattern of GLUT1, the constitutive glucose transporter. This transporter normally migrates as a 46kDa glycoprotein (p46) and is sensitive to endoglycosidase F (cleaves all *N*-linked oligosaccharides) but not endoglycosidase H (cleaves high mannose containing oligosaccharides) [McMahon and Frost, 1995]. Resistance to endoglycosidase H digestion implies the attachment of complex oligosaccharide structure on the normal GLUT1 (p46). At 24 hours of deprivation, aberrant glycosylation occurs resulting in the appearance of a lower molecular weight glycoform of GLUT1, p37 glycoform, (Figure 3-4). This glycoform migrates slightly slower than the aglycoform of GLUT1, p36 (Figure 3-5). In addition, the p37 glycoform is sensitive to both endoglycosidase F and endoglycosidase H treatment, which implies that p37 is alternatively glycosylated with respect to the normal GLUT1 (p46) [McMahon and Frost, 1995]. In contrast to the appearance of p37, glucose deprivation does not alter the migration of GLUT4 (Figure 3-6; lower band is non-specific). However, the appearance of p37 is coordinated with the induction of GRP78, even though these two proteins do not interact (Kitzman et al., 1996). Fructose, which provides substrate for *N*-linked glycosylation, prevents the appearance of the p37 glycoform and the induction of GRP78 [Figure 3-4; compare 24h pretreatment with glucose (G) vs. -glucose/+fructose (F) at 0h time point]. Cells which are pretreated with fructose (F) for 24h to reduce the glycogen pool and then deprived of all sugars, show a faster rate of p37 accumulation (4-fold difference by 12h) and GRP78 induction (5-fold difference by 24h) than cells pretreated with glucose (G).

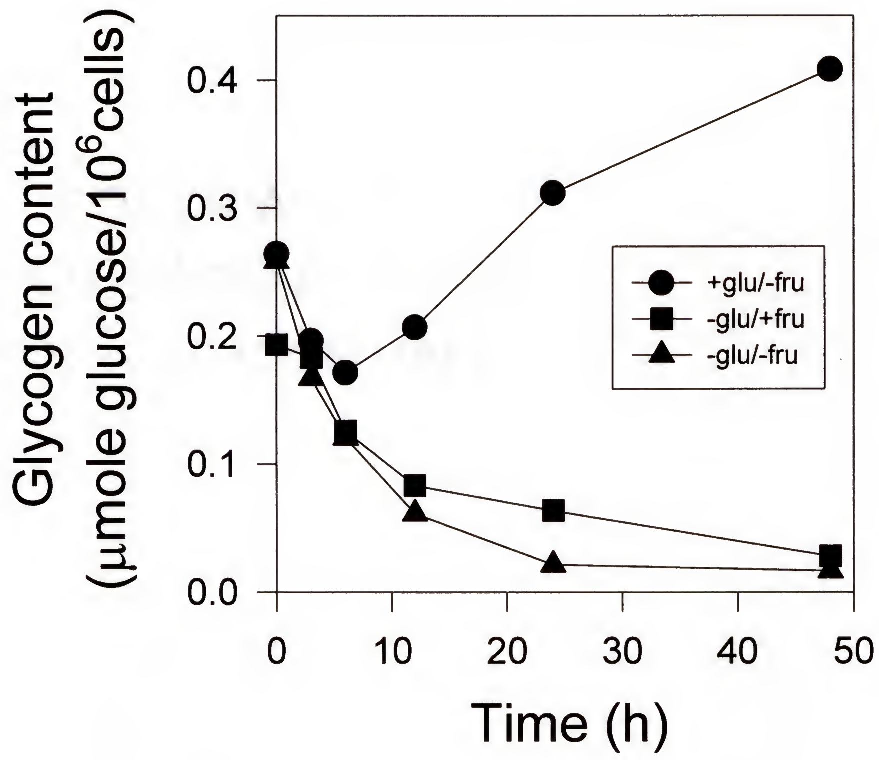

Figure 3-3 - Effect of Glucose or Fructose on Glycogen Content 3T3-L1 adipocytes were maintained in medium containing 25mM glucose (●), 25mM fructose (▲), or no sugars (■). At specific times intervals (0, 3, 6, 12, 24, and 48h), cells were collected and assayed for glucose content in glycogen.

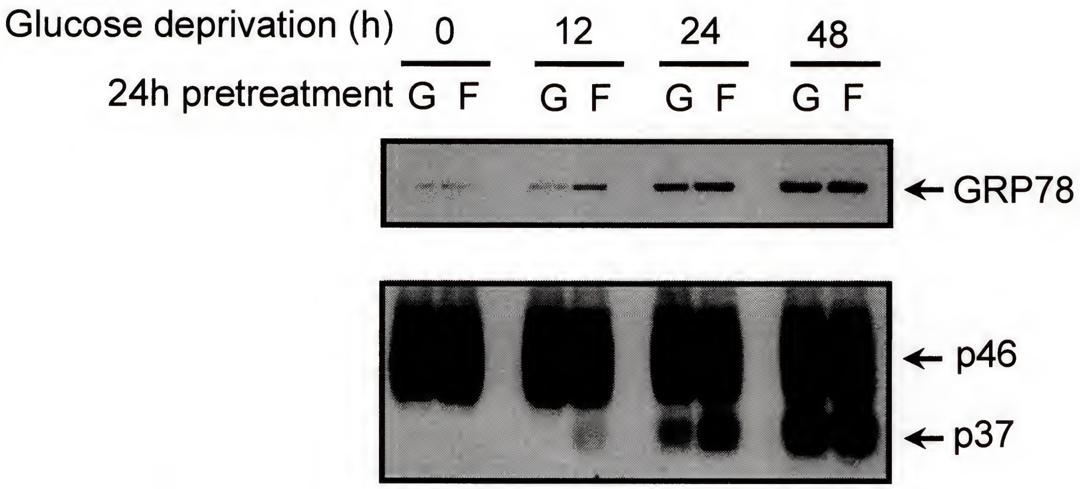

Figure 3-4 - Effect of Glucose Deprivation on Glycosylation of GLUT1 and Expression of GRP78 3T3-L1 adipocytes were pretreated with medium containing either 25mM glucose (G) or 25mM fructose (F) for 24h. After 24h, cells were deprived of sugars for specific time intervals (0, 12, 24, and 48h) at which point cells were collected. Twenty-five µg of total membrane protein was loaded per lane and run on a 7.5% SDS-PAGE. Western analysis was performed using anti-GRP78 or anti-GLUT1 antibodies. P46 is the constitutive form of GLUT1; p37 is the aberrantly glycosylated glycoform of GLUT1.

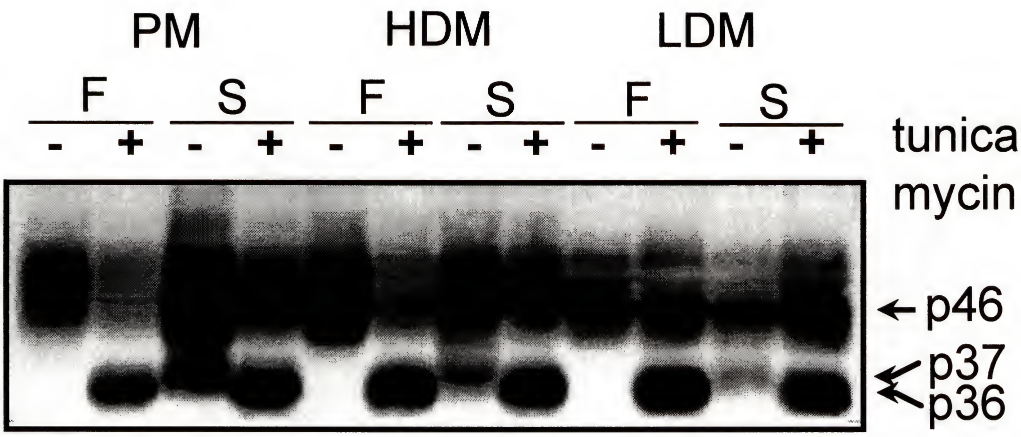

Figure 3-5 - Effect of Tunicamycin Treatment on the Migration of GLUT1 3T3-L1 adipocytes were maintained in medium containing 0mM glucose (S) or 25mM glucose (F) in the presence or absence of 2.5μg/mL tunicamycin for 24h. Cells were collected and total membranes were prepared. Twenty-five μg of total membrane protein was loaded per lane and run on a 7.5% SDS-PAGE. Western analysis was performed using anti-GLUT1 antibodies. P46 is the constitutive form of GLUT1; p37 is the aberrantly glycosylated glycoform of GLUT1; and p36 is the aglycoform of GLUT1.

Thus, glycogen provides a buffer for protein glycosylation which contributes to the extended lag time of GRP78 induction in 3T3-L1 adipocytes.

Subcellular Distribution of GLUT1 and GLUT4

To examine the subcellular localization of GLUT1 and GLUT4, a subfractionation procedure (Weber et al., 1988) that was modified by Fisher and Frost (1996) was used. In the glucose-fed condition, GLUT4 mainly localized to the LDM fraction which is enriched in endosomal vesicles, whereas GLUT1 (p46) localized mainly to the plasma membrane (Figure 3-6). The Na+/K+ ATPase, which is a resident of the plasma membrane, showed about 10% cross-contamination of the HDM fraction (Fisher and Frost, 1996). Glucose deprivation did not appear to affect targeting of GLUT1 to the plasma membrane or GLUT4 to the LDM fraction.

Induction of Molecular Chaperones

The endoplasmic reticulum (ER) is the major site for the folding and assembly of newly synthesized glycoproteins. Glucose deprivation alters protein glycosylation, which in turn leads to misfolding of proteins (Gallagher et al., 1988; Machamer and Rose, 1988; Ng et al., 1990; Melnick et al., 1992). It is this latter process that drives the induction of GRP78 during glucose

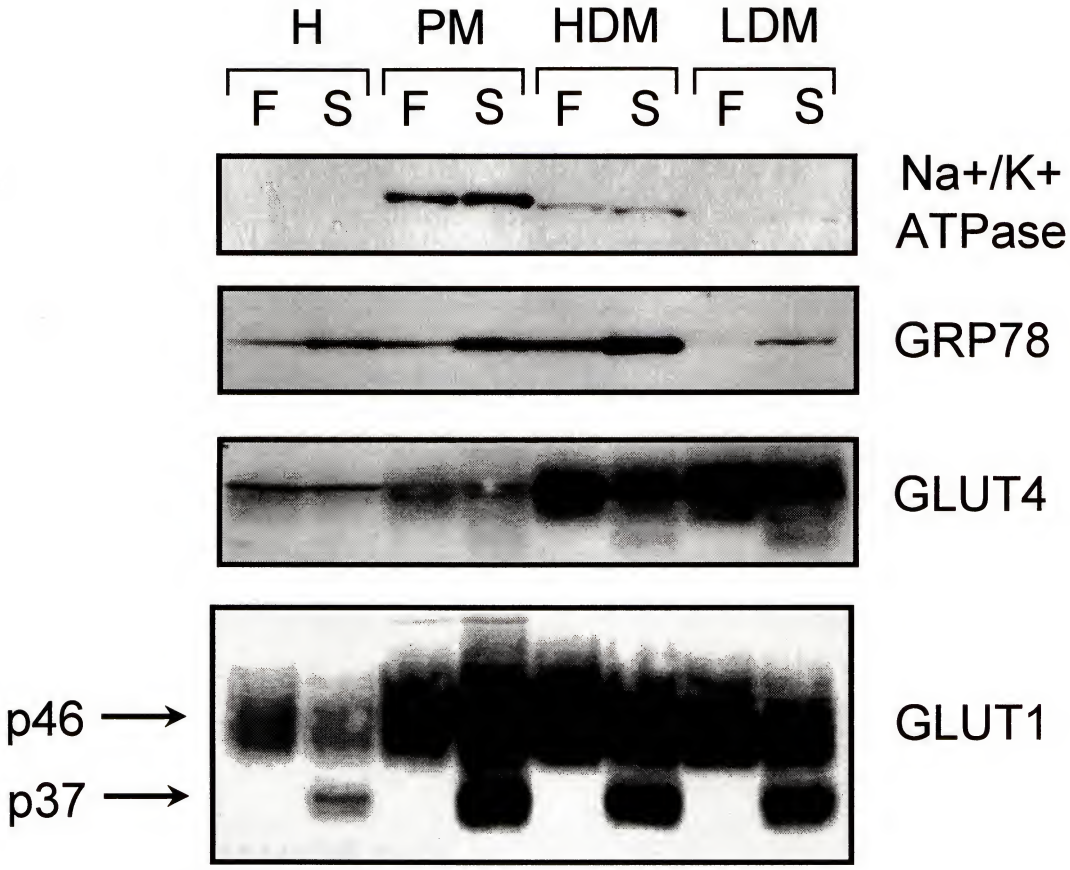

Figure 3-6 - Subcellular Localization of GLUT1, GLUT4, and GRP78 3T3-L1 adipocytes were maintained in medium containing 25mM glucose (F) or 0mM glucose (S) for 24h. After 24h, cell homogenates (H) were subfractionated into plasma membranes (PM), high density membranes (HDM), and low density membranes (LDM). Fifty μg of each fraction was loaded per lane and run on a 7.5% SDS-PAGE. Western analysis was performed using anti-Na^+/K^+ ATPase, anti-GRP78, anti-GLUT4, or anti-GLUT1 antibodies.

deprivation. Shown in Figure 3-6 is the effect of glucose deprivation on GRP78 expression. Note the localization to the HDM fraction and the significant increase in response to glucose deprivation. In addition to GRP78, glucose deprivation also induced a two-fold increase in expression of other ER molecular chaperones, such as, 94kDa Glucose-regulated protein (GRP94), calnexin, and calreticulin (Figure 3-7). Upon further examining these four ER molecular chaperones by two-dimensional gel electrophoresis, GRP78 migrated as a discrete spot with a pI of 5.5 ± .2 while the other three chaperones showed multiple isoforms with a wide pI range of 4-7 (Figure 3-8).

Conclusions

Cells respond to glucose deprivation in a number of ways. Within 3h of glucose deprivation, glucose uptake increases, reaching a 9-fold increase by 24h. Twenty-four hours of glucose deprivation is sufficient to deplete 90% of the glycogen content and cause the appearance of an aberrantly glycosylated GLUT1 (p37). In contrast, glucose deprivation fails to alter the normal processing of GLUT4. Both GLUT1 and GLUT4 have a single *N*-linked consensus site located in between the first and second transmembrane region. However, the *N*-linked oligosaccharide structures

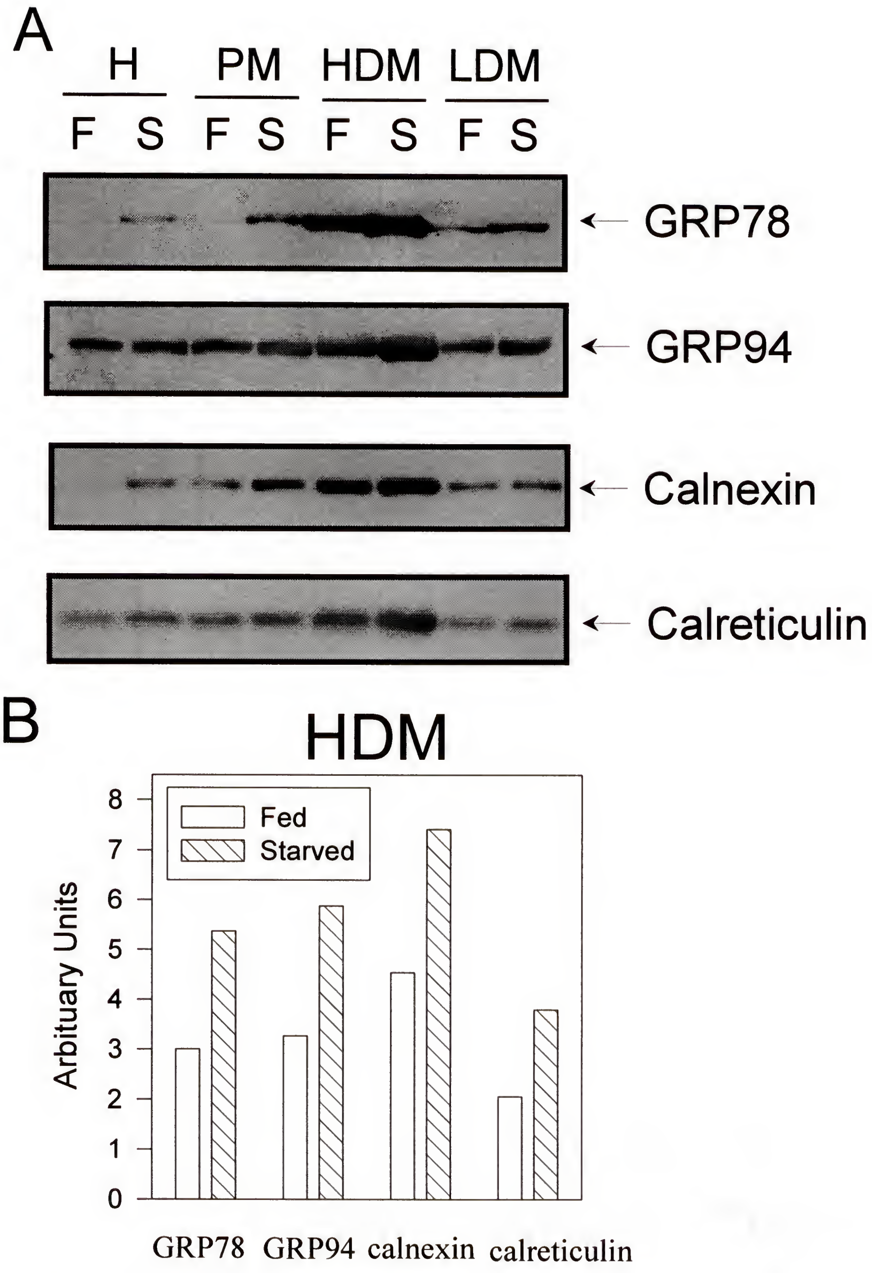

Figure 3-7 - Effect of Glucose Deprivation on the Expression of ER Molecular Chaperones 3T3-L1 adipocytes were maintained in medium containing 25mM glucose (F) or 0mM glucose (S) for 24h. After 24h, cell homogenates (H) were subfractionated into plasma membranes (PM), high density membranes (HDM), and low density membranes (LDM). *Panel A*, 50µg of each fraction was loaded per lane and run on a 7.5% SDS-PAGE. Western analysis was performed using anti-GRP78, anti-GRP94, anti-calnexin, or anti-calreticulin antibodies. Densitometric analysis of HDM fractions is represented in *Panel B*.

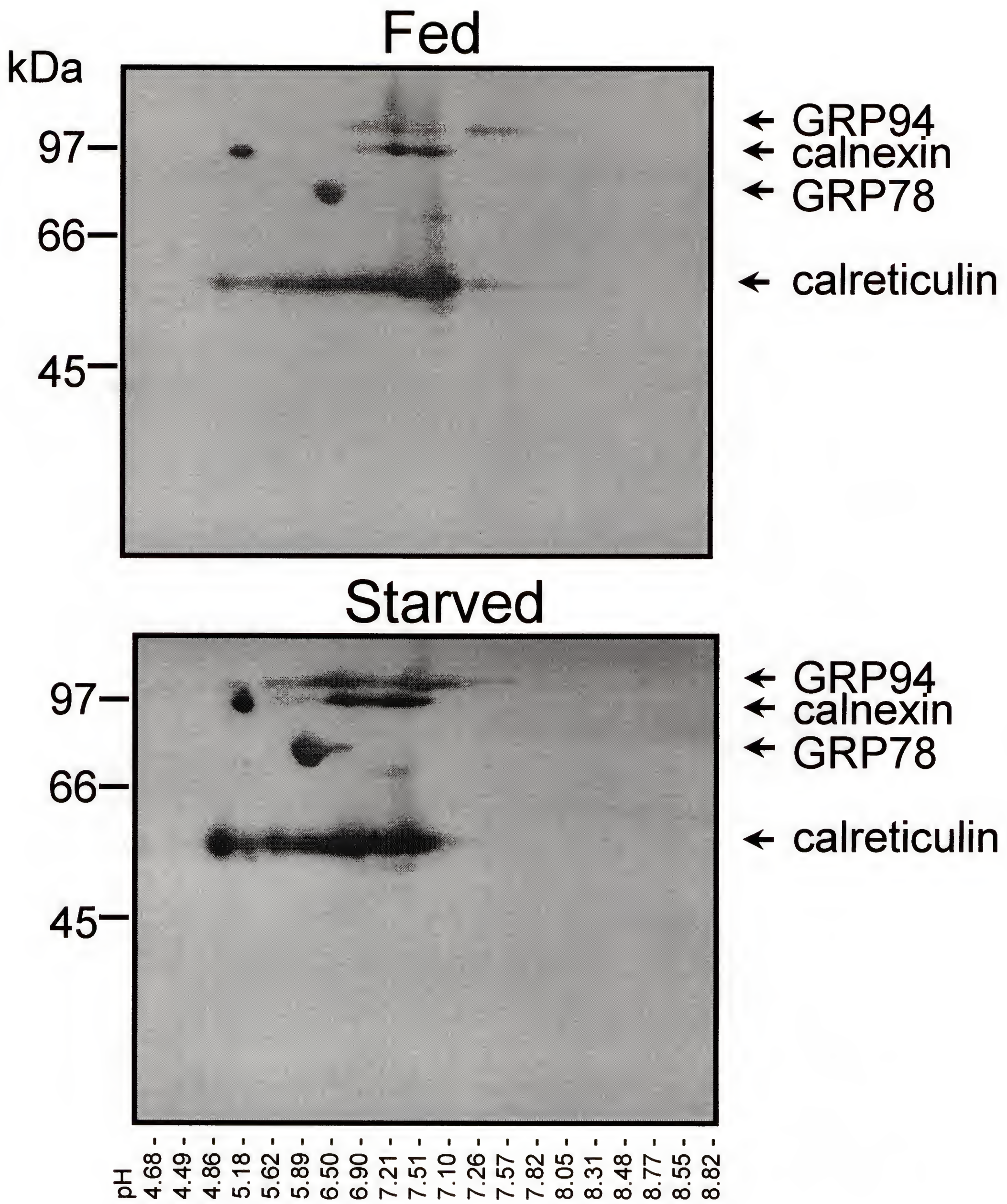

Figure 3-8 - Two-dimensional Analysis of ER Molecular Chaperones 3T3-L1 adipocytes were maintained in medium containing 25mM glucose (Fed) or 0mM glucose (Starved) for 24h. After 24h, HDM fractions were isolated. Four hundred μg of protein was solubilized in isoelectric focusing (IEF) solution before running the first-dimension (IEF), followed by the second-dimension (7.5% SDS-PAGE). Western analysis was performed using anti-GRP78, anti-GRP94, anti-calnexin, and anti-calreticulin antibodies. The vertical axis represents the molecular weight standards while the horizontal axis represents the pH gradient.

differ in that GLUT1 is heterogeneously glycosylated (Horuk et al., 1986). How this difference in oligosaccharide structure and not in the number of *N*-linked glycosylation sites contributes to the appearance of the alternative form of GLUT1, but not GLUT4 is unknown. In addition, both p37 and GLUT4 are processed to PM and LDM fractions, respectively. Furthermore, it is unknown why p37 does not interact with GRP78. Perhaps this observation can be explained in part by the structure of GLUT1, which is predicted to be a 12 transmembrane spanning protein. Although it is known that co-translational glycosylation affects the folding and/or assembly of several known proteins, a single aberrant glycosylation on GLUT1 on a short loop (32 amino acids) connecting the first and second transmembrane region may not affect folding. The transmembrane domains may insert into the lipid bilayer whether the GLUT1 is glycosylated or not. Therefore, since GRP78 only binds to exposed hydrophobic stretches of a protein (i.e., due to misfolding), it may not bind to p37. It would be interesting to know if p37 is functional at the PM. If the kinetics of p37 (i.e., Km for 2-deoxyglucose uptake) is different than for GLUT1, then it would imply that a single aberrant glycosylation of p37 does affect structure and/or function. In support, Asano et al.,

(1991) have shown that site-directed mutation of the single *N*-linked site on GLUT1 increases the Km for 2-deoxyglucose uptake by 2 - 2.5 fold. The effect of alternative glycosylation on structure and function will be further addressed using insulin receptor as a model.

CHAPTER 4
IDENTIFICATION AND CHARACTERIZATION OF INSULIN RECEPTOR PROCESSING INTERMEDIATES

Introduction

GLUT1, which possesses a single *N*-linked glycosylation site, would provide a simple model for examining the effect of aberrant glycosylation on protein processing. However, the extensive transmembrane structure may drive folding independent of its glycosylation status (refer to Conclusion section in Chapter 3). Glycosylation plays an important role in the maturation of a protein. Glucose deprivation, which alters normal glycosylation, provides a tool for examining the effect of aberrant glycosylation on protein processing. In 3T3-L1 adipocytes, glucose deprivation results in the synthesis of a lower molecular weight glycoform of GLUT1 (p37) but not GLUT4. This may be related to the delayed turnover of GLUT4 relative to GLUT1 (Sargeant and Paquet, 1993). Interestingly, aberrant glycosylation of GLUT1 does not prevent processing to the plasma membrane (McMahon and Frost, 1995). While p37 appears to be targeted to the PM, the functional status of p37 at the cell surface is yet to be determined. The aglyco form of GLUT1 (due to site directed mutation of the *N*-linked site), which is targeted to the cell surface, displayed higher Km for 2-deoxyglucose uptake than wild type GLUT1 (Asano et al., 1991). Thus GLUT1 belongs to the set of proteins whose processing may not be determined by glycosylation. In this system, glycosylation plays a different role, perhaps regulation of functional activity.

Glucose deprivation is handled in a cell-specific manner. In 3T3-L1 adipocytes, for example, the p37 form of GLUT1 is glycosylated as determined by N-glycosidase F sensitivity (McMahon and Frost, 1995). In normal rat kidney cells and 3T3-C2 fibroblasts, the lower molecular weight isoform of GLUT1 is resistant to N-glycosidase F, indicating that this isoform is not glycosylated (Haspel et al, 1986, Haspel et al, 1991). One possible reason for this difference lies in the size of the endogenous pool of stored glucose, i.e., glycogen. While adipocytes have significantly less glycogen than either muscle or liver, they still have nearly 100 times that of fibroblasts. Thus, when glycogen is mobilized in the absence of extracellular glucose, this pool is depleted more rapidly in fibroblasts than adipocytes. Adipocytes may be able to provide a significant buffer during glucose stress while the fibroblasts and perhaps other cell types are unable to do so.

Insulin receptor (IR) provides a more complicated model for examining the effect of aberrant glycosylation on processing. IR is a cell surface receptor composed of two α-subunits (each containing 14 potential *N*-linked sites), a single transmembrane domain, and two β-subunits (each containing 4 potential *N*-linked sites). The proreceptor must fold properly in order to be cleaved into the α- and β-subunits and to produce functional receptors. Glycosylation inhibitors, such as tunicamycin, castanospermine, and 1-deoxynojirimycin, and site-directed mutagenesis of *N*-linked sites, have been shown to cause accumulation in the ER. However, no one has closely examined the effect of glucose deprivation on insulin receptor processing. Glucose deprivation provides an advantage over glycosylation inhibitors and site-directed mutagenesis in that inhibition of glycosylation can be reversed with glucose readdition. This section examines the effect of glucose deprivation on insulin receptor processing.

Results

Subcellular Localization of the Insulin Receptor in 3T3-L1 Adipocytes

Using a subfractionation procedure developed in our lab (Fisher and Frost, 1996), we examined the distribution of the insulin receptor in control (F) adipocytes. Western blot analysis using a polyclonal antibody against the IR β-subunit revealed two forms of the receptor: the proreceptor which migrated as a 190kDa protein and the mature receptor, represented by the β-subunit, which migrated as a 95kDa protein (upper panel, Figure 4-1). Both the proreceptor and mature receptor were found in the HDM fraction which we have shown is composed of both ER and Golgi membranes (26). Only mature receptor was localized to the PM fraction which represented about 70% of the total IR pool (Table 4-1). No IR was found in the LDM fraction, which we and others have shown contains the translocatable pool of GLUT4 (James et

Table 4-1 - Subcellular Distribution of IR

	PM[a]IRβ	HDM[a]IRβ	Proreceptor	Alternative
	%	%	%	%
Fed	72 ± 14	24 ± 12	4 ± 3	
Starved	60 ± 14	17 ± 9		23 ± 13

[a] Values shown are percentage of the maximum.
These data represent a composite of eight independent experiments (n=8) performed as described in Figure 4-1. Units are represented as the average percentage ± SD of the total IR pool (PM + HDM). The LDM fraction is not considered in this calculation, since it contains no IR.

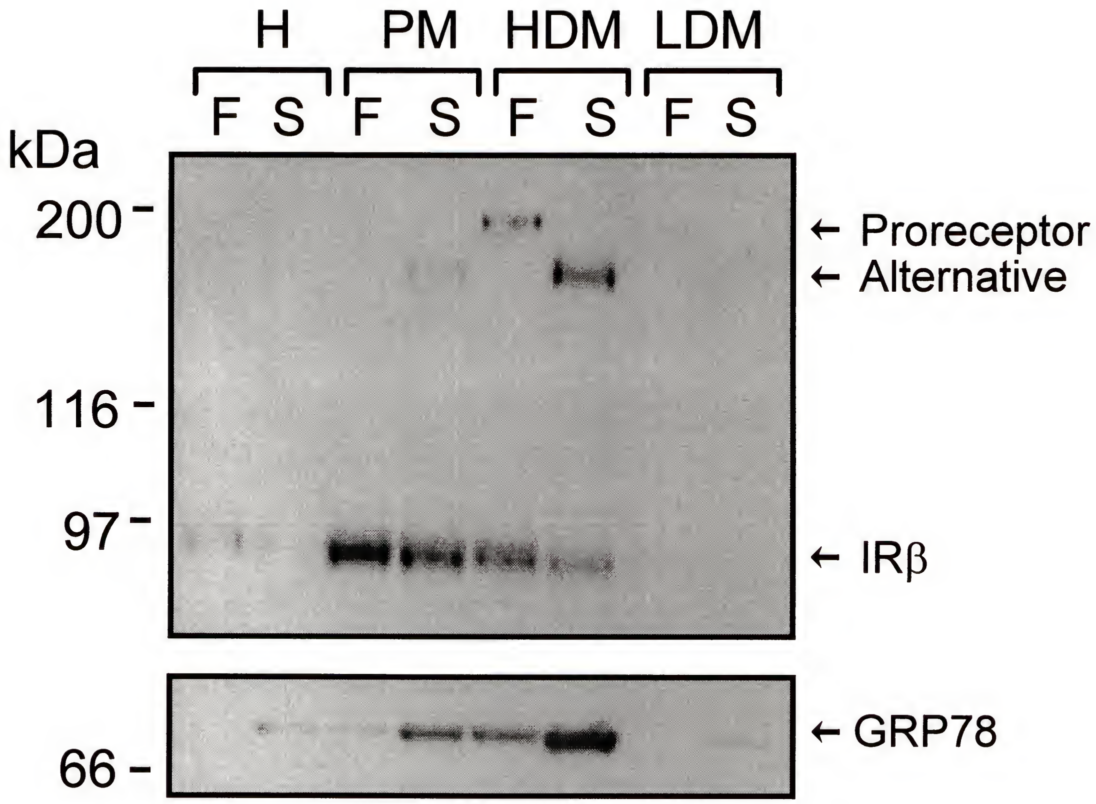

Figure 4-1 - Subcellular Distribution of IR in 3T3-L1 Adipocytes 3T3-L1 adipocytes were maintained in medium with (F) or without (S) 25mM glucose for 24h, after which the cell homogenate (H) was fractionated into PM, HDM, and LDM. An aliquot (50μg) of each fraction was run on a 7.5% SDS-PAGE. Western analysis was performed using anti-IRβ or anti-GRP78 antibodies, detected by ECL.

al., 1987; Czech and Buxton, 1993; Thomson et al., 1997). In cells deprived of glucose for 24h (S), the proreceptor migrated as a 170kDa species (upper panel, Figure 4-1). This "alternative" proreceptor represented nearly 25% of the total IR pool which was 6-fold more than the normal proreceptor in control cells (Table 4-1). Mature receptor was noted in both the HDM and PM fraction of glucose-deprived cells although expression was somewhat reduced relative to controls. This experiment was repeated eight times (n=8) in order to obtain statistics. Using the paired t-test, there was no statistical difference in the levels of IRβ (PM or HDM) from the glucose-deprived cells relative to controls. However, there was a general trend of less mature IRβ in glucose-deprived cells.

We also examined the expression of GRP78, an ER molecular chaperone. Confirming our earlier work (Fisher and Frost, 1996; Kitzman et al., 1996), we show that GRP78 is found predominantly in the HDM fraction and significantly elevated in glucose-deprived cells (lower panel, Figure 4-1). The apparent localization of GRP78 to the PM is due to the 10% contamination of ER membranes, an artifact of subfractionation in both control and glucose-deprived cells (Fisher and Frost, 1996).

Time-dependent Accumulation of the Alternative Proreceptor

In glucose-fed cells, the level of normal proreceptor and β-subunit remained relatively constant over time [Figure 4-2A and B]. In contrast, glucose deprivation led to the appearance of the alternative proreceptor by 12h with continued accumulation through 24h. The appearance of the alternative proreceptor by 12h of glucose deprivation correlates closely with the 42% depletion of the glycogen pool by 12h and >90% depletion by 24h (Figure 3-2). The 24h and 48h time points showed nearly identical accumulation denoting a new steady state. With the increase in the alternative proreceptor, a decrease in the level of IRβ in both the HDM and PM fractions was noted by 48h of glucose deprivation. By 48h of glucose deprivation, the alternative proreceptor represented the major insulin receptor species, suggesting that the alternative proreceptor is not processed but is rather retained in the ER compartment.

Synthesis of Insulin Receptor

To confirm that the alternative proreceptor is not processed with glucose deprivation, glucose-fed and glucose-deprived cells were metabolically labeled with [^{35}S]methionine/cysteine followed by immunoprecipitation

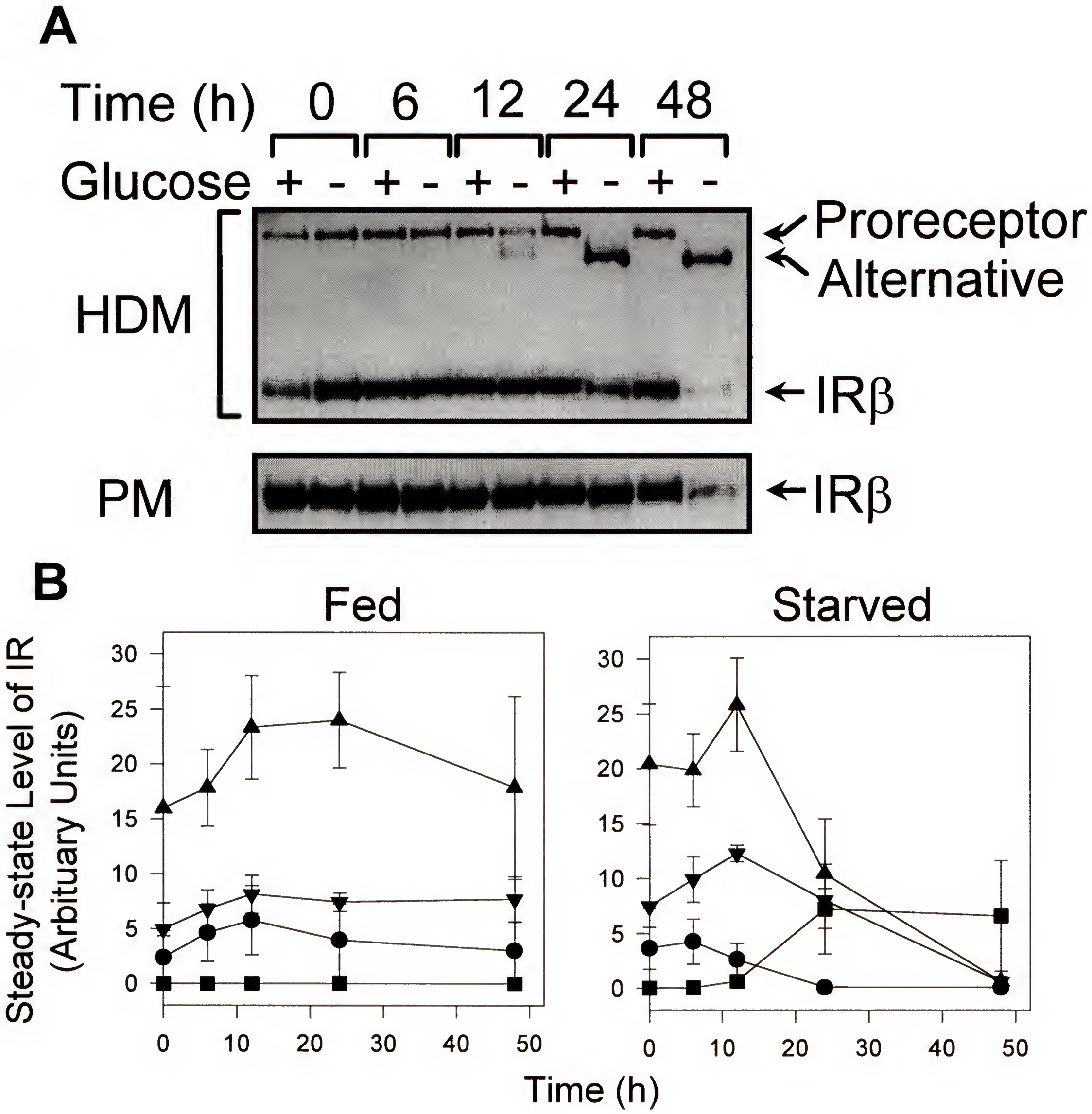

Figure 4-2 - Time-dependent Accumulation of Alternative Proreceptor Cells were maintained in medium with (F) or without (S) 25mM glucose for specific times (0, 6, 12, 24, and 48h). At each time point, the cell homogenates were fractionated into PM and HDM. An aliquot (50μg) of each fraction was run on a 7.5% SDS-PAGE, and Western analysis was performed using anti-IRβ antibodies (*A*). *B*, densitometric analysis of *A* represented as the average of three independent experiments (n=3) ± SD. ●, normal proreceptor; ■, alternative proreceptor; ▲, IRβ (HDM); ▼, IRβ (PM). Note that the HDM and PM imunoblots were developed with different exposure times (for relative intensities, see Figure 4-1).

[Figure 4-3A]. Densitometric analysis of these data is shown in Figure 4-3B. In both the glucose-fed and glucose-deprived cells, the normal and alternative proreceptors, respectively, were visible by 10min of labeling. The intensity of this labeling increased through the 3h pulse for both the normal and alternative proreceptors. In control cells, both α-and β-subunits became clearly visible by 1h of pulse. This indicates that the normal proreceptor was processed into mature receptor. Over the 3h pulse, no mature receptor was generated from the alternative proreceptor in glucose-deprived cells.

Characterization of the Oligosaccharide Structure on the Insulin Receptor

Because the alternative proreceptor migrated more rapidly than did the normal proreceptor, we tested whether the alternative proreceptor was glycosylated. Cells treated with *N*-glycosidase F, which removes all *N*-linked sugars, resulted in an aglyco-proreceptor species which migrated identically whether from glucose-fed or glucose-deprived cells (compare lanes 1 and 4 in the upper panel of Figure 4-4). While we expected that *N*-glycosidase F treatment of the normal proreceptor would result in accelerated migration, we were surprised that the same

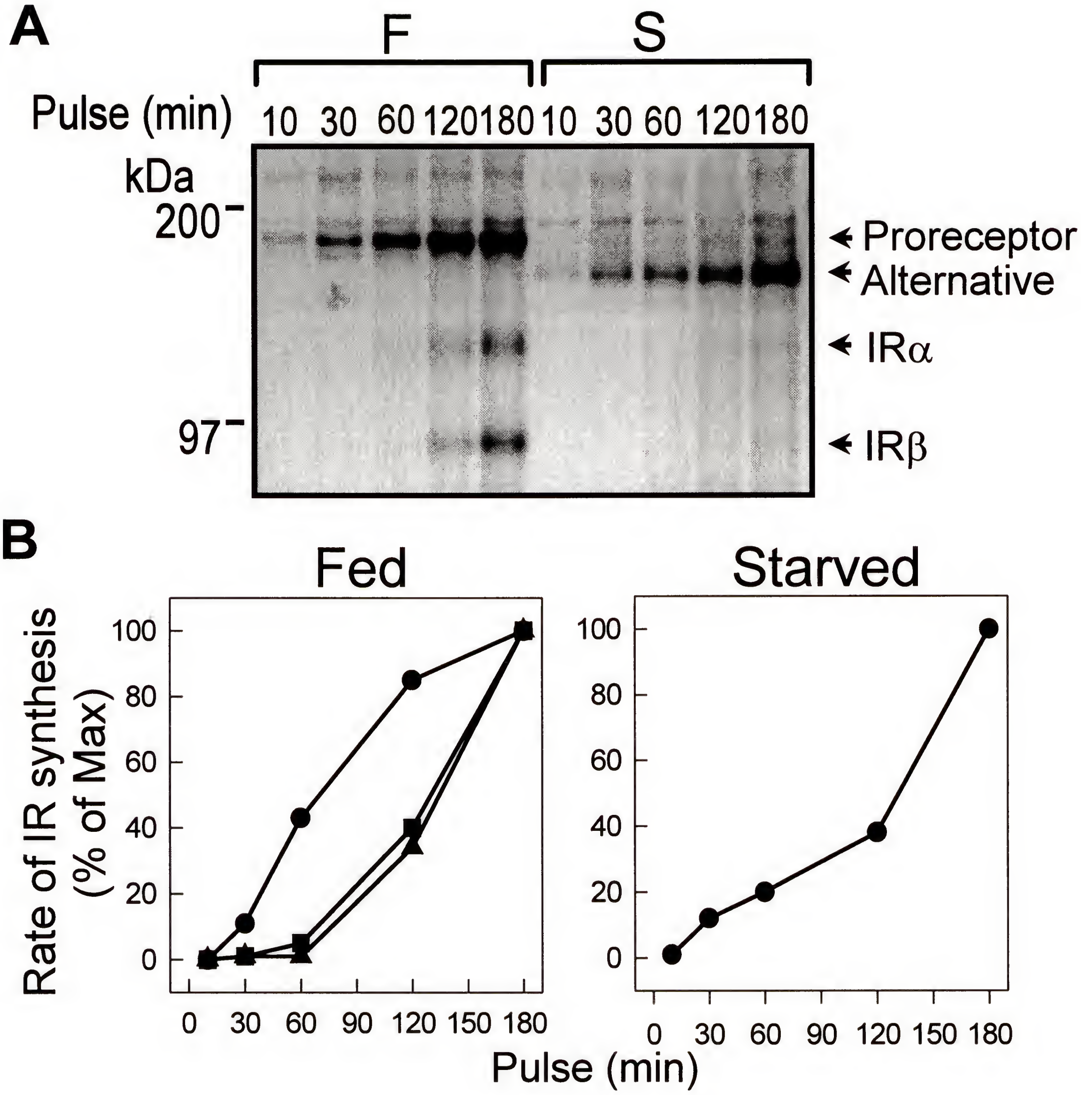

Figure 4-3 - Synthesis of IR *Panel A*, cells were maintained in medium with (F) or without (S) 25mM glucose for a total of 24h. Within that 24h period, cells were incubated for 1h in methionine- and cysteine-free medium (with or without glucose) followed by incubation in 200μCi/mL of [^{35}S]methionine/cysteine for 10, 30, 60, 120, or 180min. At each time point, total membranes (1.4mg) were extracted and precleared twice before immunoprecipitating with anti-IRβ antibody. Immunoprecipitates were resolved by 7.5% SDS-PAGE followed by autoradiography. *Panel B*, densitometric analysis of IR synthesis is represented as the percentage of maximum arbitrary units over the pulse time. These data are representative of two independent experiments (n=2). ●, normal (Fed) or alternative (Starved) proreceptor; ■, IRβ (HDM);▲, IRβ (PM).

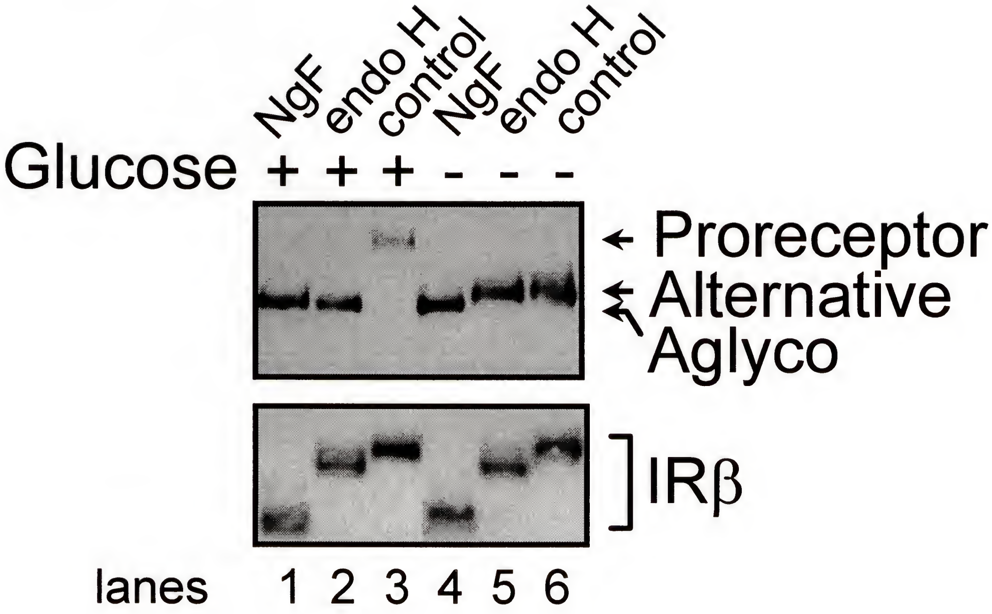

Figure 4-4 - Effect of Glycosylation on IR Migration Cells were maintained in medium with (F) or without (S) 25mM glucose for 24h. Aliquots (50μg) of HDM fractions from glucose-fed and glucose-deprived cells were treated with *N*-glycosidase F (NgF) or endoglycosidase H (endo H) before running on a 5% SDS-PAGE. Western analysis was performed using anti-IRβ antibody. This experiment is representative of two independent experiments (n=2).

occurred in glucose-deprived cells. This implies the attachment of a unique *N*-linked oligosaccharide core structure to the alternative proreceptor. This is supported by the fact that the alternative proreceptor was resistant to endo H treatment (lane 5) which is in contrast to the sensitivity of the normal proreceptor to endo H (lane 2). Sensitivity to endo H treatment indicates that the normal proreceptor contains high mannose oligosaccharides, which is consistent with earlier work (Ronnett et al., 1984). The β-subunit also showed sensitivity to endo H, indicating that at least some of the *N*-linked sites remain as high mannose structures. Note that the β-subunit behaves similarly in control and glucose-deprived samples. As shown in Figures 4-1 and 4-2, the steady state level of the mature receptor changes by only 10% at 24h of deprivation and derives from normal proreceptor.

In order to determine if both the α- and β-subunits are aberrantly glycosylated, the alternative proreceptor was first labeled with [^{3}H]mannose and then digested with furin *in vitro*. As shown in Figure 4-5, a 10μM concentration of [^{3}H]mannose was sufficient to label the oligosaccharide chains on the alternative proreceptor. Furin, a serine

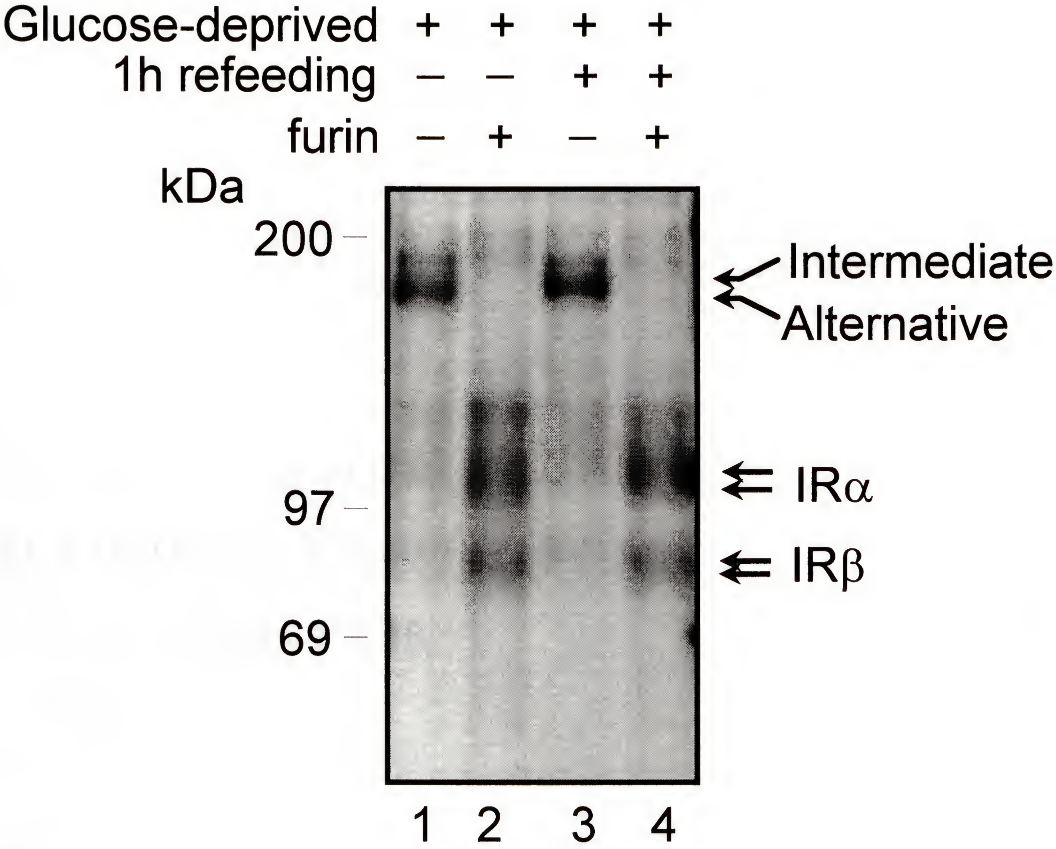

Figure 4-5 - Digestion of the Alternative Proreceptor with Furin Cells were maintained in medium without 25mM glucose for 21h. Cells were then replaced in glucose-free medium containing 420μCi/plate [^{3}H]mannose for 3h. Cells were then either collect or further chased in complete medium for 1h before collecting cells. The radiolabeled IR was immunoprecipitated. To the IR immune complex, 1μL furin (60U) was added and incubated for 2h before separating the immunoprecipitates by 7.5% SDS-PAGE followed by autoradiography.

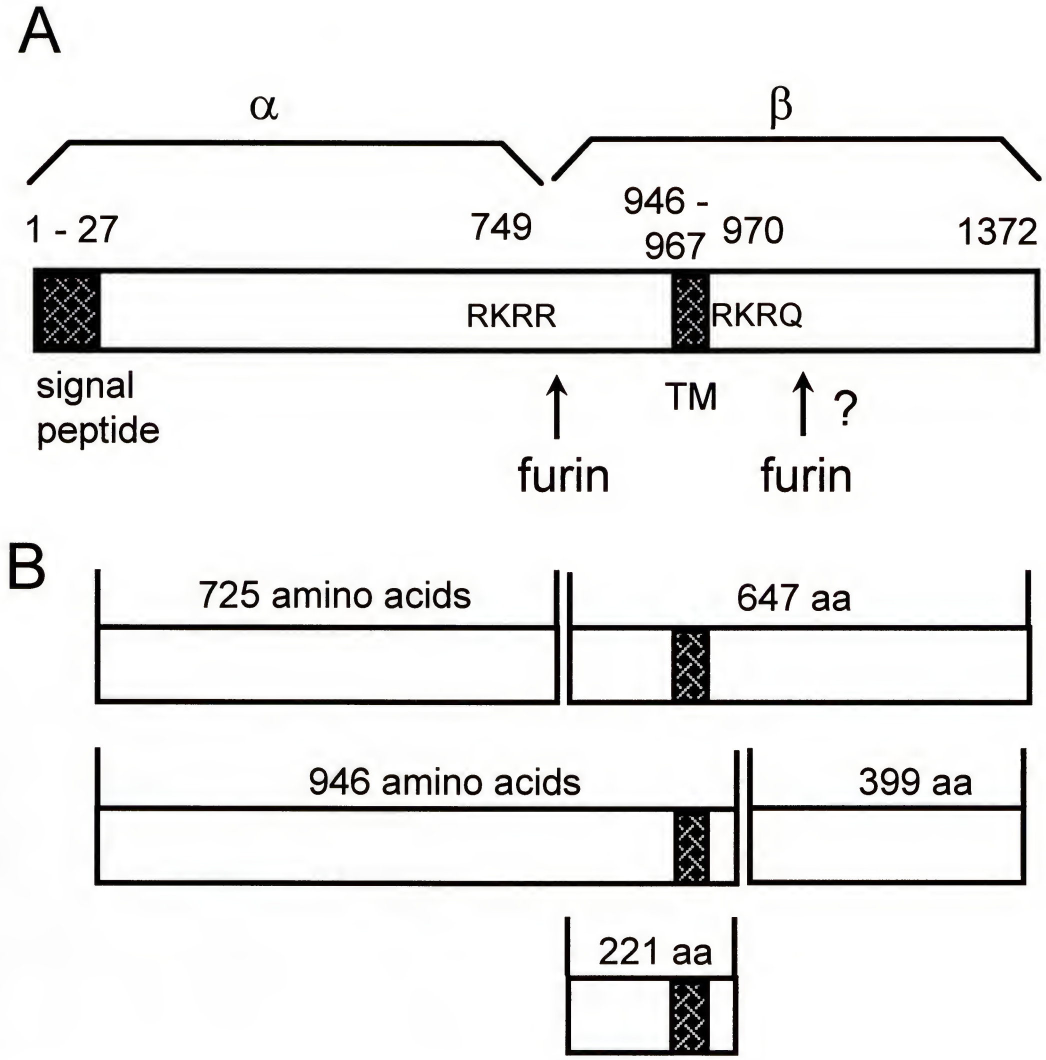

Figure 4-6 - A Model of Insulin Receptor Species Resulting from Two Furin Cleavage Sites Insulin proreceptor (mouse) is represented as a single polypeptide of 1,372 amino acids (*Panel A*). The physiological cleavage site (RKRR, each letter represents an amino acid) and a potential site (RKRQ) of furin are represented by arrows. Transmembrane domain is abbreviated as TM. Potential species resulting from two furin cleavages are represented in *Panel B*. The 725 amino acid (aa) and 647 aa species represent the normal α- and β-subunits, respectively.

endoprotease that is responsible for *in vivo* cleavage of the IR into the α- and β-subunits, was able to cleave the alternative proreceptor as well. However, instead of the expected α- and β-subunits, three bands were produced from the furin digest (lane 2). The lower band represents the β-subunit. We base this identification on similar experiments analyzed by Western blot analysis (data not shown). We also predict that the middle band is the α-subunit which migrates more rapidly than normal α-subunit due to reduced glycosylation.

The appearance of an upper band was unexpected. However, this higher molecular weight band could be explained if furin also cleaves at another furin-like cleavage site (amino acid position 970 - 973 of mouse insulin receptor) [Figure 4-6]. The resulting α- and β-species from the two furin cleavages (one physiological and the other non-physiological site) are represented in *Panel B*. Thus, the upper band could represent the 946 amino acid species, which contains the α-subunit and part of the β-subunit including the transmembrane domain. In Panel B, the 221 amino acid species would have run off the gel and thus, not detected. However, the lack of the 399 amino acid species in the gel is not known. This model of two furin cleavage sites poses two other problems. The first and last arginine residue of the physiological cleavage site (RKRR) are necessary for cleavage by furin (Yoshimasa et al., 1990; Bravo et al., 1994). In the furin-like site (RKRQ), the last position is occupied by an glutamine residue, although it maintains a positive charge. Furthermore, this furin-like site lies three amino acids from the transmembrane domain, which may not provide furin with the sufficient space for binding. Currently, we are searching for an antibody against the IRα in an attempt to identify and confirm the identity of the middle and upper bands.

Lane 3 represents the intermediate proreceptor which resulted from refeeding glucose-starved cells with complete medium containing glucose for 1h. The intermediate proreceptor is explained in Chapter 6. With respect to this experiment, digestion of the intermediate proreceptor with furin also resulted in three bands. However, the IR β-subunit in lane 3 appears to migrate slightly higher than the IR β-subunit in lane 2 (represented as two arrows in Figure 4-5). This may be due to additional glycosylation of the β-subunit (see Chapter 6). The same may be true for the α-subunit as well.

Functional Activity of the Alternative Proreceptor

The structure of a protein usually has an impact on function and frequently glycosylation impacts folding which ultimately determines structure and function. There are 18 potential *N*-glycosylation sites (14 sites on the α-subunit and 4 sites on the β-subunit). Aberrant glycosylation of these sites may affect protein folding. Although protein structure was not directly examined, the effect of aberrant glycosylation on the alternative proreceptor function was tested. As a functional assay, we examined the autophosphorylation activity of IR in the absence or presence of insulin. As shown in Figure 4-7A, the normal proreceptor showed a basal level autophosphorylation activity which could be stimulated approximately 4-fold with insulin. This data is consistent with published results from the literature (Bass et al., 1998). The alternative proreceptor also showed basal level activity. However, it did not exhibit insulin-sensitive autophosphorylation. The mature IRβ under all metabolic conditions showed a 6-fold stimulation with insulin. Recall that the mature receptor represents normal receptor processing which has occurred because of the delayed effects of glucose deprivation (see Figure 4-2).

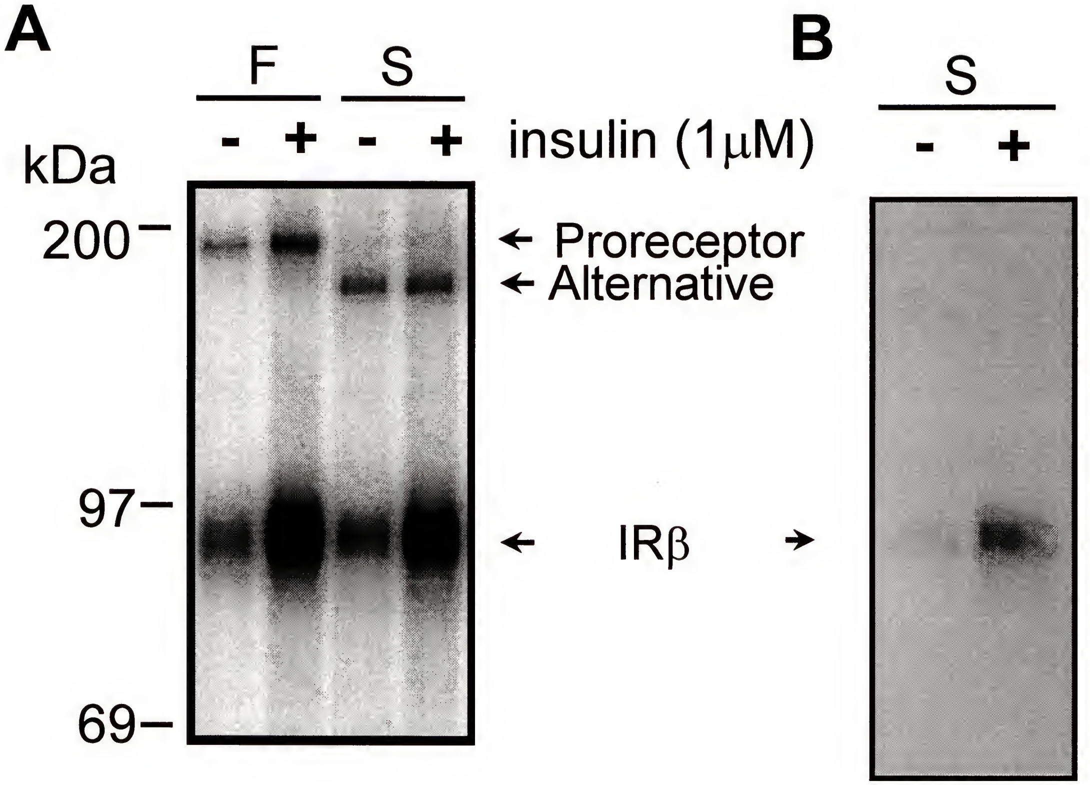

Figure 4-7 - Insulin-stimulated Autophosphorylation of IR
Cells were maintained in medium with (F) or without (S) 25mM glucose for 24h. IR was immunoprecipitated from total membrane proteins (3.5 - 4.0mg) using anti-IRβ antibody. *A*, Autophosphorylation assay using [γ-^{32}P]ATP in the absence or presence of 1μM insulin was performed directly on the IR immune complex. Immunoprecipitates were resolved by 7.5% SDS-PAGE followed by autoradiography. *B*, Immunoprecipitates were resolved by 7.5% SDS-PAGE followed by Western analysis using anti-pY antibody. Data in *A* is representative of data from 7 independent experiments (n=7).

Autophosphorylation of all three tyrosine residues (Tyr^{1146}, Tyr^{1150}, and Tyr^{1151}) on the human IR β-subunit stimulates its kinase activity 10-20 fold (White and Kahn, 1994). To confirm that autophosphorylation is occurring on tyrosine residues, immunoprecipitated IR that has been incubated in autophosphorylation solution (minus [^{32}P]ATP) was probed with a phospho-tryosine (pY) antibody by Western blot analysis (Figure 4-7B). The IR β-subunit, representing the mature receptor, showed a large stimulation with insulin, thus confirming that it is indeed autophosphorylated on tyrosine residues. However, this assay was not sensitive enough to detect either the normal or the alternative proreceptor.

Conclusions

Glucose exerts regulatory control over a number of metabolic processes including protein glycosylation. Specifically, glucose which provides substrates for protein glycosylation is necessary for normal glycosylation of the insulin proreceptor. In the presence of extracellular glucose, the insulin proreceptor is glycosylated resulting in a band which migrates as a 190kDa protein. In contrast, in the absence of extracellular glucose, an alternative proreceptor which migrates as a 170kDa protein accumulates in a time-dependent manner in the HDM fraction, which is enriched in ER and Golgi. Thus, at steady-state, the normal proreceptor represents 4% of the total IR population whereas the alternative proreceptor represents 23%. When further examining the glycosylation of the alternative proreceptor, both the α- and β-subunits of the alternative proreceptor could be radiolabeled with [^{3}H]mannose, which confirms that the alternative proreceptor is indeed glycosylated. Furthermore, glucose deprivation leads to aberrant glycosylation resulting in an endoglycosidase H resistant but endoglycosidase F sensitive species.

Aberrant glycosylation of the alternative proreceptor results in loss of function. Whereas autophosphorylation of the normal proreceptor could be stimulated 4-fold with insulin, the alternative proreceptor was not sensitive to insulin, although there was a basal level of autophosphorylation activity. There are two potential explanations for this loss of insulin-stimulated autophosphorylation activity. Either, insulin cannot bind to the α-subunit (i.e., α-subunit is misfolded) or insulin may bind to the α-subunit but cannot transmit a signal to the β-subunit for stimulation of autophosphorylation activity. The former possibility can be tested by determining the binding affinity of [I^{125}]insulin. Although the effect of aberrant glycosylation on protein folding was not directly tested, the loss of insulin-stimulated autophosphorylation of the alternative proreceptor strongly argues for misfolding of the alternative proreceptor.

Aberrant glycosylation is known to cause misfolding of proteins. Misfolded proteins are retained in the ER and degraded by cytoplasmic proteosomes. Several ER molecular chaperones (see Figure 3-6 or 3-7) including GRP78 are known to be involved in this quality control system whereby correctly folded proteins continue to the Golgi whereas misfolded proteins are retained in the ER by virtue of their interaction with a molecular chaperone(s). Misfolded proteins that are retained in the ER are then targeted for degradation. In Chapter 5, the role of GRP78 in retention and degradation of the alternative proreceptor will be addressed.

CHAPTER 5

ROLE OF GRP78 AND PROTEOSOMES IN ALTERNATIVE PRORECEPTOR DEGRADATION

Introduction

Cells possess a number of survival mechanisms to cope with adverse changes in their environment. One stress-related response mechanism is termed the unfolded protein response. The unfolded protein response is induced by a variety of stress conditions, such as glucose or amino acid deprivation, tunicamycin treatment, or sulfhydryl-reducing agents, all of which affect protein folding in the ER (Pahl and Baeuerle, 1997). The induction of the unfolded protein response leads to the transcriptional activation of several molecular chaperones, including GRP78 (also known as BiP). GRP78 is an ER resident molecular chaperone which is hypothesized to play an important role in "quality" control in the ER (Kopito, 1997). Under normal conditions, GRP78 binds transiently to newly synthesized proteins, releasing properly folded proteins for processing to the Golgi. Misfolded proteins remain bound to GRP78 and are eventually degraded by cytoplasmic proteosome (Klausner and Sitia, 1990; Ward et al., 1995). One study has addressed the role of the proteosome in insulin proreceptor degradation (Imamure et al., 1998). In that study, proteosome inhibitors, MG115 and MG132, inhibited degradation of insulin receptor with two double mutants, Asp^{1179} or Leu^{1193} point mutations with a deletion of exon 13. Furthermore, the heat shock protein, Hsp90, was shown to play a role in mediating the degradation of the mutant proreceptors.

Only two studies have examined the interaction of the insulin receptor with GRP78. In each case, overexpression of mutated receptors was necessary to examine this interaction (Accili et al., 1992; Sawa et al., 1996)). In this section, we show for the first time in a normal setting that glucose deprivation of 3T3-L1 adipocytes causes accumulation of the insulin proreceptor in the ER as a result of interaction with GRP78.

Results

Insulin Receptor Processing and Turnover

Because the alternative proreceptor was not processed, we examined its rate of degradation. Glucose-fed or glucose-deprived cells were pulsed for 1h with $[^{35}S]$methionine/cysteine and chased for specific times in the presence or absence of 25mM glucose, as appropriate,

Figure 5-1 - IR Processing and Turnover *Panel A*, Cells were maintained in medium with (F) or without (S) 25mM glucose for a total of 24h. Within that 24h period, cells were incubated for 1h in methionine- and cysteine-free medium (with or without glucose) followed by incubation in 200μCi/mL of [^{35}S]methionine/cysteine for 1h. Cells were then chased in medium with or without 25mM glucose for 1, 3, 6, 12, or 24h. Total membranes (1.4mg) were extracted and precleared twice before immunoprecipitating with anti-IRβ antibody. Immunoprecipitates were resolved by 7.5% SDS-PAGE followed by autoradiography. *Panel B*, Densitometric analysis of IR synthesis is represented as the percentage of maximum arbitrary units over the chase time (h). ●, normal (Fed) or alternative (Starved) proreceptor; ■, IRβ (HDM);▲, IRβ (PM). *Panel C*, Average sum of the normal proreceptor and α- and β-subunits from glucose-fed samples from three independent experiments (n=3) are represented as the percentage maximum arbituary units (average) over the chase time (h). The log of (% max)$_{avg}$ is plotted on the right. ●, (proreceptor + IRα + IRβ)$_{avg}$.

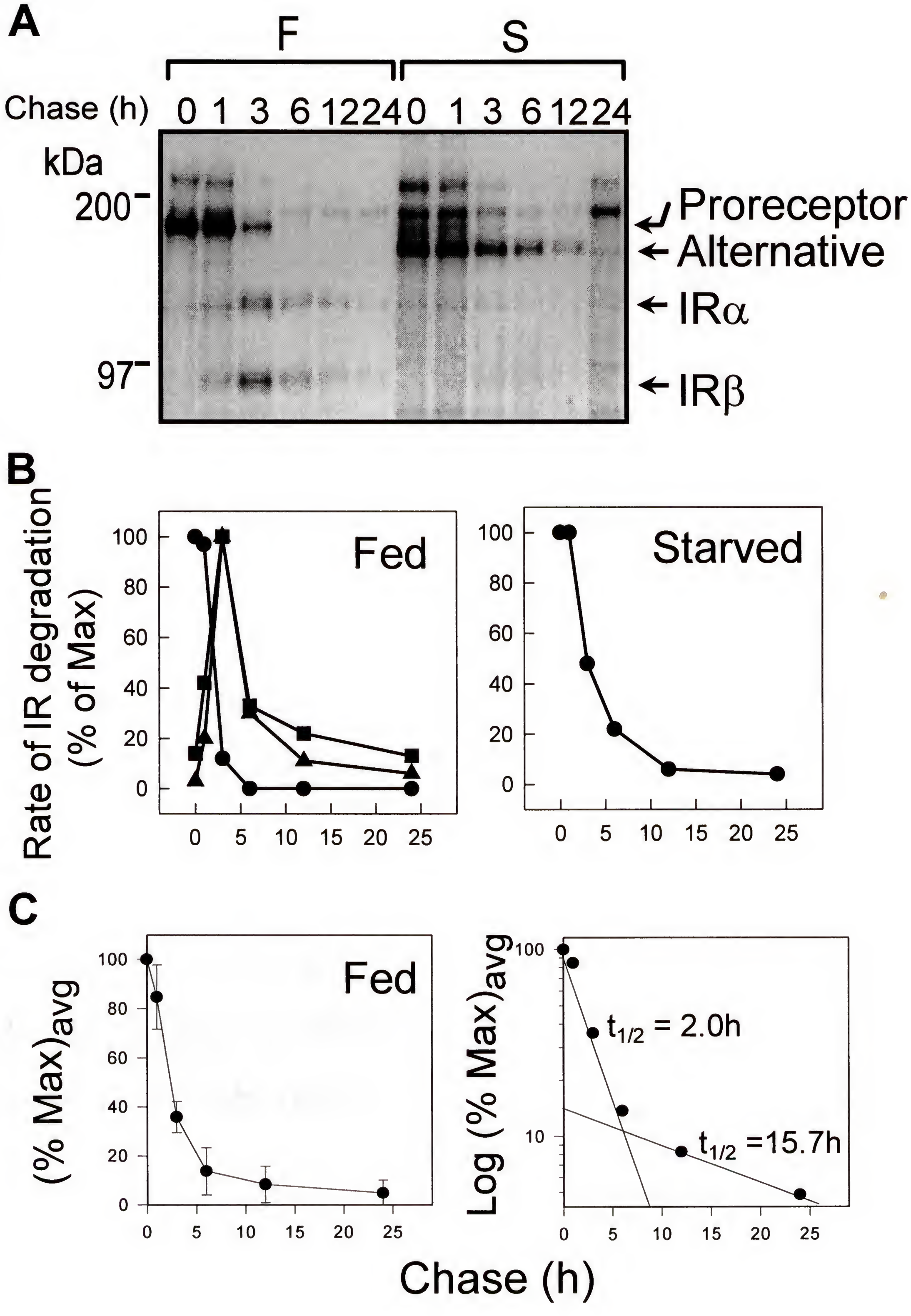
A
F
S
Chase (h)
0 1 3 6 12 24 0 1 3 6 12 24
kDa
200
97
Proreceptor
Alternative
IRα
IRβ
B
Rate of IR degradation (% of Max)
100
80
60
40
20
0
0 5 10 15 20 25
Fed
Starved
C
(% Max)avg
Fed
Log (% Max)avg
100
10
t1/2 = 2.0h
t1/2 =15.7h
Chase (h)

before immunoprecipitating IR from total membrane fractions. As shown in Figure 5-1A, the processing of normal proreceptor into the α- and β-subunits was observed by 1h of chase and reached a maximum by 3h. The half-life of the normal proreceptor was 1.3h ± 0.6h (n=3), as determined by first order regression of densitometric data (Figure 5-1B). Because cleavage of the proreceptor to individual α- and β-subunits occurs in the trans Golgi network, this represents the time it takes for the proreceptor to leave the ER and move through the various Golgi compartments. The half-life of the total IR pool (normal proreceptor, IRα, plus IRβ) displayed two-components (Figure 5-1C). The first component showed a half-life of 2.0h, which reflects the rapid processing of the proreceptor into the α- and β-subunits. The second component has a longer half-life of 15.7h, which reflects the degradation of the mature IR. This half-life corresponds well with the half-life ($t_{1/2}$ = 14.8h) measured by Ronnett et al. (1982).

In contrast, the alternative proreceptor was not processed but rather degraded slowly with a half-life of 5.1h ± 0.6h (n=3). This extended half-life corresponds well with the half-life of a mutant insulin receptor ($t_{1/2}$ =

5h) which also failed to be processed to the cell surface (Maassen et al., 1991). Furthermore, the lack of processing of the alternative proreceptor into the α- and β-subunits, means that the alternative proreceptor did not reach the trans Golgi network, where cleavage of the proreceptor and targeting to PM, lysosome, or other compartments occur. Thus, removal of the alternative proreceptor from the ER, which is delayed with respect to the normal proreceptor, must occur through another pathway.

Interaction of GRP78 with the Alternative Proreceptor

Molecular chaperones such as GRP78 are known to retain misfolded proteins in the ER. To determine if the alternative proreceptor interacts with GRP78, we performed co-precipitation assays. Figure 5-2 compares those proteins which co-precipitate with IR in the fed and deprived states. In *Panel A*, only three proteins were precipitated by the β-subunit antibody: the normal proreceptor, the α-subunit, and the β-subunit. Note that immunoprecipitation with anti-GRP78 antibodies identified no radiolabeled protein, consistent with the low synthetic rate of GRP78 observed by others in the glucose-fed state (Pouyssegur et al., 1977; Shiu et al., 1977; Kozutsumi et al., 1988). With glucose-deprived cells, the β-subunit

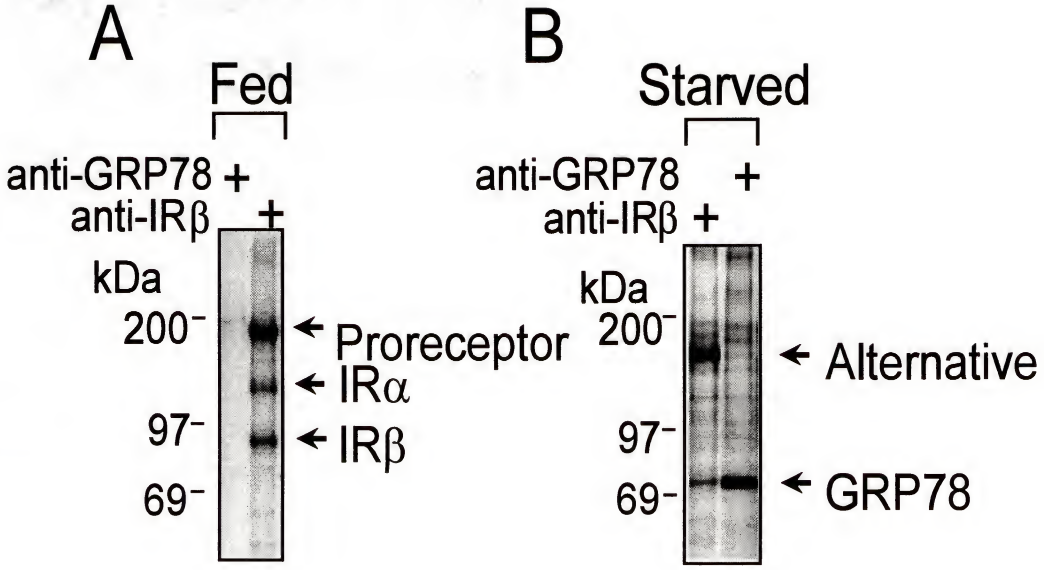

Figure 5-2 - Co-precipitation of GRP78 with IR Cells were glucose-fed (*Panel A*) or glucose-starved (*Panel B*), depleted of methionine and cysteine for 1h, and labeled with [^{35}S]methionine/cysteine for 3h. Total membranes were used for immunoprecipitation with anti-IRβ or anti-GRP78 antibodies. This experiment is representative of two independent experiments (n=2).

antibody precipitated not only the alternative proreceptor but as well a band which migrated as a 72kDa protein [*Panel B*]. Calnexin and calreticulin failed to co-precipitate with the alternative proreceptor. This implies that the aberrant oligosaccharide structure on the alternative proreceptor is not monoglucosylated. GRP78, immunoprecipitated from an identical sample, migrated in identical fashion as the 72kDa protein. Note that GRP78 co-precipitated a number of proteins, including a faint band which migrated like the alternative proreceptor. To further analyze the specificity of interaction, we took advantage of the ATP-dependence of GRP78 binding (Carlino et al., 1992; Toledo et al., 1993; Wei et al., 1995). Figure 5-3 shows that 50μM ATP was sufficient to release GRP78 from the IR immune complex collected from glucose-deprived cells. Neither high salt wash (1M NaCl) nor ADP treatment was able to dissociate the 72kDa protein from the IR (data not shown).

Finally, we used the isoelectric point of GRP78 to verify the identity of the 72kDa protein. Shown in Figure 5-4 are two-dimensional gels which compare the migration pattern of the 72kDa protein [*Panel A*] with that of authentic GRP78 [*Panel B*]. Antibodies against GRP78 precipitated two forms of the protein. It is likely that

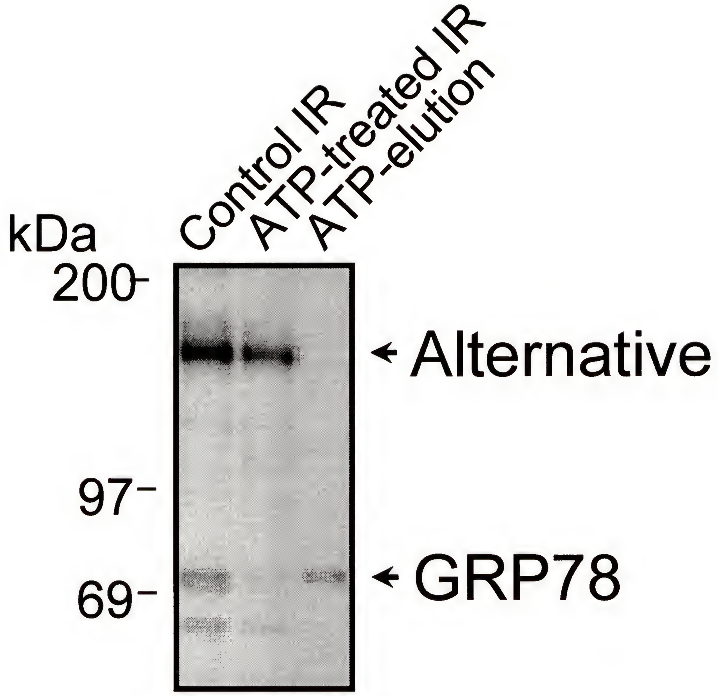

Figure 5-3 - ATP-dependent Interaction of IR with GRP78
Glucose-deprived cells were labeled for 3h and immunoprecipitated as before. The IR immune complex was treated without (control) or with 50μM ATP. The immune complex was collected and separated from the eluate. These were separately resolved by 7.5% SDS-PAGE, followed by autoradiography. This experiment is representative of two independent experiments (n=2).

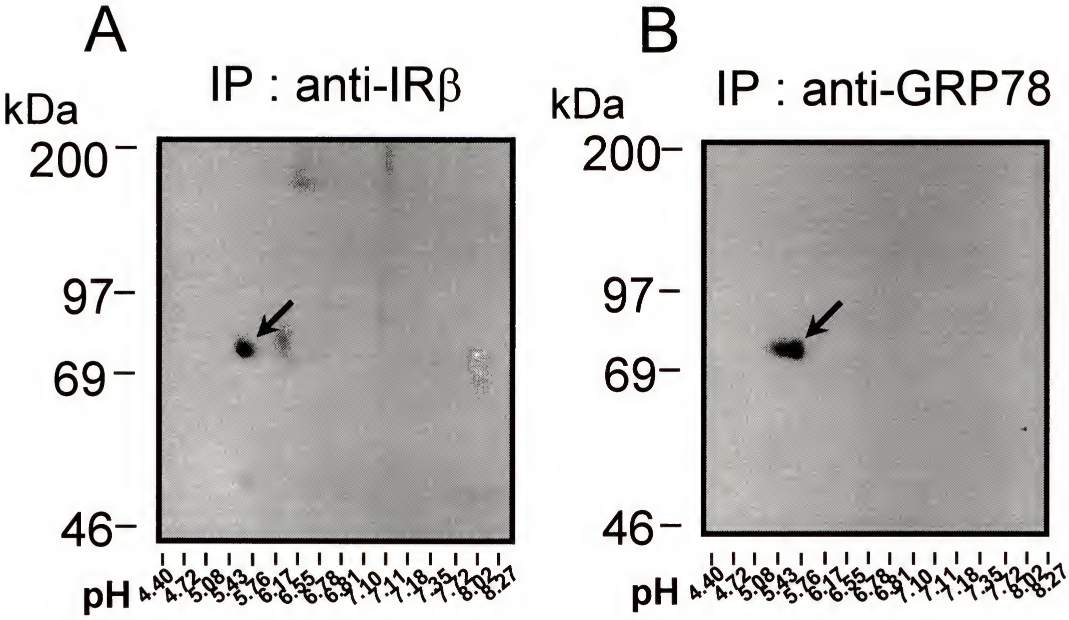

Figure 5-4 - Two-dimensional Analysis of IR and GRP78
Glucose-deprived cells were labeled for 3h and immunoprecipitated as before with either anti-IRβ or anti-GRP78 antibodies. The IR immune complexes were resolved by two-dimensional gel electrophoresis. Molecular weight is represented on the vertical axis, while the pH gradient is represented on the horizontal axis. The arrows point to the more basic form of GRP78.

one of these isoforms is either ADP-ribosylated and/or phosphorylated which causes homodimerization with itself (Freiden et al., 1992). Only in the unmodified state, does GRP78 dissociate from itself to interact with misfolded proteins. Anti-β-subunit antibodies co-precipitated only one form of GRP78 [*Panel A*] which aligned with the more basic, unmodified isoform of GRP78 [*Panel B*]. Together, data from Figures 5-2 through 5-4 provide strong support for the interaction of the alternative proreceptor with GRP78.

Proteosome-mediated Degradation of the Alternative Proreceptor

GRP78 is known to target misfolded proteins for degradation by the cytoplasmic proteosome. Although the mechanism of "ER degradation" is not well understood, many misfolded proteins have been shown to be degraded by the proteosome using proteosome-specific inhibitors such as lactacystin (a fungal metabolite) and MG132, a nonhydrolyzable peptide analogue (N-carbobenzyloxy-leucinyl-leucinyl-leucinal). As shown in Figure 5-5, the effect of lactacystin on newly synthesized and radiolabeled alternative proreceptor was tested. Contrary to our prediction, lactacystin did not inhibit loss of the alternative proreceptor. Instead, in the presence of

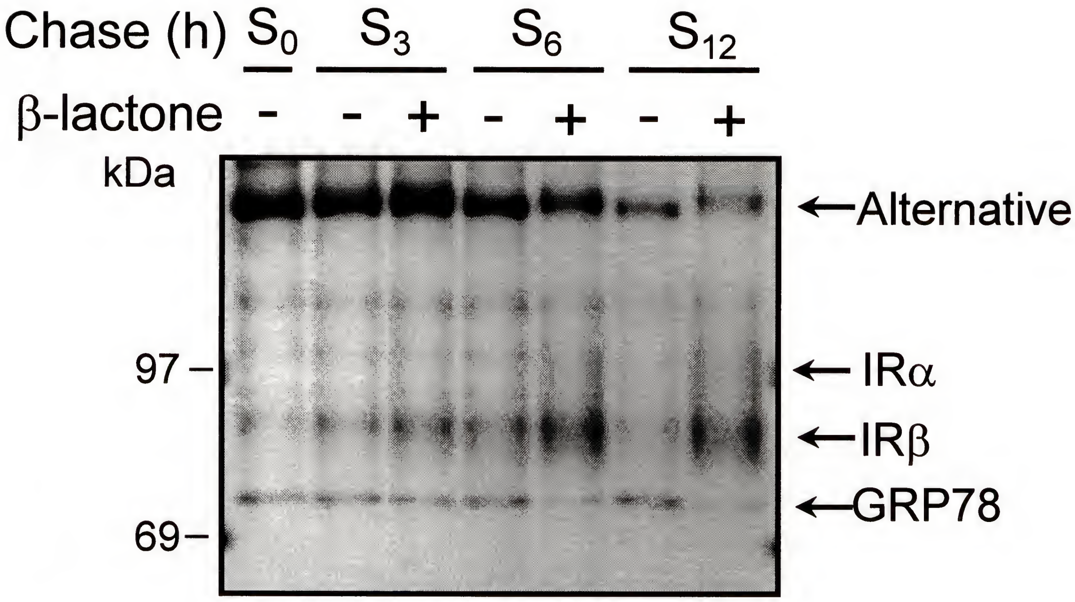

Figure 5-5 - Effect of Lactacystin on Degradation of the Alternative Proreceptor Glucose-fed or glucose-deprived cells were labeled with $[^{35}S]$methionine/cysteine (200μCi/mL) for 3h. Cells were then chased in glucose-free medium with or without 10μM lactacystin β-lactone for specific times (3, 6, or 12h). At each time point, cells were collected. Total membranes were extracted and precleared twice before immunoprecipitating with anti-IRβ antibody. Immunoprecipitates were resolved by 7.5% SDS-PAGE, followed by autoradiography.

lactacystin, there was an increase in intensity of a 90kDa band which corresponds to the β-subunit. The intensity of this band reached a maximum by 6h of chase in the absence of glucose. It appears that inhibiting the proteosome forced the alternative proreceptor into the processing path, allowing furin-specific cleavage. However, the 90kDa protein could also represent an intermediate in the proteosome-dependent degradation path. If the lactacystin-sensitive step occurs after the production of the intermediate, then blocking that step would cause accumulation of the intermediate. Lactacystin inhibits trypsin-like, chymotrypsin-like, and peptidylglutamyl activities of the proteosome. Proteolytic activities of the proteosome not inhibited by lactacystin include branched chain amino acid hydrolyzing and small neutral amino acid hydrolyzing activities. There is also evidence for proteolytic activity in the ER. Loo and Clarke (1998) showed that the expression of a human P-glycoprotein with a point mutation (Arg^{113}) caused misfolding and proteolytic cleavage from a 150kDa glycosylated intermediate to a proteolytically cleaved 130kDa protein. There is another problem to be addressed if we consider that the 90kDa band to be the furin-cleaved β-subunit. An arrow points to the molecular weight range where the α-subunit should migrate

(Figure 5-5), but there is no detection of the α-subunit. One plausible explanation is that the α-subunit has not formed its proper disulfide bonds with the β-subunit during folding of the alternative proreceptor. If this is the case, then the α-subunit would not be expected to co-precipitate with the furin-cleaved β-subunit using an antibody against the β-subunit. At present, we have not distinguished between these various possibilities.

The result of the lactacystin experiment was confirmed with the use of another proteosome inhibitor, MG132. As shown in Figure 5-6, MG132 produced the same result as that of lactacystin. Thus, taken together, these two data support processing rather than inhibition of the alternative proreceptor in the presence of proteosome inhibitors.

To show that the lysosome does not play a role in the degradation of the alternative proreceptor, three lysosomal inhibitors (ammonium chloride, leupeptin, and chloroquin) were tested. As well the effect of brefeldin A, an agent which collapses the Golgi and ER into the same compartment was tested. Neither MG132, ammonium chloride (NH_4Cl), leupeptin, chloroquin, nor brefeldin A (BFA) prevented

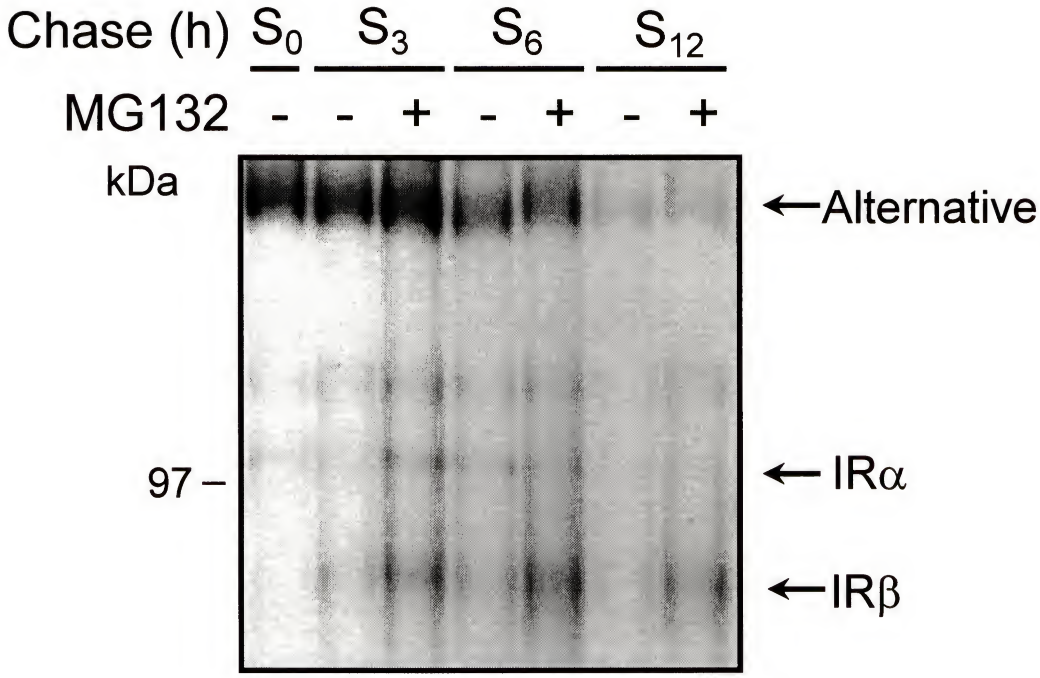

Figure 5-6 - Effect of MG132 on Degradation of the Alternative Proreceptor Glucose-fed or glucose-deprived cells were labeled with [^{35}S]methionine/cysteine (200μCi/mL) for 3h. Cells were then chased in glucose-free medium with or without 50μM MG132 for specific times (3, 6, or 12h). At each time point, cells were collected. Total membranes were extracted and precleared twice before immunoprecipitating with anti-IRβ antibody. Immunoprecipitates were resolved by 7.5% SDS-PAGE, followed by autoradiography.

degradation of the alternative proreceptor, and only MG132 resulted in an increase in β-subunit (Figure 5-7). Thus, the lysosome does not play a role in the degradation of the alternative proreceptor.

Conclusions

Glucose deprivation of 3T3-L1 adipocytes resulted in degradation of the alternative proreceptor, rather than processing, with a half-life of 5h. Failure of the alternative proreceptor to process properly resulted in accumulation in the ER by virtue of its interaction with GRP78 (an ER resident protein), but not calnexin or calreticulin. The interaction between GRP78 and the alternative proreceptor was specific because ATP, and not ADP or NaCl, was able to disrupt this interaction.

The proteosome has been shown to be responsible for the degradation of mutant insulin receptors (Imamure et al., 1998). The proteosome inhibitor studies support a role for the involvement of proteosome in the degradation of the alternative proreceptor. The proteosome inhibitors, lactacystin and MG132 which together inhibit four of the five known proteolytic activities, were unable to inhibit degradation of the alternative proreceptor. However, the presence of either lactacystin or MG132 in the chase medium

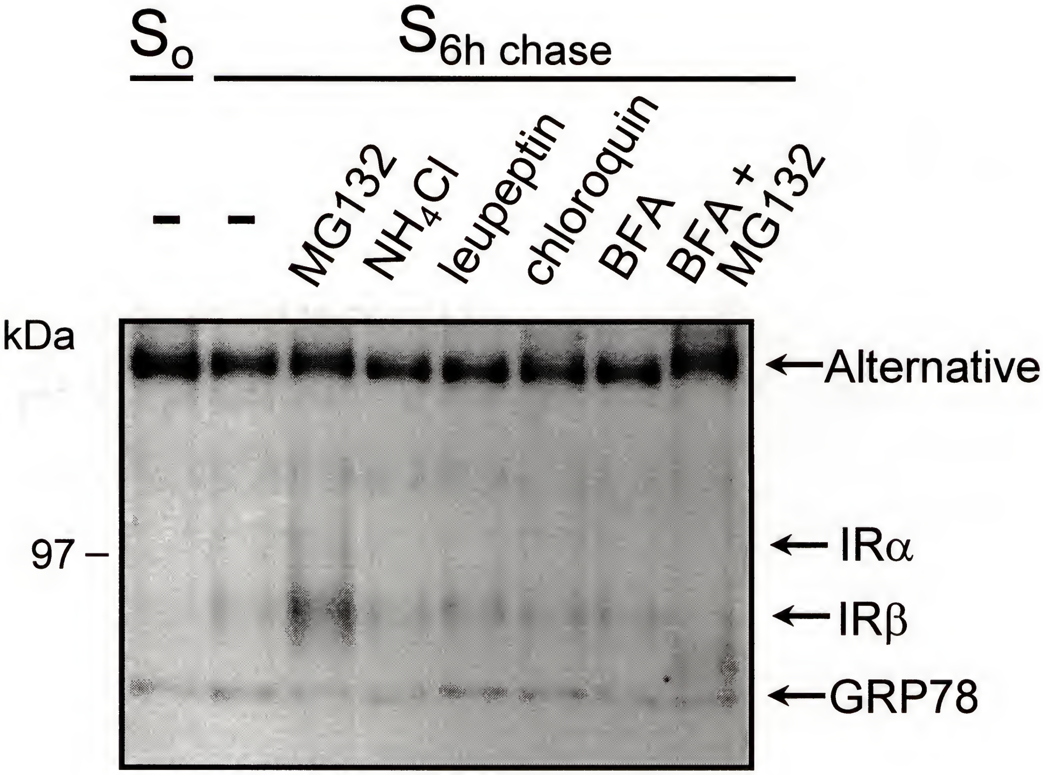

Figure 5-7 - Effect of Lysosomal Inhibitors on the Degradation of the Alternative Proreceptor Glucose-fed or glucose-deprived cells were labeled with [^{35}S]methionine/cysteine (200μCi/mL) for 3h. Cells were then chased in glucose-free medium with or without inhibitors (50μM MG132, 50μM NH_4Cl, 50μM leupeptin, 50μM chloroquin, 5μg/mL brefeldin A) for 6h. Total membranes were extracted and precleared twice before immunoprecipitating with anti-IRβ antibody. Immunoprecipitates were resolved by 7.5% SDS-PAGE, followed by autoradiography.

may have allowed time for the alternative proreceptor to escape the degradative pathway and be processed by the furin endoprotease, resulting in the 90kDa β-subunit. This β-subunit is most likely still membrane-bound since immunoprecipitation is carried out with total membrane proteins. The α-subunit failed to be co-precipitated with the β-subunit, which implies a lack of covalent bonding with the β-subunit. If this is the case, then there is the possibility that the α-subunit may be secreted into the chase medium whereas the β-subunit is processed to the cell surface and/or degraded through the lysosomal pathway. Thus, our studies support the proteosome-mediated degradation of misfolded proteins that are bound to ER molecular chaperones such as GRP78.

CHAPTER 6
REPROCESSING OF THE ALTERNATIVE PRORECEPTOR WITH GLUCOSE REFEEDING

Introduction

Glucose deprivation poses a significant stress to cells. One of the criticisms of glucose deprivation concerns the viability of cells after such a harsh condition. In response to this criticism, it should be mentioned that 3T3-L1 adipocytes, previously glucose-deprived for 24h, still maintain their monolayer and adipocyte morphology. It is also known that cells can adapt to glucose stress by altering cellular metabolism and processes including glucose transport, glycogen utilization, and protein glycosylation. Further, returning glucose-deprived cells to medium containing glucose reverses the effects of glucose deprivation. Kitzman et al. (1993) have shown that there is a 10-fold change in glucose uptake in 3T3-L1 adipocytes maintained in glucose-free medium compared to controls (glucose-fed) by 15h. Returning the deprived cells to complete medium containing 25mM glucose, returns glucose transport to a basal level (glucose-fed) by 4h of refeeding. Likewise, McMahon and Frost (1996) have shown that cells deprived of glucose for 24h showed a greatly decreased glycogen pool. Returning these glucose-deprived cells back to complete medium containing 25mM glucose returned glycogen levels to that of control (glucose-fed) cells by 24h of refeeding. McMahon and Frost (1995) also showed that by 36h of glucose deprivation p37 is the only GLUT1 form synthesized. Within 1h of glucose refeeding, only the normal p46 glycoform of GLUT1 was detected. Thus, these studies demonstrate that the effects of glucose deprivation can be reversed with no apparent harm to the cells.

Examining reversibility of a cellular process not only confirms cell viability, but more importantly, allows characterization of a process in recovery. Irreversible effects manifested by mutation or certain inhibitors can not be examined in this manner. As an example, Garant et al. (1999) have shown that short term treatment of Chinese hamster ovary cells overexpressing the human IR with the tripeptide glutathione (GSH) or N-acetyl-L-cysteine (NAC) led to a reversible reduction of intermolecular α-α disulfides. These disulfides were different from the Class I disulfides [$\alpha(\mathrm{Cys}^{524})$-$\alpha(\mathrm{Cys}^{524})$ and $\alpha(\mathrm{Cys}^{682})$-$\alpha(\mathrm{Cys}^{682})$] that are characterized by irreversible reduction with low concentrations of dithiothreitol (DTT) and Class II disulfide [$\alpha(\mathrm{Cys}^{647})$-$\beta(\mathrm{Cys}^{872})$] that are characterized by its irreversible reduction with strong reducing conditions and/or denaturation prior to reduction. Reduction of Class I disulfides results in species that are capable of insulin-induced autophosphorylation and activation of tyrosine kinase activity. Reduction of Class II disulfides prevents oligomerization and impairs insulin signaling. Reduction of novel disulfides on the α-subunits by GSH or NAC did not affect Class I or II disulfides or its oligomeric structure, but did affect insulin-induced autophosphorylation and activation of tyrosine kinase activity. Removal of GSH or NAC restores the native thiol redox status.

In this section, the reversibility of the effect of aberrant glycosylation on IR processing will be examined. Examining this reversible phenomenon led to the discovery of a novel recovery path.

Results

Restoration of Processing of the Alternative Proreceptor

To determine if the alternative proreceptor could be salvaged from the degradation path, glucose-deprived cells were refed with medium containing 25mM glucose for specific times (Figure 6-1). Glucose-fed or starved cells were labeled with [35S]methionine/cysteine for 1h and glucose-starved cells were further chased in medium containing glucose. Note that with only 1h pulse, the α- and β-subunits in the glucose-fed samples are not always visible. Interestingly, by 1h of glucose readdition, the alternative proreceptor shifted to a higher molecular weight isoform. Note that the processed alternative proreceptor migrated between the normal and alternative proreceptor. The appearance of this "intermediate" proreceptor suggests the attachment of additional oligosaccharides to the alternative proreceptor (see below). Also note that with glucose refeeding, the interaction with GRP78 was significantly reduced. Surprisingly, 3h after glucose readdition, only faint traces of α- and β-subunits were visible. Note that the film was overexposed in order to visualize the α- and β-subunits (also see Figure 6-5). The intensity of these bands never approached that of the

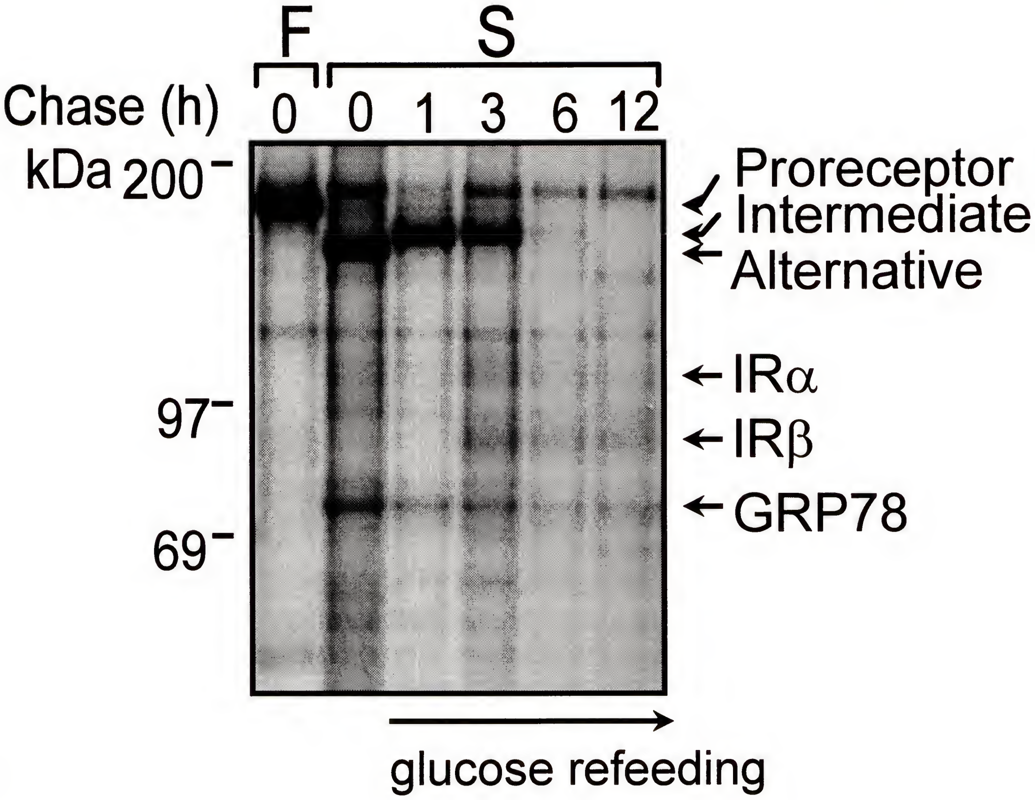

Figure 6-1 - Processing of the Alternative Proreceptor in the Presence of Glucose Cells were glucose-fed (F) or glucose-deprived (S) and labeled for 1h as before. Glucose-deprived cells were then chased in complete medium for 1, 3, 6, or 12h. At each time point, total membranes were collected for immunoprecipitation with anti-IRβ antibody. These data are representative of four independent experiments (n=4).

processed normal proreceptor. Rather, most of the intermediate proreceptor disappeared between 3 and 6h. This implies that glucose readdition not only promotes post-translational attachment of the *N*-linked oligosaccharides to the alternative proreceptor, but also accelerates proreceptor degradation. Only a minor fraction appears to be processed.

To show that the shift in migration of the alternative proreceptor is due to oligosaccharide processing, sensitivity to endo H was tested (Figure 6-2). Whereas the alternative proreceptor was resistant to endo H treatment (compare lanes 3 and 4), the intermediate proreceptor was sensitive to endo H (compare lanes 6 and 8). The newly acquired sensitivity to endo H implies either (1) the addition of mannose residues to pre-existing structures or (2) cleavage of the pre-existing structures and/or the attachment of newly synthesized oligosaccharide chains. To test the second hypothesis, tunicamycin (an inhibitor of *N*-linked glycosylation) was added during glucose refeeding (Figure 6-3). We have previously shown that it takes 3h in these cells to observe the effects of tunicamycin (Kitzman et al., 1996). Therefore, we pulsed for 1h as before, and then chased in the absence of glucose with or without tunicamycin for 3h before refeeding with glucose.

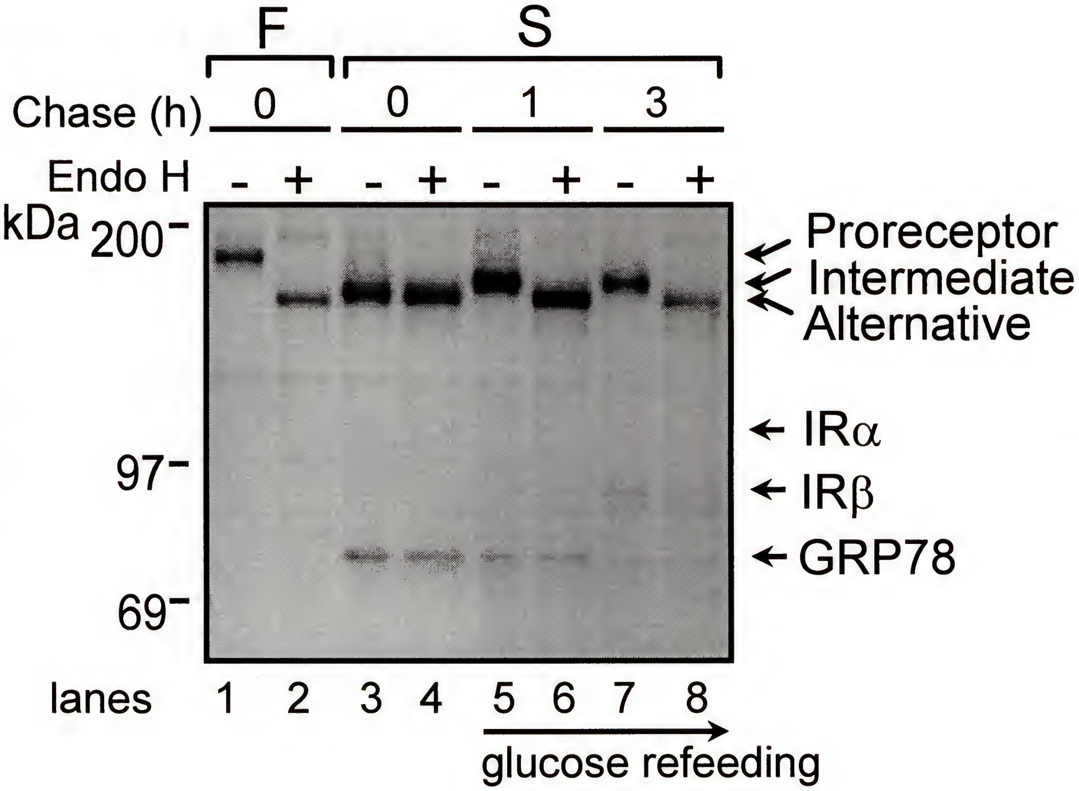

Figure 6-2 - Effect of Endo H Treatment during Glucose Refeeding Cells were glucose-fed (F) or glucose-deprived (S) and labeled for 1h. Glucose-deprived cells were chased in complete medium for 1 or 3h (lanes 5-8). At each time point, total membranes were collected for immunoprecipitation with anti-IRβ antibody. The immune complexes were then treated with or without endo H before resolving by 7.5% SDS-PAGE.

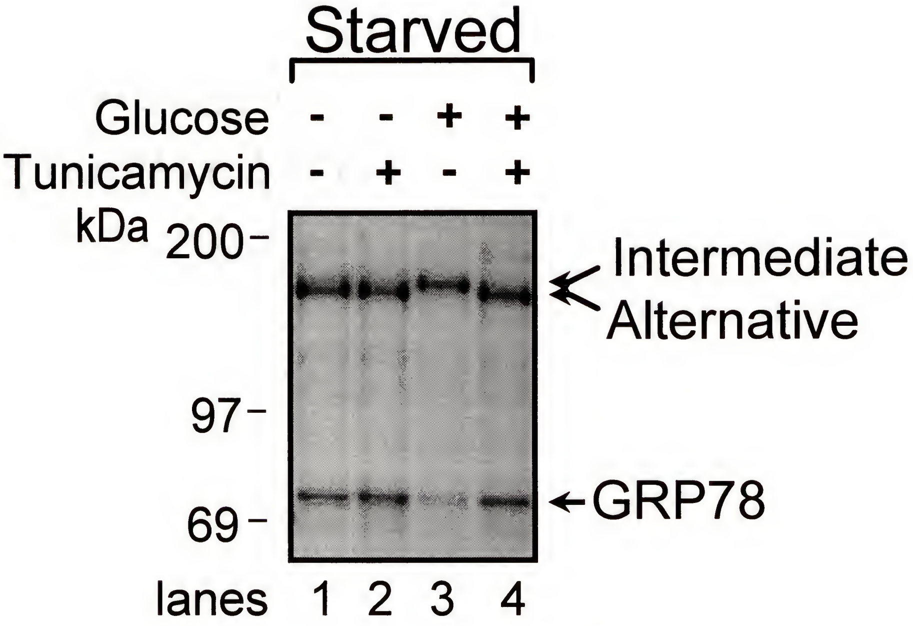

Figure 6-3 - Effect of Tunicamycin Treatment during Glucose Refeeding Cells were glucose-fed (F) or glucose-deprived (S) and labeled for 1h. Glucose-deprived cells were chased in medium without glucose in the presence or absence of tunicamycin (2.5μg/mL) for 3h (lanes 1 and 2). The glucose-free medium was then replaced with complete medium with or without tunicamycin for 1h (lanes 3 and 4). IR was immunoprecipitated and resolved by 7.5% SDS-PAGE.

Tunicamycin had no effect on the alternative proreceptor maintained in the absence of glucose (lanes 1 and 2). In contrast, tunicamycin prevented the glucose-induced shift to the intermediate form (lanes 3 and 4). This suggests that the reprocessing of the alternative proreceptor requires *N*-linked glycosylation and thus attachment of newly synthesized core structures to unoccupied *N*-linked glycosylation sites. Note once again that significantly less GRP78 co-precipitates with the intermediate form of the proreceptor.

Finally, we tested whether the oligosaccharides attached to the alternative proreceptor during glucose deprivation are retained in the intermediate form. For this study, we used [^{3}H]mannose as the oligosaccharide tag. Shown in Figure 6-4 is the result. Indeed the alternative proreceptor incorporated [^{3}H]mannose, further supporting its status as a glycoprotein. In contrast, GRP78 which has been shown to co-precipitate with the alternative proreceptor failed to be labeled with [^{3}H]mannose, which supports findings that GRP78 is not glycosylated. Interestingly, 1h after glucose readdition, the labeled proreceptor shifted to the intermediate form with no loss in radioactivity (39,700cpm, alternative proreceptor; 36,300cpm, intermediate proreceptor). Thus, the original,

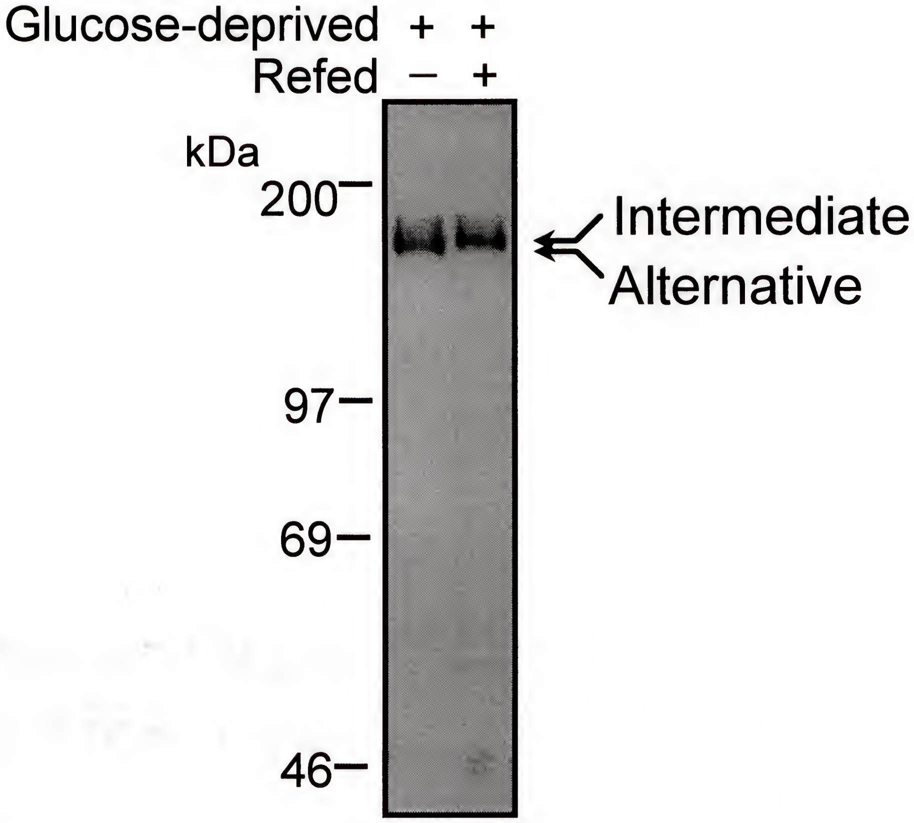

Figure 6-4 - Labeling the Alternative Proreceptor with [^{3}H]mannose Glucose-deprived cells were labeled with 10μM of [^{3}H]mannose (210μCi/mL of glucose-free medium) for 3h. Cells were then chased in complete medium for 1h. IR was immunoprecipitated and resolved by 7.5% SDS-PAGE.

abbreviated *N*-linked oligosaccharide(s) was retained during glucose-induced reprocessing. With additional chase periods (1, 2, 4, and 6h) in the presence of glucose (Figure 6-5), the intermediate proreceptor was rapidly degraded, just as in Figure 6-1. The film was overexposed in order to again show that there are faint traces of α- and β-subunits, which represent a minor pathway. The normal proreceptor was also visible with a darker exposure. This was surprising because only 10μM [^{3}H]mannose was added to the labeling medium which contains 25mM glucose. There is one technical fault that needs to be addressed here regarding this experiment. In this particular experiment, the dye front at the bottom of the SDS-PAGE gel was not run out as far as some of the other experiments (i.e., see Figure 6-4). This led to a loss of separation between the alternative and intermediate proreceptors.

Proteosome-mediated Degradation of the Intermediate Proreceptor

With the readdition of glucose in the chase medium, the alternative proreceptor acquires new *N*-linked glycosylation, resulting in an intermediate glycoform. This intermediate proreceptor is mostly degraded with faint traces of processed β-subunits. Since the major pathway is

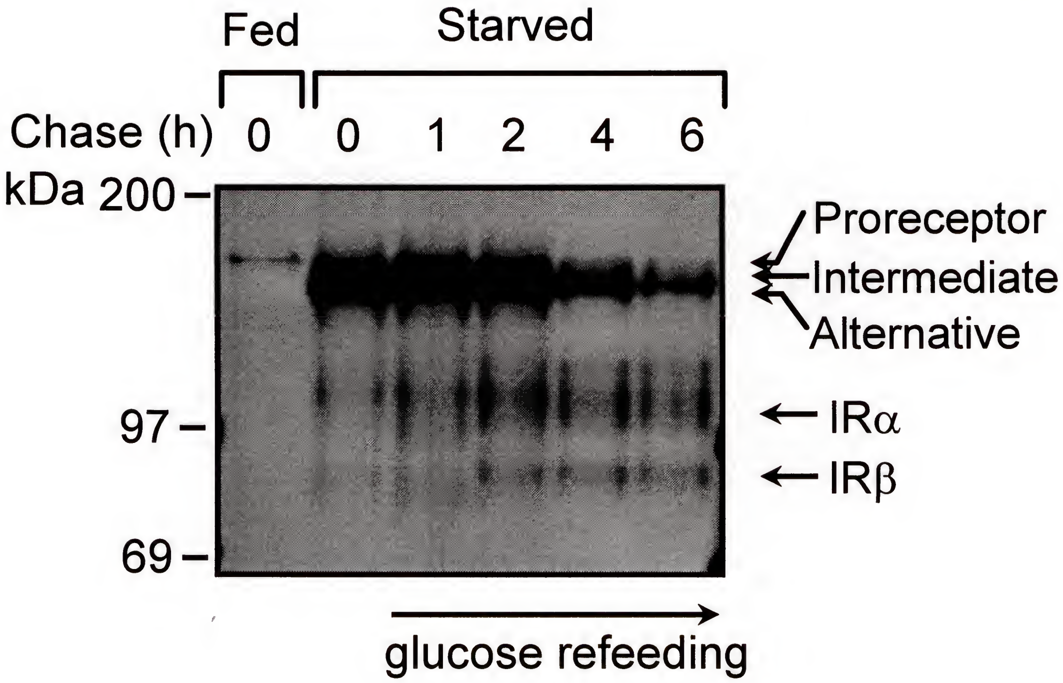

Figure 6-5 - Processing of [^{3}H]mannose-labeled Alternative Proreceptor in the Presence of Glucose Cells were glucose-fed (F) or glucose-deprived (S) and labeled for 3h with [^{3}H]mannose (210μCi/mL). Glucose-deprived cells were then chased in complete medium for 1, 3, 6, or 12h. At each time point, total membranes were collected for immunoprecipitation with anti-IRβ antibody.

still degradation, we tested the effect of a proteosome inhibitor, MG132, on degradation of the intermediate proreceptor. In Figure 6-6, glucose-deprived cells were labeled for 3h and then refed with complete medium containing 25mM glucose in the absence or presence of 50μM MG132 for 2, 4, or 6h. There was significant inhibition of degradation observed in the presence of MG132 as compared to non-treated controls at each chase time point. Furthermore, the intensity of the β-subunits increased over time in the MG132-treated cells. This processing of the β-subunit is reminiscent of the experiments in Figures 5-5 and 5-6 where treatment of glucose-deprived cells with MG132 or lactacystin induced some processing of the alternative proreceptor into the β-subunits. However, in this experiment, MG132 was able to inhibit the degradation of the intermediate proreceptor. The only difference between the previous experiments (Figures 5-5 and 5-6) and this experiment is the presence of glucose in the chase medium. For some unknown reason(s), the presence of glucose prevents degradation of the intermediate proreceptor by the proteosome inhibitor, MG132. Whether glucose exerts this effect directly on degradation or

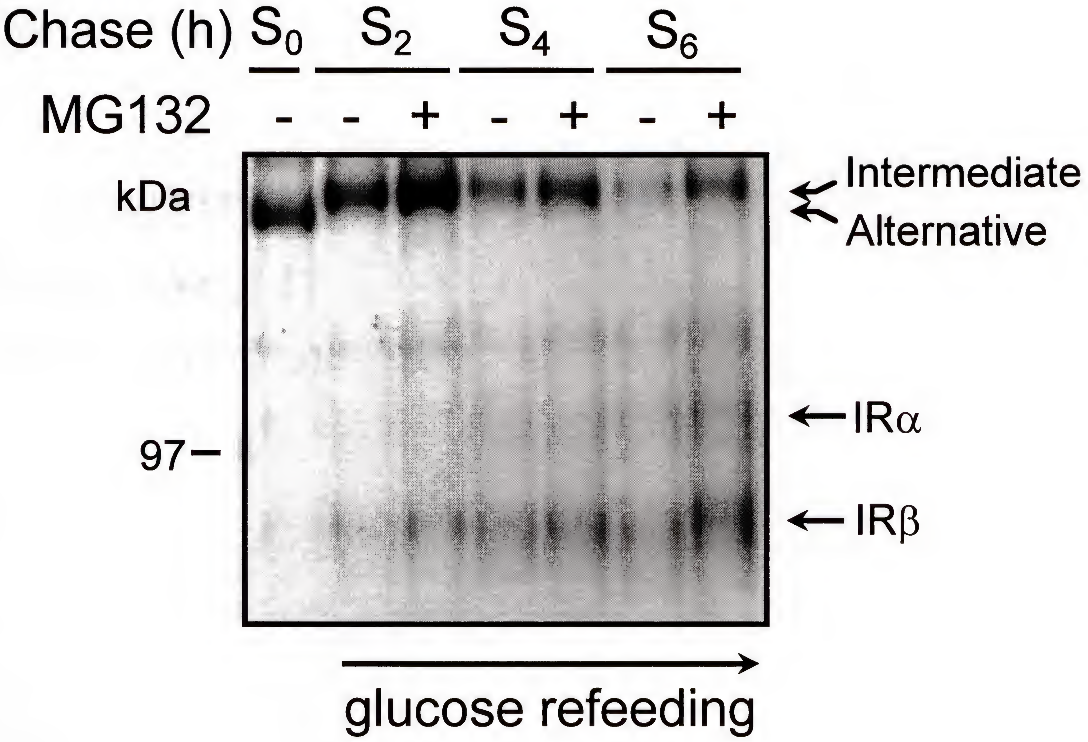

Figure 6-6 - Effect of MG132 on Degradation of the Intermediate Proreceptor Cells were glucose-deprived (S) and labeled for 3h as before. Glucose-deprived cells were then chased in complete medium for 1, 3, 6, or 12h in the absence or presence of 50μM MG132. At each time point, total membranes were collected for immunoprecipitation with anti-IRβ antibody. Immunoprecipitates were resolved by 7.5% SDS-PAGE, followed by autoradiography.

through new *N*-linked glycosylation is uncertain at this point.

Model of Reprocessing Mechanism

One of the advantages of glucose deprivation over inhibitors of glycosylation and mutation is its reversibility, which allowed us to uncover the novel processing of the alternative proreceptor to the intermediate form. Based on our current data we present the following model to explain the effects of glucose deprivation and refeeding on insulin receptor processing (Figure 6-8). The model predicts the utilization of only a limited number of the 18 possible *N*-linked glycosylation sites during glucose deprivation because of the small difference in the migration of the alternative versus the aglyco proreceptor. Substantial underglycosylation and/or attachment of truncated oligosaccharides leads to the interaction with GRP78, retention in the ER, and targeted degradation. Glucose refeeding permits post-translational processing which requires *N*-linked glycosylation of a limited number of unoccupied sites. Newly acquired endo H sensitivity predicts the attachment of normal $Glc_3Man_9GlcNAc_2$ core structures to these sites. Some sites may not be accessible to oligosaccharide transferases due to protein folding or spatial orientation. While *N*-

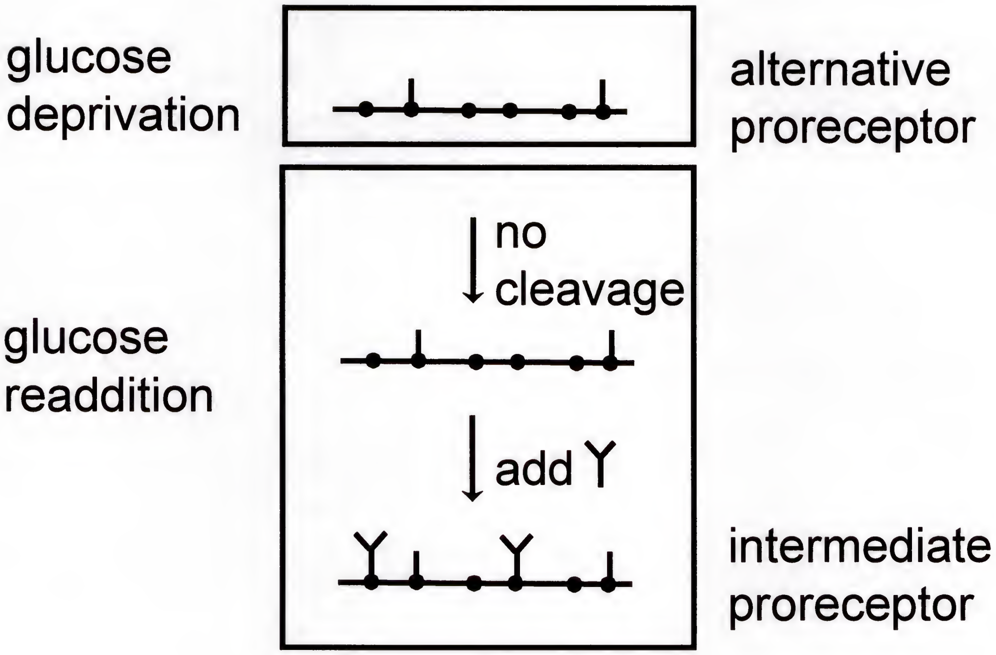

Figure 6-7 - Model of Reprocessing Mechanism For simplicity, the IR is represented here as having only 6 out of the 18 *N*-linked glycosylation sites. The upper boxed area represents the alternative proreceptor synthesized during glucose deprivation while the lower boxed area represents the intermediate proreceptor generated during glucose readdition. See text for discussion. **I**, alternative oligosaccharide; **Y**, normal oligosaccharide; ●, *N*-linked glycosylation sites.

glycosidase F activity has been noted in a number of systems, whether in cytoplasm or ER (Romisch and Ali, 1997; Suzuki et al., 1998; Suzuki et al., 1994), glucose-induced reprocessing does not require removal of the truncated oligosaccharide(s). Despite the retention of the original truncated oligosaccharides, the intermediate species is released from GRP78. This allows a small fraction of the intermediate proreceptor to be processed to mature α- and β-subunits while the majority undergoes accelerated degradation. We are currently pursuing experiments to further refine the model.

Conclusions

Glucose deprivation was used as a tool to examine the reversibility of aberrant glycosylation on IR processing. In Chapter 4, we have shown that glucose deprivation resulted in aberrant glycosylation of the insulin proreceptor that caused accumulation in the ER by its interaction with GRP78, but not calnexin or calreticulin. The alternative proreceptor was then degraded rather than processed. We show for the first time that glucose refeeding of glucose-deprived cells resulted in post-translational *N*-linked glycosylation of the alternative proreceptor as shown by the acquisition of endo H sensitivity and inhibition by tunicamycin treatment. This new *N*-linked glycosylation caused a shift in molecular mass to an intermediate form, migrating in between the normal and alternative proreceptor.

Labeling the oligosaccharide structure of the alternative proreceptor with [^{3}H]mannose before refeeding cells with glucose resulted in maintenance of radioactivity from the alternative to the intermediate proreceptor. This implies that the aberrant oligosaccharide structures are not cleaved, but remain attached to the intermediate proreceptor. This further implies that during glucose deprivation, not all of the potential *N*-linked sites are occupied. Thus, post-translational addition of new *N*-linked oligosaccharides does not require the removal of the aberrant oligosaccharide structures.

Glucose-induced reprocessing of the alternative proreceptor resulted in an acquisition of IR function. The alternative proreceptor displayed a basal level autophosphorylation activity. However, this activity was not stimulated with insulin. Glucose refeeding resulted in insulin-stimulated autophosphorylation activity of the intermediate proreceptor that was comparable to the control (glucose-fed). This implies that folding in the absence of glucose can be reversed with glucose refeeding to yield a functional receptor, at least with respect to insulin-induced autophosphorylation. However, contrary to our predictions, the functional intermediate proreceptor was still degraded.

Glucose refeeding resulted in accelerated degradation of the intermediate proreceptor by the cytoplasmic proteosome. Glucose refeeding led to a more rapid degradation of the intermediate proreceptor ($t_{1/2}$ = 1h) than the alternative proreceptor ($t_{1/2}$ = 5h). The reason for this observation is still unclear. This is even more puzzling because there is significantly less co-precipitation of GRP78, although the radioactivity between the alternative and intermediate proreceptors at 1h of chase in presence of glucose are the same. This suggests that either the intermediate proreceptor is folded correctly which reverses the interaction with GRP78 or GRP78 is released much earlier than the onset of degradation of the intermediate proreceptor. There is also a third possibility in that an increase in lumenal ATP (derived from glucose metabolism) causes the release of GRP78 from the intermediate proreceptor.

Even with glucose refeeding, degradation was still the major pathway for the intermediate proreceptor. However, there were some faint traces of the β-subunits (and possibly the α-subunits). Interestingly, inhibition of the cytoplasmic proteosome resulted in inhibition of the intermediate proreceptor and an increase in processing into the β-subunits over time.

CHAPTER 7
CONCLUSIONS AND FUTURE DIRECTIONS

Conclusions

Glycosylation inhibitors and site-directed mutagenesis of *N*-linked glycosylation sites have provided evidence for an important role of glycosylation in IR processing and function. We have extended these studies by using glucose deprivation for the first time as a tool to monitor reversible changes in IR glycosylation. Our data show that glucose deprivation alters *N*-linked glycosylation of the insulin proreceptor. This causes accumulation of an alternative glycoform of the proreceptor in an intracellular membrane compartment where it binds GRP78, consistent with ER localization. Although several investigators have shown that overexpressed or mutant insulin receptor interacts with GRP78 (Accili et al., 1992; Sawa et al., 1996), we are the first to show that IR interacts with GRP78 in a more normal setting.

We also show that the rate of synthesis of the alternative proreceptor appears similar to that of the normal proreceptor. However, the alternative proreceptor is not processed into the α- and β-subunits as compared to the normal proreceptor. Rather, the alternative proreceptor disappears more slowly than the normal proreceptor suggesting ER mediated degradation, perhaps directed by its interaction with GRP78. In support of an ER mediated degradation of the alternative proreceptor, inhibition of cytoplasmic proteosomes resulted in significantly more processing of the β-subunit. In contrast, lysosomal inhibitors had no effect.

The effect of glucose deprivation on metabolic processing including glucose transport and glycogen synthesis is a reversible phenomenon. We have further extended our studies by examining the reversibility of glucose deprivation on processing of the alternative proreceptor. This has allowed us to discover a novel pathway whereby processing of the alternative proreceptor can be stimulated with readdition of glucose, resulting in an intermediate proreceptor. This shift to a higher molecular mass requires *N*-linked glycosylation. This also leads to a rapid loss of proreceptor from the ER. This loss appears to represent accelerated degradation with only a minor maturation component. At present, we do not understand this surprising result. However, degradation of the intermediate proreceptor can be inhibited with proteosome inhibitors. Inhibition of degradation also resulted in more processing of the β-subunits. In contrast, lysosomal inhibitors had no effect on degradation or processing into the β-subunits.

Rearick et al. (1981) have shown that glucose deprivation of CHO cells leads to the attachment of an immature oligosaccharide structure at *N*-linked consensus sites. This alternative oligosaccharide structure ($Man_5GlcNAc_2$) is resistant to endo H digestion whereas the normal *N*-linked oligosaccharide core ($Glc_3Man_9GlcNAc_2$) is cleaved by endo H. Our data show that an endo H-resistant oligosaccharide is attached to the proreceptor of 3T3-L1 adipocytes during glucose deprivation which is consistent with a $Man_5GlcNAc_2$ structure. Previously, we have shown that glucose deprivation leads to the synthesis of an alternatively glycosylated form of the constitutive glucose transporter, GLUT1 (Kitzman et al., 1993). In contrast to IR, the alternative form of GLUT1 is targeted to the plasma membrane (McMahon and Frost, unpublished data). Thus, IR but not GLUT1 requires the normal *N*-linked oligosaccharide structure for processing to PM. Of course there are major differences between insulin receptors and GLUT1. As the IR contains multiple glycosylation sites in contrast to the single site on GLUT1, a major question arises as to whether underglycosylation, glycosylation with a truncated oligosaccharide, or a combination of both influence IR processing. Our data demonstrate that glucose deprivation results in both underglycosylation and attachment of truncated oligosaccharides making these possibilities difficult to distinguish. Given that the first four *N*-linked glycosylation sites significantly influence processing (Collier et al., 1993; Caro et al., 1994), it will be important to determine the consequence of glucose deprivation at these sites.

Glucose deprivation of 3T3-L1 adipocytes also leads to insulin resistance (van Putten and Krans, 1985). Yet, Tordjman et al. (1990) have shown that glucose deprivation does not alter the level of the GLUT4 glucose transporter. Thus our data explain, in part, the development of insulin resistance by the reduction of cell surface insulin receptor as a result of retention and degradation of the proreceptor in the ER. In this way, our glucose deprivation model resembles Carbohydrate Deficient Glycoprotein Syndrome type 1a which is caused by a genetic deficiency of phosphomannomutase (van Schaftingen and Jaeken, 1995). It is proposed that proteins which require glycosylation for processing, like the insulin receptor, are retained in the ER by global depletion of substrate for protein glycosylation.

Aberrant glycosylation of the insulin receptor is not the only cause for its retention in the ER. Several different types of mutations have been identified in the insulin receptor of patients with genetic forms of insulin resistance. Three specific point mutations impair transport of the mutant receptors to the cell surface (Accili et al., 1991; Accili et al., 1991; Kadowaki et al., 1990; Kadowaki et al., 1990). Accili et al. (1992) have reconstructed these mutants (Asn15Lys; His209Arg; Phe382Val) *in vitro* and overexpressed them in NIH 3T3 fibroblasts. Of these, the R209 and V382 mutants were found in a complex with GRP78. The K15 mutant did not interact with GRP78, despite its retention in the ER.

Future Directions

The experiments conducted in this research project emphasize the importance of proper glycosylation for insulin receptor processing. Aberrant glycosylation of the IR has been inferred from glycosidase sensitivity. Accumulation of the alternative proreceptor in the ER by its interaction with GRP78 has been demonstrated. Involvement of the cytoplasmic proteosome in the degradation of the alternative and intermediate proreceptor has been confirmed. A new pathway, involving the addition of new *N*-linked oligosaccharides to a folded and partially active alternative proreceptor, has been discovered. However, there are still many details left unanswered. This section will address some of these unanswered questions.

The use of several different methodologies including glycosylation inhibitors, site-directed mutagenesis, and glucose deprivation have demonstrated the importance of *N*-linked glycosylation on IR processing. Furthermore, site-directed mutagenesis studies have shown the importance of several sites on the α- and β-subunits for processing into a mature and functional receptor. However, we are more interested in the actual sites that are aberrantly glycosylated during glucose deprivation. Identification of specific *N*-linked sites and their importance for proper processing, folding, and acquisition of function will provide valuable information as to the differential effect of glycosylation on IR versus GLUT1. One of the difficulties imposed by this experiment is the number of potential *N*-linked sites on the IR (14 potential sites on the α-subunit and 4 sites on the β-subunit). In order to simplify this matter, the β-subunit should be examined first since there are only 4 known *N*-linked sites. As shown before, the α- and the β-subunits can be separated by digestion with furin. The procedure for this experiment would be as follows. Cells deprived of glucose will be radiolabeled with [^{3}H]mannose and immunoprecipitated as before. Furin would then be added directly onto the immune complex. This will release the α-subunit into solution while the β-subunit remains bound to the IRβ antibody which is bound to protein A-sepharose. The β-subunit can be further digested with trypsin for microsequencing. Treating the β-subunit with *N*-glycosidase F will release the radiolabeled aberrant oligosaccharides which can be analyzed for composition and/or sequence.

Another important question that needs to be addressed concerns the structure of the alternative proreceptor. It has been implied from the autophosphorylation studies that the alternative proreceptor is partially misfolded due to its lack of insulin-stimulated autophosphorylation activity. It was also implied from the co-precipitation studies in which GRP78 co-precipitates with the alternative but not the normal proreceptor. GRP78 only interacts stably with proteins that have exposed hydrophobic areas, areas that would normally be embedded in the hydrophobic core of the protein. However, it would be important to demonstrate that the alternative proreceptor is indeed misfolded. One method that could be pursued is the use of non-reducing electrophoresis to examine the migration of the alternative versus the normal proreceptor. In this procedure, glucose-fed or glucose-deprived cells could be radiolabeled with [35S]methionine/cysteine and IR immunoprecipitated as before. The immunoprecipitates could be analyzed for dimer or heterotetramer configuration.

Another important question that needs to be addressed concerns the absence of the α-subunit in the glucose refeeding studies. Trace amounts of the β-subunit are present during the chase in the presence of glucose, but not the α-subunit. This difference is further emphasized with the addition of proteosome inhibitors during the chase in the presence of glucose. The simplest way to examine the α-subunit would be to repeat these experiments in which IR is immunoprecipitated with an anti-IRα antibody. Unfortunately, antibodies generated against IRα have poor affinity.

Answers to these questions will further our understanding of the role that glucose deprivation plays in glycosylation and processing of the IR. This will in turn give us a broader picture of protein glycosylation.

LIST OF REFERENCES

Accili, D., Frapier, C., Mosthaf, L., McKeon, C., Elbein, S.C., Permutt, M.A., Ramos, E., Lander, E., Ullrich, A., and Taylor S.I. (1989) EMBO J. 8, 2509-2517.

Accili, D., Kadowaki, T., Kadowaki, H., Mosthaf,, L., Ullrich, A., and Taylor, S.I. (1996) J. Biol. Chem. 267, 586-590.

Accili, D., Mosthaf, L., Ullrich, A., and Taylor S.I. (1991) J. Biol. Chem. 266, 434-439.

Anfinsen, C.B., Haber, E., Sela, M., and White, F.H. (1961) Proc. Nat. Acad. Sci. U.S.A. 47, 1309-1314.

Arakaki, R.F., Hedo, J.A., Collier, E., and Gorden, P. (1987) J. Biol. Chem. 262, 11886-11892.

Asano, T., Katagiri, H., Takata, K., Lin, J.L., Ishihara, H., Inukai, K., Tsukuda, K., Kikuchi, M., Hirano, H., Yazaki, Y., and Yoshitomo, O. (1991) J. Biol. Chem. 266, 24632-24636.

Balch, W.E. and Rothman, J.E. (1985) Arch. Biochem. Biophys. 240, 413-425.

Bass, J., Chiu, G., Argon, Y., and Steiner, D.F. (1998) J. Cell. Biol. 141, 637-646.

Bastian, W., Zhu, J., Way, B., Lockwood, D., and Livingston, J. (1993) Diabetes 42, 966-974.

Bause, E. (1983) Biochem. J. 209, 331-336.

Blok, J., Gibbs, E.M., Lienhard, G.E., Slot, J.W., and Geuze, H.J. (1988) J. Cell Biol. 106, 69-76.

Blond-Elguindi, S., Fouie, A.M., Sambrook, J.F., and Gething, M-J. (1993) J. Biol. Chem. 268, 12730-12735.

Blount, P. and Merlie, J.P. (1991) J. Cell. Biol. 113, 1125-1132.

Brady, M.J., Printen, J.A., Mastick, C.C., and Saltiel, A.R. (1997) J. Biol. Chem. 272, 20198-20204.

Bravo, D.A., Gleason, J.B., Sanchez, R.I., Roth, R.A., and Fuller, R.S. (1994) J. Biol. Chem. 269, 25830-25837.

Brodsky, J.L. and Schekman, R. (1993) J. Cell Biol. 123, 1355-1363.

Brot, N., Redfield, B., Qiu, N-H., Chen, G-J., Vidal, V., Carlino, A., and Weissbach, H. (1994) Proc. Natl. Acad. Sci. 91, 12120-12124.

Calderhead, D.M., Kitagawa, K., Tanner, L.I., Holman, G.D., and Lienhard, G.E. (1990) J. Biol. Chem. 265, 13800-13808.

Carlino, A., Toledo, H., Skaleris, D., DeLisio, R., Weissbach, H., and Brot, N. (1992) Proc. Natl. Acad. Sci. U.S.A. 89, 2081-2085.

Carlsson, L. and Lazarides, E. (1983) Proc. Natl. Acad. Sci. 80, 4664-4668.

Caro, L.H.P., Ohali, A., Gorden, P., and Collier, E. (1994) Diabetes 43, 240-246.

Chang, S.C., Woden, S.K., Nakaki, T., Kim, Y.K., Lin, A.Y., Kung, L., Attenello, J.W., and Lee, A.S. (1987) Proc. Natl. Acad. Sci. U.S.A. 84, 680-684.

Chapman, R., Sidrauski, C., and Walter, P. (1998) Annu. Rev. Cell. Dev. Biol. 14, 459-485.

Chessler, S.D. and Byers, P.H. (1993) J. Biol. Chem. 268, 18226-18233.

Choudhury, P., Liu, Y., and Sifers, R.N. (1997) News Physiol. Sci. 12, 162-166.

Collier, E., Carpentier, J-L., Beitz, L., Caro, L.H. P., Taylor, S.I., and Gorden, P. (1993) Biochemistry 32, 7818-7823.

Collier, E., and Gorden, P. (1991) Diabetes 40, 197-203.

Czech, M.P. and Buxton, J.M. (1993) J. Biol. Chem. 268, 9187-9190.

Dankert, J.R., Shiver, J.W., Esser, A.F. (1985) Biochemistry 24, 2754-2762.

Ebina, Y., Ellis, L., Jarnagin, K., Edery, M., Graf, L., Clauser, E., Ou, J., Masiarz, F., Kan, Y.W., Goldfine, I.D., Roth, R.A., and Rutter, W.J. (1985) Cell 40, 747-758.

Ellis, R.J. (1987) Nature 328, 378-379.

Fiege, J., Keller, G., and Scheffler, I.E. (1988) J. Cell. Physiol. 136, 33-42.

Fisher, M.D. and Frost, S.C. (1996) J. Biol. Chem. 271, 11806-11809.

Flaherty, K.M., DeLuca-Flaherty, C., and McKay, D.B. (1990) Nature 346, 623-628.

Flynn, G.C., Chappell, T.G., and Rothman, J.E. (1989) Science 245, 385-390.

Freiden, P.J., Gaut, J.R., and Hendershot, L.M. (1992) EMBO J. 11, 73-70.

Frost, S.C. and Lane, M.D. (1985) J. Biol. Chem. 260, 2646-2652.

Gallagher, P., Henneberry, J., Wilson, I., Sambrook, J., and Gething, M-J. (1988) J. Cell Biol. 107, 2059-2073.

Garant, M.J., Kole, S., Maksimova, E.M., and Bernier, M. (1999) Biochemistry 38, 5896-5904.

Gavel, Y. and von Heijne, G. (1990) Protein Eng. 3, 433-442.

Gething, M-J. (1996) Current Biol. 6, 1573-1576.

Gething, M-J. and Sambrook, J. (1992) Nature 355, 33-45.

Gibson, R., Schlesinger, S., and Kornfeld, S. (1979) J. Biol. Chem. 252, 3600-3707.

Golden, P.L., Maccagnan, T.J., and Pardridge, W.M.(1997) J. Clin. Invest. 99, 14-18.

Goldstein, B.J., and Kahn, C.R. (1988) J. Biol. Chem. 263, 12809-12812.

Green, H. and Kehinde, O. (1976) Cell 7, 105-113.

Green, H. and Meuth, M. (1974) Cell 3, 127-133.

Haas, I.G. and Wabl, M. (1983) Nature 306, 387-389.

Hammond, C. and Helenius, A. (1994) J. Cell Biol. 126, 41-52.

Harlow, E. and Lane, D. (1988) Antibodies: A Laboratory Manual Cold Spring Harbor Laboratory, New York, 55-57.

Hartl, F.U. (1996) Nature 381, 571-580.

Haspel, H.C., Mynarcik, D.C., Ortiz, P.A., Honkanen, R.A., and Rosenfeld, M.G. (1991) Molec. Endo. 5, 61-72.

Haspel, H.C., Wilk, E.W., Birnbaum, M.J., Cushman, S.W., and Rosen, O.M. (1986) J. Biol. Chem. 261, 6778-6789.

Hedo, J.A., Kahn, C.R., Hayashi, M., Yamada, K.M., and Kasuga, M. (1983) J. Biol. Chem. 258, 10020-10026.

Hendershot, L.M., Ting, J., and Lee, A.S. (1988) Mol. Cell. Biol. 8, 4250-4256.

Hendrick, J.P. and Hartl, F.U. (1993) Annu. Rev. Biochem. 62, 349-384.

Herzberg, V.L., Grigorescu, F., Edge, A.S.B., Spiro, R.G., and Kahn, C.R. (1985) Biochem. Biophys. Res. Commun. 129, 789-796.

Horuk, R., Matthaei, S., Olefsky, J.M., Baly, D.L., Cushman, S.W., and Simpson, I.A. (1986) J. Biol. Chem. 261, 1823-1828.

Hunt, C. and Morimoto, R.I. (1985) *Proc. Natl. Sci. U.S.A*. *82*, 6455-6459.

Imamura, T., Haruta, T., Takata, Y., Usui, I., Iwata, M., Ishihara, H., Ishiki, M., Ishibashi, O., Ueno, E., Sasaoka, T., and Kobayashi, M. (1998) *J. Biol. Chem*. 273, 11183-11188.

Imperiali, B. and Rickert, K.W. (1995) *Proc. Natl. Acad*. *Sci. U.S.A*. *92*, 97-101.

Isaka, T., Yoshida, M., Owada, M., and Toyoshima, K. (1975) *Virology* *65*, 226-237.

James, D.E., Lederman, L., and Pilch, P.F. (1987) *J. Biol*. *Chem*. *262*, 11817-11824.

Kadowaki, T., Kadowaki, H., Accili, D., and Taylor, S.I. (1990) *J. Biol. Chem*. *265*, 19143-19150.

Kadowaki, T., Kadowaki, H., Rechler, M.M., Serrano-Rios, M., Roth, J., Gorden, P., and Taylor, S.I. (1990) *J. Clin. Invest*. *86*, 254-264.

Kang, P-J., Ostermann, J., Shilling, J., Neupert, W., Craig, E.A., Phanner, N. (1990) *Nature* *348*, 137-143.

Kim, P.S. and Arvan, P. (1995) *J. Cell. Biol*. *128*, 29-38.

Kitzman, H., McMahon, R.J., Aslanian, A.M., Fadia, P.M., and Frost, S.C. (1996) *Mol. Cell. Biochem*. *162*, 51-58.

Kitzman, H., McMahon, R.J., Williams, M.G., and Frost, S.C. (1993) *J. Biol. Chem*. *268*, 1320-1325.

Klausner, R.D. and Sitia, R. (1990) *Cell* *62*, 611-614.

Knutson, V.P. (1991) *FASEB J*. *5*, 2130-2138.

Kopito, R.R. (1997) *Cell* 88, 427-430.

Kornfeld, R. and Kornfeld, S. (1985) *Annu. Rev. Biochem*. *54*, 631-664.

Kornfeld, S. (1992) *Annu. Rev. Biochem*. *61*, 307-330.

Kozutsumi, Y., Segal, M., Normington, K., Gething, M-J., and Sambrook, J. (1988) Nature 332, 462-464.

Laemmli, U.K. (1970) Nature 227, 680-685.

Leconte, I., Auzan, C., Debant, A., Rossi, B., and Clauser, E. (1992) J. Biol. Chem. 267, 17415-17423.

Leconte, I., Carpentier, J-L., and Clauser, E. (1994) J. Biol. Chem. 269, 18062-18071.

Lee A.S. (1987) TIBS 12, 20-23.

Lee, G.J. (1995) Methods Cell Biol. 50, 325-334.

Leno, G.H. and Ledford, B.E. (1989) Eur. J. Biochem. 186, 205-211.

Little, E., Ramakrishnan, M., Roy, B., Gazit, G., and Lee, A.S. (1994) Crit. Rev. Euk. Gene Expr. 4, 1-18.

Loo, T.W. and Clarke, D.M. (1998) J. Biol. Chem. 273, 32373-32376.

Maassen, J.A., Van der Vorm, E.R., Van der Zon, G.C.M., Klinkhamer, M.P., Krans, H.M.J., and Moller, W. (1991) Biochemistry 30, 10778-10783.

Macario, A.J.L. (1995) Int. J. Clin. Lab. Res. 24, 59-70.

Machamer, C.E. and Rose, J.K. (1988) J. Biol. Chem. 263, 5948-5954.

Markwell, M.A., Haas, S.M., Lieber, L.L., and Tolbert, N.E. (1978) Anal. Biochem. 87, 206-210.

Martin, L.B., Shewan, A., Millar, C.A., Gould, G.W., and James, E.E. (1998) J. Biol. Chem. 273, 1444-1452.

McMahon, R. and Frost, S.C. (1996) Am. J. Physiol. 2270, E640-E645.

Melnick, J., Aviel, S., and Argon, Y. (1992) J. Biol. Chem. 267, 21303-21306.

Min J., Okada, S., Kanzaki, M., Elmendorf, J.S., Coker, K.J., Ceresa, B.P., Syu, L-J., Noda, Y., Saltiel, A.R., and Pessin, J.E. (1999) Mol. Cell 3, 751-760.

Munro, S. and Pelham, H. (1986) Cell 46, 291-300.

Munro, S. and Pelham, H (1987) Cell 48, 899-907.

Ng, D.T.W., Hiebert, S.W., and Lamb, R.A. (1990) Mol. Cell. Biol. 10, 1989-2001.

Ou, W.J., Cameron, P.H., Thomas, D.Y., Bergeron, J.J. (1993) Nature 364, 771-776.

Pahl, H.L. and Baeuerle, P.A. (1997) Trends Cell. Biol. 7, 50-55.

Panneerselvam, K., Etchison, J.R., and Freeze, H.H. (1997) J. Biol. Chem. 272, 23123-23129.

Pfleiderer, G. (1963) Methods of Enzymatic Analysis Academic Press, New York, 91-1-3.

Piper, R.C., Hess, L.J., and James, D.E. (1991) Am. J. Physiol. 260, C570-C580.

Pouyssegur, J., Shiu, R.P.C., and Pastan I. (1977) Cell 11, 941-947.

Puig, A. and Gilbert, H.F. (1994) J. Biol. Chem. 269, 25889-25896.

Rearick, J.I., Chapman, A., and Kornfeld, S. (1981) J. Biol. Chem. 256, 6255-6261.

Reed, B.C., Ronnett, G.V., and Lane, M.D. (1981) Proc. Natl. Acad. Sci. U.S.A. 78, 2908-2912.

Robertson, B.J., Moehring, J.M., and Moehring, T.J. (1993) J. Biol. Chem. 268, 24274-24277.

Robinson, A.S., Bockhaus, J.A., Voegler, A.C., and Wittrup, K.D. (1996) J. Biol. Chem. 271, 10017-10022.

Romisch, K. and Ali, B.R.S. (1997) Proc. Natl. Acad. Sci. U.S.A. 94, 6730-6734.

Ronnett, G.V., Knutson, V.P., Kohanski, R.A., Simpson, T.L., and Lane, M.D. (1984) J. Biol. Chem. 259, 4566-4575.

Ronnett, G.V., Knutson, V.P., and Lane, M.D. (1982) J. Biol. Chem. 257, 4285-4291.

Ronnett, G.V., and Lane, M.D. (1981) J. Biol. Chem. 256, 4704-4707.

Rudd, P.M. and Dwek, R.A. (1997) Crit. Rev. Biochem. Mol. Biol. 32, 1-100.

Sanders, S.L., Whitfield, K.M., Vogel, J.P., Rose, M.D., and Schekman, R.W. (1992) Cell 69, 353-365.

Sargeant, R.J. and Paquet, M.R. (1993) Biochem. J. 290, 913-919.

Sawa, T., Imamura, T., Haruta, T., Sasaoka, T., Ishiki, M., Takata, Y., Takada, Y., Morioka, H., Ishihara, H., Usui, I., and Kobayashi, M. (1996) Biochem. Biophys. Res. Commun. 218, 449-453.

Schroder, H., Langer, T., Hartl, F.U., and Bakau, B. (1993) EMBO J. 12, 4137-4144.

Scidmore, M.A., Okamura, H.H., and Rose, M.D. (1993) Mol. Biol. Cell. 11, 1145-1159.

Semple-Rowland, S.L., Adamus, G., Cohen, R.J., and Ulshafer, R.J. (1991) Electrophoresis 12, 307-312.

Sevilla, L., Tomas, E., Munoz, P., Guma, A., Fischer, Y., Thomas, J., Ruiz-Montasell, Bo, Testar, X., Palacin, M., Blasi, J., and Zorzano, A. (1997) Endocrinology 138, 3006-3015.

Shakin-Eshleman, S.H., Spitalnik, S.L., and Kasturi, L. (1996) J. Biol. Chem. 271, 6363-6366.

Shiu, R.P.C., Pouyssegur, J., and Pastan, I. (1977) Proc. Natl. Aca. Sci. U.S.A. 74, 3840-3844.

Sidrauski, C., Chapman, R., and Walter, P. (1998) Trends Cell. Biol. 8, 245-249.

Simons, J.F., Ferro-Novick, S., Rose, M.D., and Helenius, A. (1995) J. Cell Biol. 130, 41-49.

Skowyra, D., Georgopoulos, C., and Zyliez, M. (1990) Cell 62, 939-944.

Stone, K.R., Smith, R.E., and Joklik, W.K. (1974) Virology 58, 86-100.

Stuart, R.A., Cur, D.M., Craig, E.A., and Neupert, W. (1994) Trends Biochem. Sci. 19, 87-92.

Suzuki, C.K., Bonifacino, J.S., Lin, A.Y., Davis, M.M., and Klausner, R.D. (1991) J. Cell. Biol. 114, 189-205.

Suzuki, T., Park, H., Kitajima, K., and Lennarz, W.J. (1998) J. Biol. Chem. 273, 21526-21530.

Suzuki, T., Seko, A., Kitajima, K., Inoue, Y., and Inoue, S. (1994) J. Biol. Chem. 269, 17611-17618.

Thomas, P.J., Qu, B-H., and Pedersen, P.L. (1995) TIBS 20, 456-459.

Thomson, M.J., Williams, M.G., and Frost, S.C. (1997) J. Biol. Chem. 272, 7759-7764.

Ting, J., Wooden, S.K., Kriz, R., Kelleher, K., Kaufman, R.J., and Lee, A.S. (1987) Gene 55, 147-152.

Toledo, H., Carlino, A. Vidal, V., Redfield, B., Nettleton, M.Y., Kochan, J.P., Brot, N., and Weissbach, H. (1993) Proc. Natl. Acad. Sci. U.S.A. 90, 2505-2508.

Tordjman, K.M., Leingang, K.A., and Mueckler, M.M. (1990) Biochem. J. 271, 201-207.

Towbin, H., Stachelin, T., Gordon, J. (1979) Proc. Natl. Acad. Sci. U.S.A. 76, 4350-4354.

Tsugeki, R. and Nishimura, M. (1993) FEBS 320, 198-202.

Ullrich, A., Bell, J.R., Chen, E.Y., Herrera, R., Petruzelli, L.H., Dull, T.J., Gray, A., Coussens, L., Liao, Y.C., Tsubokawa, M., Mason, A., Seeburg, P.H., Grunfeld, C., Rosen, O.M., and Ramachandran, J. (1985) Nature 313, 756-761.

Van der Vorm, E.R., Kuipers, A., Kielkopf-Renner, S., Krans, H.M.J., Moller, W., and Maassen, J.A. (1994) J. Biol. Chem. 269, 14297-14302.

Van Putten, J.P.M. and Krans, H.M.J. (1985) J. Biol. Chem. 260, 7996-8001.

Van Schaftingen, E., and Jaeken, J. (1995) FEBS Lett. 377, 318-320.

Vidal, V., Qiu, N., Redfield, B., Carlino, A., Broth, N., and Weissbach, H. (1996) Arch. Biochem. Biophy. 330, 314-318.

Voet, D. and Voet, J. (1990) Biochemistry John Wiley and Sons, New York, 116-118.

Vogel, J.P., Misra, L.M., and Rose, M.D. (1990) J. Cell Biol. 110, 1885-1895.

Volchuk, A., Wang, Q., Ewart, H.S., Liu, Z., He, L., Bennett, M.K., and Klip, A. (1996) Mol. Biol. Cell 7, 1075-1082.

Wada, I., Kai, M., Imai, S., Sakane, F., and Kanoh, H. (1997) EMBO J. 16, 5420-5432.

Ward, C.L., Omura, S., and Kopito, R.R. (1995) Cell 83, 121-127.

Weber, T.M., Joost, H-G., Simpson, I.A., and Cushman, S.W. (1988) In Receptor Biochemistry and Methodology. Kahn R.C. and Harrison, L.C., eds. pp. 171-187, Alan R. Liss, Inc., New York.

Wei, J., Gaut, J.R., and Hendershot, L.M. (1995) J. Biol. Chem. 270, 26677-26682.

Wei, J. and Hendershot, L.M. (1995) J. Biol. Chem. 270, 26670-26676.

Welch, W., Garrels, J., Thomas, P., Lin, J., and Feramisco, J. (1983) J. Biol. Chem. 258, 7102-7111.

Weng, S. and Spiro, R.G. (1997) Biochem. J. 322, 655-661.

White, M.F. and Kahn, C.R. (1994) J. Biol. Chem. 269, 1-4.

Wiese, R.J., Mastick, C.C., Lazar, D.F., Saltiel, A.R. (1995) J. Biol. Chem. 270, 3442-3446.

Wild, J., Altman, E., Yura, T., and Gross, C.A. (1992) Genes and Dev. 6, 1165-1172.

Williams, A.M. and Enns, C.A. (1991) J. Biol. Chem. 266, 17648-17654.

Wilson, I.B., Gavel, Y., and von Heijne, G. (1991) Biochem. J. 275, 529-534.

Yang, Y., Janich, S., Cohn, J.A., and Wilson, J.M. (1993) Proc. Natl. Acad. Sci. U.S.A. 90, 9480-9484.

Yoshimasa, Y., Paul, J.I., Whittaker, J., and Steiner, D.F. (1990) J. Biol. Chem. 265, 17230-17237.

Zhou, A., Webb, G., Zhu, X., and Steiner, D.F. (1999) J. Biol. Chem. 274, 20745-20748.

Zhu, X., Zhao, X., Burkholder, W.F., Gragerov, A., Ogata, C.M., Gottesman, M.E., Hendrickson, W.A. (1996) Science 272, 1606-1614.

BIOGRAPHICAL SKETCH

Joseph Bumsuh Hwang was born in Seoul, South Korea in 1970. His family, including an older sister, immigrated to U.S.A. where they attained U.S. citizenship. He was raised in Jacksonville, Florida until he attended college at Emory University in Atlanta, Georgia. There he graduated with a bachelor's degree in chemistry and biology. He continued his education under the guidance of Dr. Susan C. Frost in the Department of Biochemistry and Molecular Biology at the University of Florida in pursuit of his doctorate. While in Gainesville, Florida he married Hyunok Lim on July 26, 1997. He will continue his post-doctoral training under the guidance of Dr. Alan Saltiel in the Department of Physiology at the University of Michigan at Ann Arbor.

I certify that I have read this study and that in my opinion it conforms to acceptable standards of scholarly presentation and is fully adequate, in scope and quality, as a dissertation for the degree of Doctor of Philosophy.

Susan C. Frost

Susan C. Frost, Chair
Associate Professor of
Biochemistry and Molecular
Biology

I certify that I have read this study and that in my opinion it conforms to acceptable standards of scholarly presentation and is fully adequate, in scope and quality, as a dissertation for the degree of Doctor of Philosophy.

Nancy Denslow

Nancy D. Denslow
Associate Scientist in
Biochemistry and Molecular
Biology

I certify that I have read this study and that in my opinion it conforms to acceptable standards of scholarly presentation and is fully adequate, in scope and quality, as a dissertation for the degree of Doctor of Philosophy.

Ben M. Dunn

Ben M. Dunn
Distinguished Professor of
Biochemistry and Molecular
Biology

I certify that I have read this study and that in my opinion it conforms to acceptable standards of scholarly presentation and is fully adequate, in scope and quality, as a dissertation for the degree of Doctor of Philosophy.

Peter M. McGuire

Peter M. McGuire
Assistant Professor of
Biochemistry and Molecular
Biology

I certify that I have read this study and that in my opinion it conforms to acceptable standards of scholarly presentation and is fully adequate, in scope and quality, as a dissertation for the degree of Doctor of Philosophy.

William Dunn

William Dunn
Associate Professor of
Anatomy and Cell Biology

This dissertation was submitted to the Graduate Faculty of the College of Medicine and to the Graduate School and was accepted as partial fulfillment of the requirements for the degree of Doctor of Philosophy.

December, 1999

Dean, College of Medicine

Winfred M Phillips

Dean, Graduate School